OCT 1 - 1958

# JET PROPULSION

A publication of the
AMERICAN ROCKET SOCIETY
Research and Development

BIND

VOLUME 28 SEPTEMBER 1958 NUMBER 9

SCIENCE & TECHNOLOGY

SURVEY ARTICLE

Some Recent Advances in the Mechanics of Terrestrial Flight . . *Angelo Miele* 581

CONTRIBUTED ARTICLES

Observation of High Intensity Radiation by Satellites 1958 Alpha and Gamma . . . . . *J. A. Van Allen, G. H. Ludwig, E. C. Ray and C. E. McIlwain* 588

Flame Stabilization in the Boundary Layer of Heated Plates . . . . . *Richard W. Ziemer and Ali Bulent Cambel* 592

Erosive Burning of a Colloidal Solid Propellant . . . *Jean A. Vandenkerckhove* 599

Supersonic Aerodynamic Experiments Using Very High Temperature Air Wind Tunnels . . . . . *D. E. Bloxsom Jr.* 603

Use of Capacitor Discharges to Produce High Temperature, High Pressure Air . . . . . *D. E. Bloxsom Jr.* 609

Measurement of Turbulent Heat Transfer Rates on the Aft Portion and Blunt Base of a Hemisphere Cylinder in the Shock Tube . . . . . *Josef Rabinowicz* 615

TECHNICAL NOTES

A Comparison of Turbojets and Ramjets for High Speed Flight . . . . . *M. Arens* 620

Simulation of Free Flight Structural Characteristics by Captive Missile I. Computer Analysis . . . . . *P. Lieberman* 622

DEPARTMENTS

New Patents 626 Book Reviews 630 Technical Literature Digest 634

*Thiokol*

# HUNTER-BRISTOL

## DIVISION—at BRISTOL, PENNSYLVANIA

Thiokol's Hunter-Bristol Division is an outstanding pioneer in rocket-powered test systems, such as rocket sleds to test pilot-ejection devices. Located at Bristol, Pennsylvania, Hunter-Bristol also produces aircraft and missile support equipment, air frame modifications, thrust and weighing stands and vital auxiliary power units. Its special engineering and production facilities are equipped to produce and test such equipment as igniters and fuses, as well as custom-engineered metal and electronic products for military and commercial use.

Engineers, scientists — perhaps there's a place for you in Thiokol's expanding organization. Our new projects present challenging problems and the chance for greater responsibility.

Thiokol®
CHEMICAL CORPORATION

TRENTON, N. J. · ELKTON, MD. · HUNTSVILLE, ALA. · MARSHALL, TEXAS · MOSS POINT, MISS.
BRIGHAM CITY, UTAH · DENVILLE, N. J. · BRISTOL, PA.

® Registered trademark of the Thiokol Chemical Corporation for its liquid polymers, rocket propellants, plasticizers and other chemical products

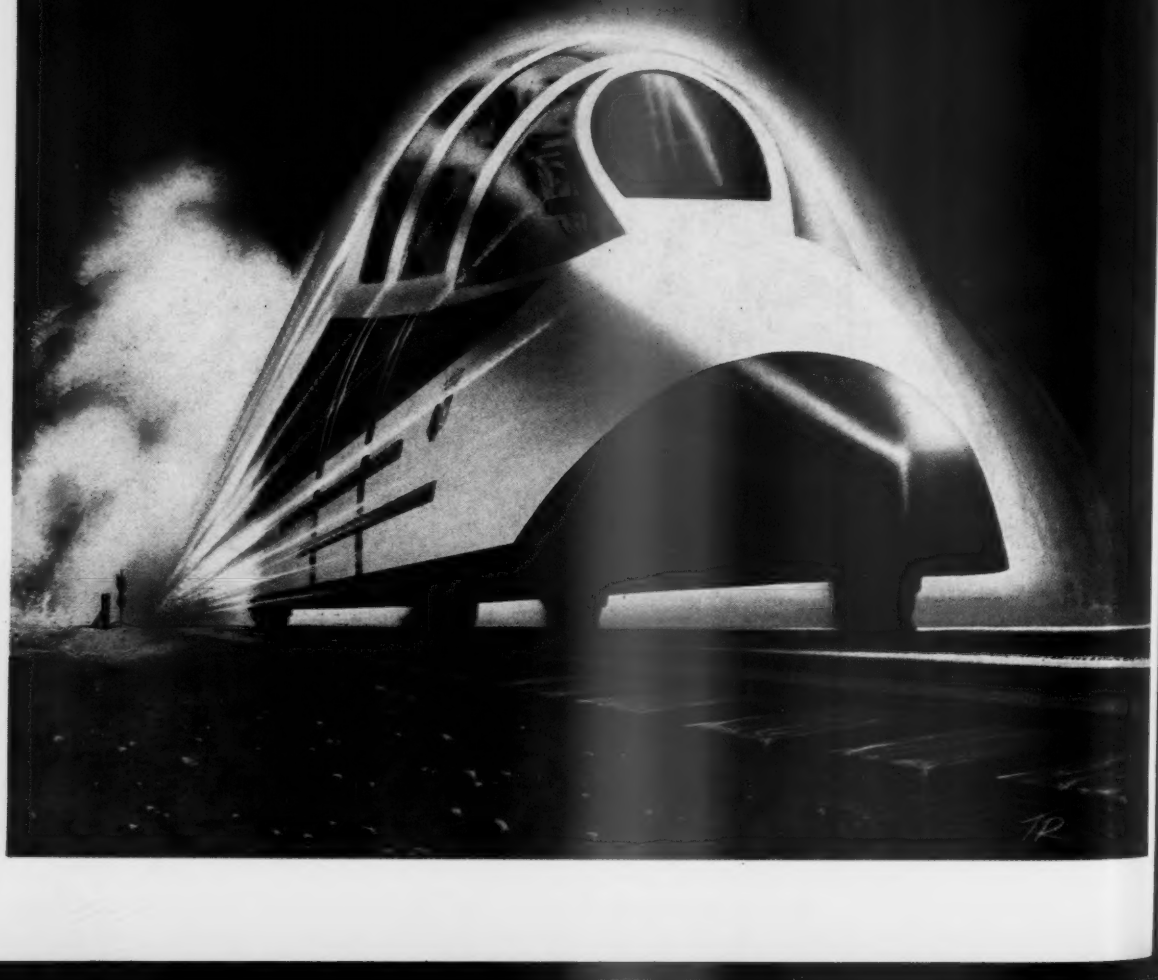

LOS ANGELES PUBLIC LIBRARY
OCT 1 - 1958

# STRAIGHT TALK TO ENGINEERS

## *from Donald W. Douglas, Jr.*

*President, Douglas Aircraft Company*

In your field, as most of you well know, it's easy to be complicated . . . it's hard to be simple. At Douglas, I'm happy to say, we do things the "hard" way. This matter of simplicity is vitally important. We work intensive hours, days and months to achieve it.

Why this extra effort? Well, simple things work easier, last longer, are more easily maintained and are lots more reliable. We are rewarded for our greater engineering effort with a product that performs better for our various customers.

We know that good engineers, working in an atmosphere which stimulates them to do their best, have been largely responsible for our success. If you enjoy solving challenging problems in the simplest manner, we'd like to talk with you about joining us.

Please write to Mr. C. C. LaVene
Douglas Aircraft Company, Box J-620
Santa Monica, California

# JET PROPULSION

*A publication of the*

AMERICAN ROCKET SOCIETY

*Research and Development*

IRWIN HERSEY—DIRECTOR OF PUBLICATIONS

*EDITOR* MARTIN SUMMERFIELD

*ASSISTANT EDITOR* BARBARA NOWAK

*ART EDITOR* JOHN CULIN

*ASSOCIATE EDITORS*

ALI BULENT CAMBEL, *Northwestern University*
IRVIN GLASSMAN, *Princeton University*
M. H. SMITH, *Princeton University*

*CONTRIBUTORS*

MARSHAL FISHER, *Princeton University*
GEORGE F. McLAUGHLIN

*ADVERTISING PRODUCTION MANAGER*

WALTER BRUNKE

*ADVERTISING & PROMOTION MANAGER*

WILLIAM CHENOWETH

*ADVERTISING REPRESENTATIVES*

D. C. Emery & Associates
155 East 42 St., New York, N. Y.
Telephone: Yukon 6-6855

James C. Galloway & Co.
6535 Wilshire Blvd., Los Angeles, Calif.
Telephone: Olive 3-3223

Jim Summers & Associates
35 E. Wacker Dr., Chicago, Ill.
Telephone: Andover 3-1154

R. F. and Larry Pickrell
318 Stephenson Bldg., Detroit, Mich
Telephone: Trinity 1-0790

Louis J. Bresnick
304 Washington Ave., Chelsea 50, Mass.
Telephone: Chelsea 3-3335

John W. Foster
239 4th Ave., Pittsburgh, Pa.
Telephone: Atlantic 1-2977



## AMERICAN ROCKET SOCIETY

Founded 1930

*OFFICERS*

President — George P. Sutton
Vice-President — John P. Stapp
Executive Secretary — James J. Harford
Secretary — A. C. Slade
Treasurer — Robert M. Lawrence
General Counsel — Andrew G. Haley

*BOARD OF DIRECTORS*

*Terms expiring on dates indicated*

Krafft Ehricke, 1959
S. K. Hoffman, 1958
Simon Ramo, 1960
H. W. Ritchey, 1959
H. S. Seifert, 1958
K. R. Stehling, 1958
Martin Summerfield, 1959
Wernher von Braun, 1960
Maurice J. Zucrow, 1960

*TECHNICAL DIVISION CHAIRMEN*

Lawrence S. Brown, Instrumentation and Guidance
Milton U. Clauser, Magnetohydrodynamics
Kraft A. Ehricke, Space Flight
Stanley V. Gunn, Nuclear Propulsion
Y. C. Lee, Liquid Rocket
Brooks T. Morris, Ramjet
David G. Simons, Human Factors
John Sloop, Propellants and Combustion
Ivan E. Tuhy, Solid Rocket

*COMMITTEE CHAIRMEN*

S. K. Hoffman, Finance
Simon Ramo, Publications
H. W. Ritchey, Membership
H. S. Seifert, Program
Kurt Stehling, Awards
Martin Summerfield, Policy


## Scope of JET PROPULSION

This Journal is a publication of the American Rocket Society devoted to the advancement of the field of jet propulsion through the dissemination of original papers disclosing new knowledge or new developments. As used herein, the term "jet propulsion" embraces all engines that develop thrust by rearward discharge of a jet through a nozzle or duct; and thus it includes air-consuming engines and underwater systems as well as rockets. JET PROPULSION is open to contributions dealing not only with propulsion but with other aspects of jet-propelled flight, such as flight mechanics, guidance, telemetering, and research instrumentation. Increasing emphasis will be given to the scientific problems of extraterrestrial flight.

## Information for Authors

Manuscripts must be as brief as the proper presentation of the ideas will allow. Exclusion of dispensable material and conciseness of expression will influence the Editors' acceptance of a manuscript. In terms of standard-size double-spaced typed pages, a typical maximum length is 22 pages of text (including equations), 1 page of references, 1 page of abstract, and 12 illustrations. Fewer illustrations permit more text, and vice versa. Greater length will be acceptable only in exceptional cases.

Short manuscripts, not more than one quarter of the maximum length stated for full articles, may qualify for publication as Technical Notes or Technical Comments. They may be devoted to new developments requiring prompt disclosure or to comments on previously published papers. Such manuscripts are usually published within two months of the date of receipt.

Sponsored manuscripts are published occasionally as an ARS service to the industry. A manuscript that does not qualify for publication according to the above-stated requirements as to subject, scope or length, but which nevertheless deserves widespread distribution among jet propulsion engineers, may be printed as an extra part of the Journal or as a special supplement, if the author or his sponsor will reimburse the Society for actual publication costs. Estimates are available on request. Acknowledgment of such financial sponsorship appears as a footnote on the first page of the article. Publication is prompt since such papers are not in the ordinary backlog.

Manuscripts must be double spaced on one side of paper only with wide margins to allow for instructions to printer. Include a 100 to 200 word abstract. State the authors' positions and affiliations in a footnote on the first page. Equations and symbols may be handwritten or typewritten; clarity for the printer is essential. Greek letters and unusual symbols should be identified in the margin. If handwritten, distinguish between capital and lower case letters, and indicate subscripts and superscripts. References are to be grouped at the end of the manuscript and are to be given as follows: for journal articles: authors first, then title, journal, volume, year, page numbers; for books: authors first, then title, publisher, city, edition, and page or chapter numbers. Line drawings must be clear and sharp to make clear engravings. Use black ink on white paper or tracing cloth. Lettering should be large enough to be legible after reduction. Photographs should be glossy prints, not matte or semi-matte. Each illustration must have a legend; legends should be listed in order on a separate sheet.

Manuscripts must be accompanied by written assurance as to security clearance in the event the subject matter lies in a classified area or if the paper originates under government sponsorship. Full responsibility rests with the author.

Submit manuscripts in duplicate (original plus first carbon, with two sets of illustrations) to the Editor, Martin Summerfield, Professor of Aeronautical Engineering, Princeton University, Princeton, N. J. Preprints of papers presented at ARS national meetings are automatically considered for publication.


JET PROPULSION is published monthly by the American Rocket Society, Inc., and the American Interplanetary Society at 20th & Northampton Sts., Easton, Pa., U. S. A. Editorial offices: 500 Fifth Ave., New York 36, N. Y. Price: $12.50 per year, $2.00 per single copy. Second-class mail privileges authorized at Easton, Pa. Notice of change of address should be sent to the Secretary, ARS, at least 30 days prior to publication. Opinions expressed herein are the authors and do not necessarily reflect the views of the Editors or of the Society


© Copyright 1958 by the American Rocket Society, Inc.

# Some Recent Advances in the Mechanics of Terrestrial Flight

ANGELO MIELE[1]

Purdue University, Lafayette, Ind.

**The author was born in 1922 in Italy. Following a classical education, he attended the University of Rome and was awarded a doctorate in Aeronautical Engineering in 1946. Dr. Miele has held positions in engineering, teaching, research and consulting in Italy, Argentina and the United States. He is now a professor at Purdue University, where he has taught for the last three years. He has acted as a consultant to Douglas Aircraft Company and Allison Division of General Motors Corporation; and has directed research projects sponsored by the National Advisory Committee for Aeronautics, Office of Scientific Research of the United States Air Force and Army Ballistic Missile Agency. Dr. Miele's research has been mainly concerned with the mechanics of terrestrial and extraterrestrial flight and with the application of the Calculus of Variations to the general theory of aircraft, missile and satellite performance. He is the author of approximately forty scientific papers, published in American and European journals.**

## Introduction

THE mechanics of flight of an aircraft is an important branch of the aeronautical sciences. The scope of this subject—a final synthesis of classical mechanics, theoretical and experimental aerodynamics and theory of jet engines—is the determination of the performance of a flying machine. Its particular objective is to provide a solution for the following fundamental and complementary problems:

1 To define the operational utility of an aircraft or missile which has already been designed.

2 To determine the basic configuration of an aircraft or a missile for a given mission to be accomplished.

In the years preceding World War II it was a common belief among engineers that the mechanics of flight had reached a conclusive and rather stagnant stage of development. The progress achieved in the last fifteen years has disproved this belief. In fact, the advent of jet engines as aircraft propulsion systems and the parallel increase in flight velocities have generated a wealth of important and unsolved problems of applied mathematics. Some of these problems, which cannot be handled by conventional methods of performance analysis, are mainly responsible for the engineering revival of the branch of mathematics known as the Calculus of Variations.

## Object of the Present Paper

This article offers a critical sketch of some recent advances in the mechanics of terrestrial flight. In spite of the considerable amount of bibliographical information included, no claim for completeness is made. Consequently, the author apologizes to those original writers who, because of oversight or space considerations, have been excluded from the present survey.

In this paper the aircraft is conceived as a particle. The aerodynamic lag is disregarded and attention is focused on two categories of questions associated with motion in a vertical plane:[2] Problems of steady or quasi-steady flight, and problems of nonsteady flight.

## Problems of Steady or Quasi-Steady Flight

The quasi-steady approach is useful in the analysis of those conditions of flight where the acceleration can be regarded as negligible. Initially developed for conventional aircraft, the quasi-steady approach has also been of interest for aircraft propelled by air-breathing jet engines. As an example, the cruising flight of a turbojet powered commercial aircraft can be well analyzed by means of this approach. The latter has the merit of leading to simple analytic relationships of great usefulness for design purposes.

Inherent in the quasi-steady approach is the fact that each point of the flight path of an aircraft can be investigated independently of the preceding one and of the following one. Thus, the so-called point performance can be studied within the framework of elementary algebra. Furthermore, associated with the *optimum* flight conditions are analytical problems amenable to treatment by the Ordinary Theory of Maxima and Minima.

Let

$T$ = thrust
$D$ = drag
$L$ = lift
$W$ = weight
$\theta$ = inclination of the vector velocity with respect to a horizontal plane
$\omega$ = inclination of the vector thrust with respect to the vector velocity
$h$ = altitude
$V$ = flight velocity

Consider a drag function of the form $D = D(h, V, L)$ and a thrust function $T = T(h, V, \alpha)$ where $\alpha$ is a variable[3] controlling the engine performance and having a function analogous to that of the accelerator pedal in a typical automobile.

With the above considerations in mind, and assuming that the inertia terms are negligible, the equations of motion in a vertical plane are written as

$$T(h, V, \alpha) \cos \omega - D(h, V, L) - W \sin \theta = 0$$
$$T(h, V, \alpha) \sin \omega + L - W \cos \theta = 0 \quad \ldots\ldots [1]$$

For a given weight $W$, Equations [1] represent a set of two

Received July 10, 1958.

[1] Member ARS.

[2] Due to space limitations, the problems of motion in a horizontal plane are not reviewed here. The interested reader is referred to References (1, 19, 20, 21, 69, 71).

[3] Within the context of this paper the $\alpha$-variable is termed engine control parameter or thrust control parameter or power setting. Nevertheless, its actual physical meaning is not specified, both because of the great variety of existing types of engines and for the purpose of developing a general theory. As an example, however, $\alpha$ can be identified with the number of revolutions of the turbine-compressor group for a turbojet engine having fixed geometry, or with the position of the fuel control lever, etc.

Editor's Note: This is the first of two articles on the mechanics of flight. The other to follow next month is on the subject of extraterrestrial flight and is entitled "Recent Advances in Astrodynamics" by S. Herrick and R.M.L. Baker Jr.

algebraic relations in the six variables $h$, $V$, $L$, $\theta$, $\alpha$ and $\omega$. It follows that four degrees of freedom are left, thus implying that a quadruple infinity of solutions is mathematically possible.

### Additional Constraints

In many engineering applications it is of paramount interest to study particular solutions of the algebraic system formed by Equations [1], more specifically, those solutions which simultaneously satisfy a set of $p \leq 4$ additional constraints.[4] The latter are symbolically indicated as

$$\Phi_i(h, V, L, \theta, \alpha, \omega) = 0 \qquad (i = 1, 2, \ldots, p) \ldots\ldots [2]$$

Clearly, the number ($n$) of degrees of freedom associated with the system of Equations [1 and 2] is now

$$n = 4 - p \ldots\ldots [3]$$

As a consequence, for $p \leq 3$, $n \geq 1$, so that some optimum requirement can be imposed on the flight performance, specifically, the one of extremizing (i.e., maximizing or minimizing) an arbitrarily specified function of the form

$$\Psi = \Psi(h, V, L, \theta, \alpha, \omega) \ldots\ldots [4]$$

In practical cases the $\Psi$-function can be, for instance, the range[5] per unit fuel consumed ($V/cT$), the endurance per unit fuel consumed ($1/cT$), the altitude ($h$), the flight velocity ($V$), the path inclination ($\theta$), the rate of climb ($V \sin \theta$), etc.

### Brief Literature Survey

Within the frame of expressions [1 to 4] many of the recent advances in quasi-steady flight mechanics of jet-propelled aircraft can be interpreted. First, the comprehensive papers by Lippisch (1,2)[6] deserve particular mention. They were carried out as part of the pioneering development of jet-propelled vehicles in Germany during World War II.

In the years following World War II, the performance problem attracted considerable interest in several countries. Under the assumption that the drag polar is parabolic with constant coefficients, analytical results were derived in (3 to 10).

The important range problem for a turbojet aircraft was the object of the investigations (11 to 13). In particular, the economy in fuel, which may result by flying at variable altitude (cruise-climb technique), was pointed out in (11,12).

The case of a drag polar embodying—in addition to a constant term and a term quadratic in the lift coefficient—a term linear in the lift coefficient was considered by Ludwig (14), who extended to a jet-propelled aircraft the analysis previously carried out by Wendt (15) for a piston-engined aircraft. Finally, the computation of the flight performance with compressibility effects accounted for was stressed in (3, 16 to 18).

### Optimum Conditions for a Given Configuration and Basic Determinantal Equation

Consider Equations [1 and 2], and assume $p = 3$, i.e., that three additional constraints $\Phi_1 = 0$, $\Phi_2 = 0$ and $\Phi_3 = 0$ are imposed. Assume also that the only remaining degree of freedom is to be saturated in such a way that the $\Psi$-function (Eq. [4]) is stationary. By the method of the Lagrange multipliers—and within the framework of the Ordinary Theory of Maxima and Minima—it can be shown (19) that the following optimizing condition is to be satisfied

$$\begin{vmatrix} \frac{\partial T}{\partial h}\cos\omega - \frac{\partial D}{\partial h} & \frac{\partial T}{\partial h}\sin\omega & \frac{\partial \Phi_1}{\partial h} & \frac{\partial \Phi_2}{\partial h} & \frac{\partial \Phi_3}{\partial h} & \frac{\partial \Psi}{\partial h} \\ \frac{\partial T}{\partial V}\cos\omega - \frac{\partial D}{\partial V} & \frac{\partial T}{\partial V}\sin\omega & \frac{\partial \Phi_1}{\partial V} & \frac{\partial \Phi_2}{\partial V} & \frac{\partial \Phi_3}{\partial V} & \frac{\partial \Psi}{\partial V} \\ -\frac{\partial D}{\partial L} & 1 & \frac{\partial \Phi_1}{\partial L} & \frac{\partial \Phi_2}{\partial L} & \frac{\partial \Phi_3}{\partial L} & \frac{\partial \Psi}{\partial L} \\ -W\cos\theta & W\sin\theta & \frac{\partial \Phi_1}{\partial \theta} & \frac{\partial \Phi_2}{\partial \theta} & \frac{\partial \Phi_3}{\partial \theta} & \frac{\partial \Psi}{\partial \theta} \\ \frac{\partial T}{\partial \alpha}\cos\omega & \frac{\partial T}{\partial \alpha}\sin\omega & \frac{\partial \Phi_1}{\partial \alpha} & \frac{\partial \Phi_2}{\partial \alpha} & \frac{\partial \Phi_3}{\partial \alpha} & \frac{\partial \Psi}{\partial \alpha} \\ -T\sin\omega & T\cos\omega & \frac{\partial \Phi_1}{\partial \omega} & \frac{\partial \Phi_2}{\partial \omega} & \frac{\partial \Phi_3}{\partial \omega} & \frac{\partial \Psi}{\partial \omega} \end{vmatrix} = 0 \ldots\ldots [5]$$

The above determinantal equation is fundamental for flight mechanics applications. Actually, all the optimum flight conditions of articles (1 to 18) are only particular cases of Equation [5]. The latter, therefore, unifies the best performances in a vertical plane into a single generalized statement. Thus, apparently diversified problems, such as maximum range, maximum endurance, ceiling, maximum speed, steepest ascent, fastest ascent, flattest descent, etc., are all covered[7] by the same determinantal equation.

### Optimum Aerodynamic Configurations

The method outlined in (19) not only yields the best flight performance for a given aircraft configuration, but also can be employed to solve design questions.

Assume for instance that the configuration of an aircraft[8] depends on $m$ parameters $\pi_k$ ($k = 1 \ldots m$), so that the drag function becomes $D = D(h, V, L, \pi_1, \ldots, \pi_m)$ and the weight $W = W(\pi_1, \ldots, \pi_m)$. Assume also that the above $m$ parameters must be determined so as to extremize the function [4] subject to the equations of motion and to the constraints [2], where $p = 3$. The number of degrees of freedom becomes $n = m + 1$, so that—after eliminating the Lagrange multipliers—$(m + 1)$ optimum relationships must be written. Under the hypothesis that the $\Psi$-function and the $\Phi_i$-constraints are independent of both the lift and the $\pi_k$-parameters, it can be shown (19) that the optimizing condition is represented by the combination of Equation [5] and the following $m$ additional relations

$$\frac{\partial D}{\partial \pi_k} + \frac{\partial W}{\partial \pi_k}\left(\sin\theta + \frac{\partial D}{\partial L}\cos\theta\right) = 0 \qquad (k = 1, 2, \ldots, m) \ldots [6]$$

In spite of the generality of these results, a word of caution is necessary. Unavoidably, an aircraft design is always a compromise between many contrasting requirements. As a consequence, the previously indicated optimum aerodynamic configurations must be taken *cum grano salis*.

## Problems of Nonsteady Flight

The nonsteady approach to the mechanics of flight is of interest (for instance) in the analysis of the flight paths of rocket-powered aircraft, missiles, satellite carriers, skip and glide bombers and in the study of the transient behavior[9] of aircraft propelled by air-breathing engines. For flight in a vertical plane over a flat Earth[10] the following set of differen-

---

[4] Within the context of the present paper the constraints [1] are termed fundamental; the constraints [2] are termed additional.

[5] The symbol $c = c(h, V, \alpha)$ denotes specific fuel consumption, i.e., weight of fuel consumed per unit time and unit thrust.

[6] Numbers in parentheses indicate References at end of paper.

[7] The only difference between one problem and another lies in the analytical nature of the function $\Psi$ to be extremized and of the additional constraints $\Phi_i = 0$ ($i = 1, 2, 3$) to be satisfied.

[8] In practical cases the $\pi_k$ parameters can be, for instance, the wing surface, the aspect ratio, the apex angle, etc.

[9] Typical, among these problems, is the investigation of the brachistocronic climbing technique for a turbojet aircraft.

[10] Problems of motion over a spherical, rotating Earth are discussed at the end of this paper.

tial equations is to be considered.

$$\dot{X} - V\cos\theta = 0$$
$$\dot{h} - V\sin\theta = 0$$
$$\dot{V} + g\sin\theta + \frac{D(h, V, L) - T(h, V, \alpha)\cos\omega}{m} = 0$$
$$\dot{\theta} + g\frac{\cos\theta}{V} - \frac{L + T(h, V, \alpha)\sin\omega}{mV} = 0$$
$$\dot{m} + \beta(h, V, \alpha) = 0 \qquad \ldots\ldots [7]$$

where

| | | |
|---|---|---|
| $X$ | = | horizontal distance |
| $g$ | = | acceleration of gravity |
| $m$ | = | instantaneous mass of the vehicle |
| $\beta$ | = | $cT/g$ engine mass flow |
| dot sign | = | derivative with respect to time ($t$) |

Notice that Equations [7] form a system of five differential equations in the eight unknown functions $X(t)$, $h(t)$, $V(t)$, $\theta(t)$, $m(t)$, $L(t)$, $\alpha(t)$ and $\omega(t)$. Thus, $n = 3$ degrees of freedom[11] are left, as is logical in view of the possibility of controlling the time history of: The elevator position, the thrust magnitude, and the thrust direction.[12]

### Additional Constraints

In many engineering applications it is of interest to study particular solutions of the set of differential Equations [7]; i.e., those solutions which simultaneously satisfy a set of $p \leq 3$ additional constraints

$$\phi_i(\dot{X}, \dot{h}, \dot{V}, \dot{\theta}, \dot{m}; X, h, V, \theta, m, L, \alpha, \omega, t) = 0 \qquad (i = 1, \ldots, p) \ldots [8]$$

Their effect is to reduce the number of degrees of freedom to

$$n = 3 - p \qquad \ldots\ldots [9]$$

Within the framework of expressions [7 to 9] many of the recent contributions to nonsteady flight mechanics can be interpreted. Quite appropriately, these contributions can be divided into papers dealing with optimum flight trajectories, and papers dealing with arbitrary (i.e., non-optimum) flight trajectories.

Because of space limitations, only a survey of papers of the first type is presented here. Furthermore, they are generally more significant from a mathematical standpoint. Contributions of the second type are therefore excluded, even though there is no question that several of them are certainly interesting from an engineering point of view.

### The Problems of Bolza, Mayer and Lagrange

With regard to the optimization of the flight trajectories the substantial difference between the quasi-steady approach and the nonsteady approach is the following: Because of the inertia terms, the minimal problems can no longer be handled from a *local* point of view; considerations of an integral nature are in order, in the sense that the flight path is to be treated *as a whole*. Thus, the nucleus of the problems of performance optimization shifts from the domain of the Ordinary Theory of Maxima and Minima into the realm of the Calculus of Variations. This fact, in turn, signifies a considerable increase in analytical difficulties, insofar as the optimum paths are no longer governed by equations in finite terms, but rather controlled by nonlinear systems of differential equations which are integrable, in general, only by approximate methods.

Notice that, if the additional constraints are such that $p \leq 2$, the number of degrees of freedom is $n \geq 1$. As a consequence, some optimum requirement can be imposed on the flight trajectory.[13] In this connection, the following problem (of Bolza type) is formulated (22): "In the class of functions $X(t)$, $h(t)$, $V(t)$, $\theta(t)$, $m(t)$, $L(t)$, $\alpha(t)$ and $\omega(t)$ satisfying Equations [7 and 8] and certain prescribed end conditions, find that special set such that the functional form[14]

$$\Psi = [G(X, h, V, \theta, m, t)]_i^f + \int_{t_i}^{t_f} F(\dot{X}, \dot{h}, \dot{V}, \dot{\theta}, \dot{m}; X, h, V, \theta, m, L, \alpha, \omega, t)dt \ldots\ldots [10]$$

is extremized."

It should be remarked that, if the $G$-function is *identically* zero, the Bolza problem reduces to the problem of Lagrange. If, on the other hand, the $F$-function is *identically* zero, the Bolza problem reduces to the problem of Mayer.[15] It is also stressed that, while the problem of Bolza appears to be—at first glance—more general than the other two, the three problems of Mayer, Lagrange and Bolza have, actually, the *same* degree of generality. As a matter of fact, by simple transformations (22), one problem can be taken into another and vice versa.

### General Considerations

With the theory of the first variation it can be shown that the special trajectory which solves the proposed Bolza problem must satisfy, as a necessary condition, the set of Euler-Lagrange equations (22), omitted here for brevity. The formulation of the latter becomes particularly simple if use is made of a special set of auxiliary variables, the Lagrange multipliers. The boundary conditions (partly of the fixed end points type, partly of the natural type) must be consistent with the general *transversality condition* of the Calculus of Variations (22).

It is to be noted that the analytical nature of the set of Euler equations and constraining equations is such that the attainment of solutions in a closed form is the exception, rather than the rule. An important additional difficulty stems from the circumstance that the variational problems of the mechanics of flight are *boundary value problems*, i.e., problems with conditions prescribed in part at the initial point and in part at the final point. As a consequence, the use of trial and error techniques is, except for particular cases, an unavoidable necessity.

[11] It should be emphasized that the phrase "degree of freedom" is being used in this section with a significance different from the one used in the preceding section on Problems of Steady or Quasi-Steady Flight. The symbol $n$ of the preceding section denotes the number of coordinates to be given in order to supply one particular solution of the set of *algebraic* Equations [1 and 2]. On the other hand, the symbol $n$ of this section indicates the number of functions to be specified in order to supply—with the appropriate boundary conditions—one particular solution of the set of *differential* Equations [7 and 8].

[12] In several papers of the variational literature the angle of attack ($\epsilon$) has been used in place of the lift ($L$) as a dependent variable. Analytically, Equations [7] are modified insofar as the drag becomes $D = D(h, V, \epsilon)$ and the lift $L = L(h, V, \epsilon)$. The minimal problem, therefore, is no longer studied in the ($X$, $h$, $V$, $t$, $m$, $L$, $\alpha$, $\omega$, $t$) space but in the ($X$, $h$, $V$, $\theta$, m, $\epsilon$, $\alpha$, $\omega$, $t$) space. The latter coordinate system offers—perhaps—a more immediate understanding of the analytical nature of the problem in the case where particular hypotheses are introduced in the equations of motion (see following sections).

[13] It should be emphasized that, for $n = 0$, it is still possible to optimize the boundary conditions. Problems of this type have been treated in (58).

[14] The subscript $i$ denotes initial point; the subscript $f$ refers to final point. The symbols $G$ and $F$ denote arbitrarily specified functions of the coordinates of the vehicle and their derivatives.

[15] Typical $G$-functions, having engineering interest, are: The range ($G = X$), the time ($G = t$), the flight velocity ($G = V$), the mass ($G = m$), etc.

## Review of the Variational Literature

Generally speaking, the analytical difficulties of a Bolza problem increase as the number of degrees of freedom increases. Thus, the simplest problems are those in which two degrees of freedom have been conveniently frozen, so that attention is focused on the optimization of the remaining one. Typical problems arising from the optimization of only the lift distribution (or the angle of attack) or only the thrust modulus or only the thrust direction are now reviewed. More general problems are also considered.[16]

### Programming of the Lift Distribution or the Angle of Attack

Consider the case $p = 2$, and assume that the two constraints $\Phi_1 = 0$ and $\Phi_2 = 0$ are such that they prescribe a priori both the mode of operation of the engine and the thrust direction (relative to the aircraft or to the vector velocity). One degree of freedom is consequently left, namely the degree of freedom associated with the programming of either the lift distribution or the angle of attack. Some typical problems are now presented (23 to 39).

#### Simplified Climbing Program for Turbojet Aircraft[17]

The initial investigations of the optimum[18] climbing program for turbojet aircraft were based on a somewhat simplified form of Equations [7]. The assumption was made that the mass of the aircraft is ideally a constant, and the centripetal component of the acceleration is disregarded, with only the tangential component being accounted for. Thus, approximate solutions were detected by the writer (23,24) whose analytical method, based on Green's theorem, avoids the use of indirect variational procedures. The Calculus of Variations was also avoided in a paper by Lush (25), with an intuitive graphical method based on the concept of energy-height.

On the same problem, an attack with the indirect methods of the Calculus of Variations was attempted in (26 to 28) leading, however, to incomplete results. In fact, the true Eulerian solution is discontinuous and generally formed of three different branches (dive, zoom, variable path inclination sub-arc); nevertheless, only one of the three sub-arcs forming the extremal arc was detected in (26 to 28), namely, the sub-arc flown with variable path inclination. Complete variational solutions, on the other hand, were found in (29,30).

Recently, the results indicated in (23,24) were rederived by Cartaino and Dreyfus (31) along the lines of the promising theory of dynamic programming, as developed by Bellman (70). Furthermore, solutions in a closed form for the altitude-Mach number relationship were indicated in (32), thus bypassing the so-called energy-height method commonly used by aircraft manufacturers.

#### Simplified Climbing Program for Rocket-Powered Aircraft

For a rocket-powered aircraft, the timewise variation of mass is important and must be accounted for in the study of the climbing performance. Historically, it is worth noticing that the theoretical development of new climbing techniques for rocket-powered aircraft preceded that for turbojet powered aircraft.

The two papers (1,33) are of particular interest. Even though they left the bulk of variational questions associated with the climbing flight substantially unsolved, nevertheless they shed considerable light on a new class of problems of the mechanics of flight.

It appears that in the paper by Kaiser (33) the concept of energy-height was first employed for flight mechanics application. On the other hand, the accelerated climbing flight was investigated in (1) under the assumption that the total drag coefficient is constant. As in the case of (26 to 28), the mathematical techniques employed in (1) lead to an incomplete solution, insofar as only one of the three sub-arcs forming the extremal arc associated with the problem under consideration was detected.

Recently, the brachistocronic problem with fixed end points was attacked in (34) with Green's theorem and in (35) with the indirect methods of the Calculus of Variations, under the assumption that the induced drag is negligible with respect to the zero-lift drag. In particular, analytical solutions were detected in (35) for the altitude-Mach number relationship, for both tropospheric and stratospheric flight.

#### More General Investigations

The investigations of the preceding sections were carried out under particular hypotheses, of which the essential analytical objective was to simplify the equation of motion on the normal to the flight path. By lifting the above limitations, a more general category of variational problems is originated. These problems attracted the attention of Cicala and the writer, who stressed the advantages of the Mayer formulation in an initial note (36) dealing with minimum time flight paths.

On the other hand, the Lagrange formulation was used by Behrbohm (37) who investigated—among other problems—trajectories of minimum time and of minimum fuel consumption, by referring to a parabolic polar with coefficients depending upon the Mach number.

In a recent Readers' Forum note (38) the minimum time problem was once more attacked essentially along the lines of (36), but using the altitude in place of the time as the independent variable.

Finally, a recent paper by Fraeijs de Veubeke (39) is to be mentioned. It refers particularly to the problem of maximum range and formulates the equations of motion in parametric form.

### Thrust Programming Problems

Consider again the case $p = 2$, and assume that the constraints $\Phi_1 = \Phi_2 = 0$ prescribe a priori the direction of the thrust and the distribution of lift (or some equivalent geometric condition). One degree of freedom is left, the one associated with the programming of the modulus of thrust. Papers in this area of problems (40 to 53) are now reviewed.

Concerning the level flight of a rocket-powered aircraft, the early analysis by Hibbs (40) is mentioned in connection with the problem of maximizing the range, the flying time being free of choice. An interesting characteristic of this problem is that—in addition to the constraints [7 and 8]—it involves a side condition expressed in the form of an *inequality*

$$0 \leq \beta \leq \beta_{max} \qquad [11]$$

specifying that the engine mass flow $\beta$ is bounded between an upper value and a lower value. This circumstance, in turn, leads to a discontinuous extremal arc, composed of sub-arcs of three different kinds: Sub-arcs flown with maximum thrust, sub-arcs flown by coasting and sub-arcs flown with variable thrust. Methods for handling inequality [11] were developed in (41) by the writer, who made use of Green's the-

[16] It should be emphasized that the really important characteristic of a variational problem is the number of degrees of freedom associated with the set of fundamental constraints and additional constraints being considered. Any other form of classification is—to a certain extent—arbitrary. The terminology "lift programming problems" or "thrust programming problems" or "problems where the thrust direction is programmed" has only been used with the purpose of rendering a more vivid exposition of these problems. The reader, therefore, should accept the present terminology with a note of caution.

[17] This problem, as well as the one of the following section, is better understood if the angle of attack is used in place of the lift as a dependent variable.

[18] With regard to either time or fuel consumed.

orem and by Cicala, who introduced the concept of *index value* in combination with the Weierstrass device. More general Mayer problems of the form $G = G(X, V, m, t)$ were investigated in (42).

With regard to vertical flight, it is of historical interest to notice that Goddard (43) clearly recognized that the Calculus of Variations is an important tool in the performance analysis of rockets; even though—following an oversimplified procedure—he dealt with questions of the Ordinary Theory of Maxima and Minima. Following a brief paper by Hamel (44), the variational problems of minimum propellant consumption attracted the attention of Tsien and Evans (45) and, subsequently, of Ward (46), Leitmann (47,48) and Faulkner (49). In addition, the brachistocronic problem, as well as Mayer problems of the form $G = G(h, V, m, t)$ were studied in (50,51).

Arbitrarily inclined rectilinear paths were investigated in (52), while nonlifting paths flown with minimum propellant consumption were analyzed by Bryson and Ross (53).

### Programming of the Thrust Direction

If the two constraints $\Phi_1 = \Phi_2 = 0$ prescribe a priori both the distribution of lift and the modulus of the thrust, the trajectory can still be optimized with regard to the thrust direction (54 to 56).

For the special condition of vacuum flight ($L = D = 0$), simple and intriguing results are obtained. It has been shown by Lawden (54) that, for a Mayer problem of the form $G = G(X, h, V, \theta, m, t)$, the absolute inclination in space of the vector thrust is a *bilinear* function of the time.

On the other hand, for the particular case of Mayer problems of the form $G = G(h, V, \theta, m, t)$ not involving range, the absolute inclination of the vector thrust becomes a *linear* function of the time, as shown by Fried (55). Finally, for the other particular case of Mayer problems of the form $G = G(X,h,m,t)$ where the vector velocity is free at the final point, the optimum inclination in space of the vector thrust is a constant, a result proved by Fried and Richardson (56).

### Simultaneous Optimization of Several Degrees of Freedom

The investigations of the preceding sections were concerned with problems involving only one degree of freedom, i.e., the one associated with either the lift distribution or the thrust modulus or the thrust direction. In the present paragraph questions of a more general nature, involving either two or three degrees of freedom, are analyzed (57 to 60).

First, the contributions due to Cicala (57,58) must be mentioned in connection with the programming of both the lift distribution and the modulus of the thrust. The latter problem was also studied in an interesting report by Breakwell (59). Finally, a very general theory by the writer (60) is mentioned in connection with the simultaneous optimization of lift distribution, thrust modulus and thrust direction.

### Legendre-Clebsch, Weierstrass and Jacobi-Mayer Conditions

As is known from the theory of the first variation, the optimum paths are solutions of the Euler-Lagrange differential equations. The fact that a trajectory satisfies the Euler equations, however, only guarantees its *stationary* character. To determine whether the functional $\Psi$ assumes a maximum or minimum value along the Eulerian path, a further investigation is in order. In particular, the so-called Legendre-Clebsch, Weierstrass and Jacobi-Mayer conditions must be analyzed. A general discussion of these conditions can be found in (57,58). Particular aspects of them are dealt with in (39,55,61).

It is of interest to note that in many problems of the mechanics of flight the conditions due to Legendre-Clebsch and Weierstrass *fail* to supply any information on the minimal or maximal character of the solution along a major portion of the extremal arc. This important difficulty can be overcome with some of the techniques developed in (58). Another device is based on Green's theorem, which has a particularly useful application in the study of *linear* variational problems of either the simplest type or the isoperimetric type (24, 42, 62).

### Effect of Inequalities on the Solutions

There are innumerable problems of the mechanics of flight where not only the constraints [7 and 8] must be satisfied, but also a number of additional constraints expressed in the form of inequalities.

As an example, the mass flow of a rocket engine must satisfy the inequality [11] at all points of the flight path. Other possible inequalities may involve the longitudinal acceleration, the normal acceleration, the lift, the flight altitude, the maneuverability, etc. In this connection, the following statement is pertinent: The effect of each inequality is to introduce one additional (potential) branch into the solution. Discontinuous solutions are *generally* found and the Erdmann-Weierstrass corner conditions (22) must be applied in order to join the different sub-arcs forming one extremal arc.

As an additional example, consider a high speed glider, and assume that the lift $L$ is to be consistent with the constraint

$$L \leq KW \qquad [12]$$

at all points of the flight path, $W$ being the weight and $K$ a nondimensional constant. By means of analytical methods similar to those developed in (42,51,53) it can be shown that, because of the inequality [12], the additional sub-arc

$$L - KW = 0 \qquad [13]$$

*may* appear in the composition of the extremal arc. In this connection, methods for treating problems involving discontinuous solutions can be found in several of the papers of Cicala and the writer.

### On the Relationship Between Calculus of Variations and Ordinary Theory of Maxima and Minima

An interesting link can be established between Calculus of Variations and Ordinary Theory of Maxima and Minima by means of the following procedure.

Let the acceleration terms appearing in Equations [7] decrease, tending to zero in the limit. The associated set of Euler-Lagrange equations modifies and, in the limit, yields a new set of Euler equations. The latter set supplies optimizing conditions *identical* with those given by the Ordinary Theory of Maxima and Minima for problems of quasi-steady flight. This important property of the Euler equations has been proved in (17,19,63) for particular problems, specifically, the maximum range and the maximum endurance of a turbojet powered aircraft.

### Problems of a Thermal Nature

The variational techniques surveyed in this article can also be applied to problems of a thermal nature, for instance the problem of the trajectory which minimizes the increase in skin temperature for a rocket-powered missile (64).

The analytical character of these problems is not different from those previously examined. Nevertheless, the set of constraining equations is to be completed by a further equation, the one relative to the heat balance between missile skin and surrounding medium (64).

### Variational Problems with Consideration of the Variable Gravitational Field and Rotation of the Earth

For problems where either great ranges or great velocities are involved, or for problems where a great precision is needed,

it becomes important to account for two factors:

1 The gravitational field of the Earth is not *uniform* but *central.*

2 Newton's law is rigorously true only for a reference system rigidly associated with the so-called Fixed Stars. Thus, when the equations of motion are referred to a coordinate system rigidly associated with the Earth, the corrective terms due to the so-called *transport acceleration* and *Coriolis acceleration* must be considered. The latter is of more relevant importance than the former for ballistic missiles and satellite vehicles.

When items 1 and 2 are accounted for, Equations [7] are modified and become more complicated. Nevertheless, the analytical nature of the minimal problems does not change; they still fall under the formulations of either Bolza, Mayer or Lagrange, even though the attainment of solutions in a closed form becomes more difficult.

Problems involving either one or several degrees of freedom (with sphericity and/or rotation of the Earth considered) have been investigated by Fried and Richardson (56), Breakwell (59), Miele (60), Leitmann (65), Okhotsimskii and Eneev (66) and Lawden (67,68). The latter is also the author of many contributions to the mechanics of extraterrestrial flight, excluded however from the present survey which is confined to problems of terrestrial flight.

## Summary and Conclusions

A general survey is presented of the problems of the mechanics of terrestrial flight, with particular regard to the optimization of the trajectories of both quasi-steady and nonsteady flight.

The optimum problems of quasi-steady flight are amenable to treatment by the Ordinary Theory of Maxima and Minima. For the case where the aircraft configuration is given, a new and general determinantal equation is presented. The latter covers a wide variety of problems, such as maximum range, maximum endurance, ceiling, maximum speed, steepest ascent, fastest ascent, flattest descent, etc., thus unifying all the mechanics of flight in a vertical plane into a single statement. A general solution is also presented for the aerodynamic configuration which is the best for an arbitrary performance to be optimized.

On the other hand, nonsteady flight mechanics leads to minimal problems falling in the domain of the problems of Bolza, Mayer and Lagrange of the Calculus of Variations. The recent variational literature is reviewed with particular regard to the programming of the lift distribution, thrust modulus and thrust direction. The following topics are also discussed: Legendre-Clebsch and Weierstrass conditions, effect of inequalities on the solutions, problems of a thermal nature, relationships between Calculus of Variations and Ordinary Theory of Maxima and Minima, and variational problems with consideration of the variable gravitational field and rotation of the Earth.

It is clear from the present survey that much has been achieved in recent years in the field of terrestrial flight mechanics. Many problems have been conquered. Nevertheless, an even larger domain is still unexplored, both from a theoretical standpoint and with regard to practical engineering applications.

There is an immediate need for improved methods for integrating the system of Euler equations and constraining equations and for solving the associated boundary value problems. An extension of the available closed form solutions would be of great value with regard to engineering applications. In view of the rather weak character of the maxima and minima of the mechanics of flight, the finding of short cuts and simplifications applicable to particular problems would also be valuable.

At the present time, the work in the area of *sufficient conditions* for an extremum lags far behind the work accomplished in obtaining *necessary conditions.* These sufficiency conditions have given rise to questions, the answers to some of which are still incomplete or unknown, especially in connection with discontinuous extremal solutions.

In the era of supersonic interceptors, intercontinental missiles, satellites and interplanetary vehicles, the variational methods constitute a much needed and important step forward in advanced performance calculations. The vista is now beginning to open on this application. It is the opinion of the writer that, as the industry progresses toward faster and faster vehicles, the Calculus of Variations will become the standard, rather than the specialized, tool of optimum performance analysis of aircraft and missiles.

## References


1 Lippisch, A., "Performance Theory of Airplanes with Jet Propulsion," Headquarters Air Materiel Command, Translation Report no. F-TS-685-RE, 1946.

2 Lippisch, A., "The Range of Jet-Propelled Aircraft," Cornell Aeronautical Laboratory, Translation, 1947.

3 Page, R. K., "Performance Calculation for Jet-Propelled Aircraft," *Journal of the Royal Aeronautical Society,* vol. 51, 1947, p. 440.

4 Santangelo, G., "Sulle Caratteristiche di Volo degli Aeroplani con Turboreattore," *L'Aerotecnica,* vol. 27, 1947, p. 323.

5 Freeman, H. B., "Simple Analytical Equations for the Velocity of an Airplane in Unaccelerated Level, Climbing, and Diving Flight," *Journal of the Aeronautical Sciences,* vol. 14, 1947, p. 185.

6 Tifford, A. N., "The Application of Gas Turbines to Aircraft," *Aeronautical Engineering Review,* vol. 7, 1948, p. 33.

7 Edwards, A. D., "Performance Estimation of Civil Jet Aircraft," *Aircraft Engineering,* vol. 22, 1950, p. 70, p. 94, p. 143.

8 Miele, A., "Il Calcolo delle Caratteristiche di Salita e della Quota di Tangenza degli Aeroplani Azionati da Turboreattori," *L'Aerotecnica,* vol. 30, 1950, p. 76.

9 Miele, A., "On the Speed of an Airplane in Steady Flight," *Journal of the Aeronautical Sciences,* vol. 17, 1950, p. 808.

10 Järvineva, E., "The Steepest Angle of Climb of Jet Aeroplanes in Unaccelerated Flight," *Aircraft Engineering,* vol. 23, 1951, p. 76.

11 Jonas, J., "Jet Airplane Range Considerations," *Journal of the Aeronautical Sciences,* vol. 14, 1947, p. 124.

12 Ashkenas, I. L., "Range Performance of Turbo-Jet Airplanes," *Journal of the Aeronautical Sciences,* vol. 15, 1948, p. 97.

13 Pearson, H., "The Estimation of Range of Jet-Propelled Aircraft," *Aeronautical Quarterly,* vol. 2, 1950, p. 167.

14 Ludwig, R., "Ein Beitrag zur Dimensionslosen Methode der Leistungsberechnung von Flugzeugen mit Strahltriebwerken," *Zeitschrift für Flugwissenschaften,* vol. 3, 1955, p. 141.

15 Wendt, R. E., "A Method of Airplane Performance Calculation Applicable to Any Polar," *Journal of the Aeronautical Sciences,* vol. 14, 1947, p. 243.

16 Hayes, W. D., "Performance Methods for High Speed Aircraft," *Journal of the Aeronautical Sciences,* vol. 12, 1945, p. 345.

17 Miele, A., "Variational Approach to the Stratospheric Cruise of a Turbo-Jet Powered Aircraft," *Zeitschrift für Flugwissenschaften,* vol. 7, 1958, p. 253.

18 Edelbaum, T., "Maximum Range Flight Paths," United Aircraft Corp., Report no. R-22465-24, 1955.

19 Miele, A., "Lagrange Multipliers and Quasi-Steady Flight Mechanics," Purdue University Aeronautical Engineering Dept., Report no. A-58-4, 1958.

20 Miele, A., "Steady Properly-Banked Turns of Turbo-Jet Propelled Airplanes," NACA TM no. 1382, 1955.

21 Santangelo, G., "La Virata Corretta Non-Stazionaria e Stazionaria degli Aeroplani con Gruppo Propulsore di Qualsiasi Tipo," *L'Aerotecnica,* vol. 34, 1954, p. 3.

22 Bliss, G. A., "Lectures on the Calculus of Variations," University of Chicago Press, Chicago, 1946.

23 Miele, A., "Problemi di Minimo Tempo nel Volo Non-Stazionario degli Aeroplani," *Atti della Accademia delle Scienze di Torino,* vol. 85, 1950–1951, p. 41.

24 Miele, A., "General Solutions of Optimum Problems in Non-Stationary Flight," NACA TM no. 1388, 1955.

25 Lush, K. J., "A Review of the Problem of Choosing a Climb Technique with Proposals for a New Climb Technique for High Performance Aircraft," Aeronautical Research Council, R. M. no. 2557, 1951.

26 Rutowski, E. S., "Energy Approach to the General Aircraft Performance Problem," *Journal of the Aeronautical Sciences*, vol. 21, 1954, p. 187.

27 Garbell, M. A., "Optimum Climbing Techniques for High-Performance Aircraft," Garbell Aeronautical Series, Report no. 8, 1953.

28 Kelly, L., "Optimum Climb Technique for a Jet-Propelled Aircraft," College of Aeronautics, Cranfield, Report no. 57, 1952.

29 Cicala, P. and Miele, A., "Brachistocronic Maneuvers of a Constant Mass Aircraft in a Vertical Plane," *Journal of the Aeronautical Sciences*, vol. 22, 1955, p. 286.

30 Lush, K. J., "Optimum Climb Theory and Techniques of Determining Climb Schedules from Flight Tests," AFFTC-TN-56-13, 1956.

31 Cartaino, T. F. and Dreyfus, S. E., "Application of Dynamic Programming to the Airplane Minimum Time-to-Climb Problem," Rand Corp., Report no. P-834, 1957.

32 Miele, A. and Cappellari, J. O., Jr., "Approximate Solutions to Optimum Flight Trajectories for a Turbo-Jet Powered Aircraft," Purdue University Aeronautical Engineering Dept., Report no. A-57-7, 1957.

33 Kaiser, "The Climb of Jet-Propelled Aircraft. Part I. Speed Along the Path in Optimum Climb," Ministry of Supply, RTP/TIB Translation no. GDC/15/148T, 1944.

34 Miele, A., "Optimum Climbing Technique for a Rocket-Powered Aircraft," JET PROPULSION, vol. 25, 1955, p. 385.

35 Miele, A. and Cappellari, J. O., Jr., "Approximate Solutions to the Optimum Climbing Trajectory for a Rocket-Powered Aircraft," Purdue University Aeronautical Engineering Dept., Report no. A-57-4, 1957.

36 Cicala, P. and Miele, A., "Brachistocronic Maneuvers of a Variable Mass Aircraft in a Vertical Plane," *Journal of the Aeronautical Sciences*, vol. 22, 1955, p. 577.

37 Behrbohm, H., "Optimal Trajectories in the Vertical Plane," SAAB T. N. no. 34, 1955.

38 Carstoiu, J., "On a Minimum Time Flight Path of a Jet Aircraft," *Journal of the Aeronautical Sciences*, vol. 24, 1957, p. 704.

39 Fraeijs de Veubeke, B., "Le Problème du Maximum de Rayon d'Action dans un Champ de Gravitation Uniforme," *Astronautica Acta*, vol. 4, 1958, p. 1.

40 Hibbs, A. R., "Optimum Burning Program for Horizontal Flight," JET PROPULSION, vol. 22, 1952, p. 206.

41 Cicala, P. and Miele, A., "Generalized Theory of the Optimum Thrust Programming for the Level Flight of a Rocket-Powered Aircraft," JET PROPULSION, vol. 26, 1956, p. 443.

42 Miele, A., "An Extension of the Theory of the Optimum Burning Program for the Level Flight of a Rocket-Powered Aircraft," *Journal of the Aeronautical Sciences*, vol. 24, 1957, p. 874.

43 Goddard, R. H., "A Method for Reaching Extreme Altitudes," Smithsonian Miscellaneous Collections, vol. 71, 1921, p. 1.

44 Hamel, G., "Ueber eine mit dem Problem der Rakete Zusammenhängende Aufgabe der Variationsrechnung," *Zeitschrift für Angewandte Mathematik und Mechanik*, vol. 7, 1927, p. 451.

45 Tsien, H. S. and Evans, R. L., "Optimum Thrust Programming for a Sounding Rocket," JET PROPULSION, vol. 21, 1951, p. 99.

46 Ward, L. E., "A Calculus of Variations Problem in Thrust Programming," US Naval Ordnance Test Station, T. N. no. 3503/2, 1955.

47 Leitmann, G., "A Calculus of Variations Solution of Goddard's Problem," *Astronautica Acta*, vol. 2, 1956, p. 55.

48 Leitmann, G., "Stationary Trajectories for a High-Altitude Rocket with Drop-Away Booster," *Astronautica Acta*, vol. 2, 1956, p. 119.

49 Faulkner, F. D., "The Problem of Goddard and Optimum Thrust Programming," *Proc. American Astronautical Society*, 1956.

50 Miele, A., "On the Brachistocronic Thrust Program for a Rocket-Powered Missile Travelling in an Isothermal Medium," JET PROPULSION (in publication).

51 Miele, A., "Generalized Variational Approach to the Optimum Thrust Programming for the Vertical Flight of a Rocket, Part I, Necessary Conditions for the Extremum," *Zeitschrift für Flugwissenschaften*, vol. 6, 1958, p. 69.

52 Miele, A. and Cavoti, C. R., "Optimum Thrust Programming along Arbitrarily Inclined Rectilinear Paths," Purdue University Aeronautical Engineering Dept., Report no. A-57-8, 1957.

53 Bryson, A. E. and Ross, S. E., "Optimum Rocket Trajectories with Aerodynamic Drag," JET PROPULSION, vol. 28, 1958, p. 465.

54 Lawden, D. F., "Optimal Rocket Trajectories," JET PROPULSION, vol. 27, 1957, p. 1263.

55 Fried, D. B., "On the Powered Flight Trajectory of an Earth Satellite," JET PROPULSION, vol. 27, 1957, p. 641.

56 Fried, D. B. and Richardson, J. M., "Optimum Rocket Trajectories," *Journal of Applied Physics*, vol. 27, 1956, p. 955.

57 Cicala, P., "Le Evoluzioni Ottime di un Aero," *Atti della Accademia delle Scienze di Torino*, vol. 89, 1954–1955, p. 350.

58 Cicala, P., "Soluzioni Discontinue nei Problemi di Volo Ottimo," *Atti della Accademia delle Scienze di Torino*, vol. 90, 1955–1956, p. 533.

59 Breakwell, J. V., "The Optimization of Trajectories," North American Aviation, Report no. AL-2706, 1957.

60 Miele, A., "General Variational Theory of the Flight Paths of Rocket-Powered Aircraft, Missiles and Satellite Carriers," Purdue University Aeronautical Engineering Dept., Report no. A-58-2, 1958.

61 Ross, S., "Minimality for Problems in Vertical and Horizontal Rocket Flight," JET PROPULSION, vol. 28, 1958, p. 55.

62 Miele, A., "Flight Mechanics and Variational Problems of a Linear Type," *Journal of the Aeronautical Sciences* (in publication).

63 Miele, A., "Minimal Maneuvers of High Performance Aircraft in a Vertical Plane," Purdue University Aeronautical Engineering Dept., Report no. A-58-3, 1958.

64 Miele, A., "Optimum Burning Program as Related to Aerodynamic Heating for a Missile Traversing the Earth's Atmosphere," JET PROPULSION, vol. 27, 1957, p. 1231.

65 Leitmann, G., "Trajectory Programming for Maximum Range," *Journal of the Franklin Institute*, vol. 264, 1957, p. 443.

66. Okhotsimskii, D. E. and Eneev, T. M., "Some Variation Problems Connected with the Launching of Artificial Satellites of the Earth," *Journal of the British Interplanetary Society*, vol. 16, 1958, p. 263.

67 Lawden, D. F., "Maximum Ranges of Intercontinental Missiles," *Aeronautical Quarterly*, vol. 8, 1957, p. 269.

68 Lawden, D. F., "Optimum Launching of a Rocket into an Orbit around the Earth," *Astronautica Acta*, vol. 1, 1955, p. 185.

69. Santangelo, G., "Sulla Virata Corretta Brachistocrona," *L'Aerotecnia*, vol. 33, 1953, p. 158.

70. Bellman, R., "Dynamic Programming of Continuous Processes," Rand Corp., Report no. R-271, 1954.

71. Behrbohm, H., "Optimal Trajectories in the Horizontal Plane," SAAB T. N. no. 33, 1955.

# Observation of High Intensity Radiation by Satellites 1958 Alpha and Gamma[1]

J. A. VAN ALLEN,[2] G. H. LUDWIG,[3] E. C. RAY[4] and C. E. McILWAIN[5]

State University of Iowa, Iowa City, Iowa

## Introduction

THIS is a preliminary report of results obtained concerning radiation intensities measured with a single geiger tube carried by the artificial earth satellites 1958 $\alpha$ and 1958 $\gamma$.[6]

The counting rate of the counter in 1958 $\alpha$ was transmitted continuously, and the data were recorded only when the satellite was quite near one of the 16 receiving stations distributed over the earth.

The data collected by 1958 $\gamma$ were also telemetered continuously. In addition, a small magnetic tape recorder stored the data obtained during each entire orbit. Then, as the satellite passed near one of the receiving stations, a radio command from the ground caused these data to be read out.

A preliminary study of the data obtained from 1958 $\alpha$ and several interrogations of 1958 $\gamma$ has been carried out, with the following results.

Reasonable cosmic ray counting rates have been obtained for altitudes below about 1000 km. In particular, we have obtained a plot of omnidirectional intensity vs. height in the vicinity of California for the first two weeks in February. This curve, extrapolated down to altitudes previously reached by rockets, agrees with earlier data.

At altitudes greater than about 1100 km, very high counting rates were obtained. This conclusion is the result of a somewhat lengthy analysis. Geiger tube output rates up to about 140/sec have actually been observed. In addition, periods have been found during which the geiger tube put out less than 128 pulses in 15 min. (We have a scaling factor of 128.) The considerations detailed in section 3 cause us to conclude that this is not due to equipment malfunction, but is caused by a blanking of the geiger tube by an intense radiation field. We estimate that if the geiger tube had had zero dead time, it would on these occasions have been producing at least 35,000 counts/sec.

We surmise that the radiation we have found is closely related to the soft radiation previously detected during rocket flights in the auroral zone.[7]

The radiation intensity necessary just to blank the geiger tube is equivalent to 60 mr/hr. In this connection the recommended permissible dose for human beings is 0.3 r/week.[8] The present radiation is 0.3 r in 5 hr or less.

Several geophysical effects of this radiation seem possible. It is very likely closely related to aurorae and geomagnetic storms. In addition, a rough calculation suggests that the radiation may be sufficiently intense to contribute important heating to the upper atmosphere. It will be important to investigate the amount of atmospheric ionization, light and radio noise which would be produced, under various assumptions as to the nature of the radiation.

## 1 Instrumentation for 1958 $\alpha$ and 1958 $\gamma$

The instrumentation for 1958 $\alpha$ consisted essentially of a single Geiger Mueller tube, a scaling circuit for reducing the number of pulses to be worked with, and telemetry systems for transmitting the scaler output to the ground receiving stations. The system contained in 1958 $\gamma$ was identical, with the addition of a miniature tape recorder for storing the data for the duration of each orbit and a command system to cause the telemetry of the stored information over a ground receiving station (Fig. 1).

Identical G.M. counters, scaler input circuits and scaling circuitry were used in the two cases. The G.M. counters were Anton halogen quenched counters having approximately 0.050 in. thick stainless steel walls. In addition, the counters were surrounded by the stainless steel cases of the payload, which were 0.023 in. thick. Thus the total absorption was approximately 1.5 gm cm$^{-2}$ of stainless steel (approximately

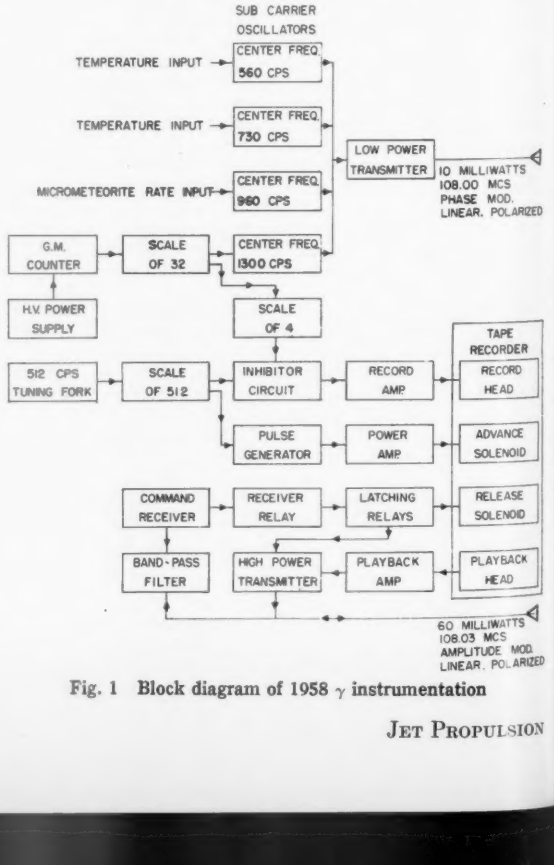


Fig. 1 Block diagram of 1958 $\gamma$ instrumentation

---

Presented at the ARS Semi-Annual Meeting, Los Angeles, Calif., June 9–12, 1958.

[1] Assisted by U.S./IGY Project 32.1 of the National Academy of Sciences and the National Science Foundation.

[2] Head, Department of Physics.

[3] Research Assistant, Department of Physics.

[4] Assistant Professor, Department of Physics.

[5] Research Assistant, Department of Physics.

[6] These satellites are sometimes called Explorer I and Explorer III, respectively.

[7] Meredith, Gottlieb and Van Allen, J. A., *Physics Review*, vol. 97, 1955, p. 201.

[8] Kinsman, S., "Radiological Health Handbook," U.S. Dept. of Health, Education and Welfare, 1955, p. 292.

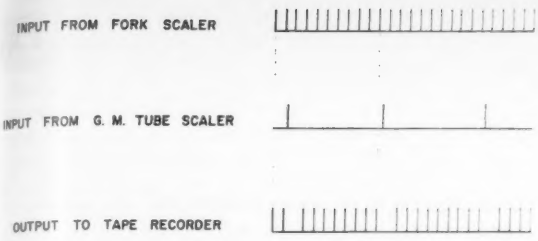


Fig. 2 **Illustration of the function of the inhibitor circuit**

75 per cent iron, 25 per cent chromium). The G.M. tubes had essentially infinite lives, small variation in counting efficiency over the range −55 to 175 C, approximately 85 per cent counting efficiency for cosmic rays, and about 0.3 per cent counting efficiency for photons of energy 660 kev. The dead time of the counters was approximately 100 microsec. The length of the counter wire was 4 in.; the inside diameter of the counter was 0.781 in.

Following the counters were current amplifiers, which directly fed the first scaler stages. The scalers were bistable transistor multivibrators, which operated over a wide range of supply voltage and over a temperature range of −15 to 85 C. This limitation was caused by the supply batteries. The scaler resolving time was 250 microsec. If input pulses at higher rates than 4000 per sec periodic were received, the scaler simply indicated a constant rate of 4000 per sec. That is to say, the scaler would not go out of operation if this rate was exceeded. It did, however, have an input pulse amplitude discrimination level, so that counter pulses of amplitude less than approximately one eighth normal were not counted.

In each of the satellites, the output of a scale of 32 was telemetered directly by the low power transmitter. In addition, it was transmitted by the high power transmitter in 1958 $\alpha$. In all cases, the shift of state of the output scaler stages caused a discontinuous shift in the frequency of the subcarrier oscillators, of which the outputs were transmitted by the appropriate transmitters. The data telemetered in this manner have been readable when the rates of input pulses to the scalers were between 0.14 pulses per sec (16 pulses or one change of state per 2 min pass) and 80 pulses per sec (limited by the bandwidth of the receiving and data reduction systems).

In 1958 $\gamma$ additional scaling circuits were included to provide a total scaling factor of 128 for the data to be stored. It was also necessary to include a time base, in order that a proper correlation could be established between the data and the satellite position. These two bits of information were combined in such a way that they could both be stored and telemetered on a single channel. Fig. 2 indicates the manner in which an inhibitor circuit effected this combination. The time base input was a train of pulses at the rate of one each sec. These pulses appeared at the output of the inhibitor, and were recorded, unless one was preceded by an output from the scale of 128, in which case it was suppressed.

The tape recorder was advanced in a discontinuous manner at the rate of one step per sec. As the tape advanced, it wound a spring for the eventual return of the tape to the starting point.

Upon receipt of a properly coded interrogation signal by the command receiver in the satellite, a relay system was activated which caused the higher power transmitter to be turned on and the tape to be released, so that the spring was free to return it to zero. The return tape speed was controlled by an eddy current damping system, so that the playback time was approximately 5 sec. As the tape returned, the information was read off the tape, telemetered, and the tape was erased. Upon completion of the cycle, the relays were reset, the transmitter turned off, and the next recording begun.

The information thus telemetered to the ground was the train of pulses emanating from the inhibitor circuit, except that it was much compressed in time. It can be seen then that scaler input pulse rates between 0 and 128 per sec were properly passed on, and that all rates above 128 per sec appeared as a rate of 128 per sec, that is, all pulses missing.

## 2 Summary of Preliminary Observations

Table I is a list of the stations receiving data and reporting them to us. The stations labeled JPL are operated under the auspices of the Jet Propulsion Laboratory at Pasadena, Calif. Those labeled NRL are operated by the Naval Research Laboratory in Washington, D. C. Data were obtained from 1958 $\alpha$ only when it was reasonably near one of these stations, since it had no provision for storing data for a later readout. We have already analyzed most of the data from the JPL stations, and some of that from the NRL stations as well. This work is continuing.

A small magnetic tape recorder in 1958 $\gamma$ stored the cosmic ray information for an entire oribit, and then played it into a transmitter on command from the ground. Data from nine of these orbits have been reduced in a preliminary way. We already have on hand many more of these passes, and are reducing the data from them in a routine way.

It is evident from the above summary that the present report is a very preliminary one. The nine cases from 1958 $\gamma$ occur during the last four days of March, and we expect ultimately to have data obtained during several weeks after those days. In addition, we have so far reduced the data from 1958 $\gamma$ only in a rather rough way, as explained in the following paragraphs. Finally, we do not yet have highly accurate data on the satellites' orbits. We do have the position of 1958 $\alpha$ as a function of time tabulated in 1 min intervals as supplied by the Vanguard computing center for the month of February. These data seem to be in error by several minutes in time, but apparently are sufficiently accurate for the purposes of the present report. So far for 1958 $\gamma$, we have only a set of orbital elements for March 26 and position vs. time for one orbit on April 1, together with estimates of the various perturbations. This information, supplied to us by the Vanguard Computing Center, has made it possible for us to estimate the orbit during the last days of March with reasonable accuracies. In particular, we estimate that our error in determining the time of passage through perigee is not more than about 5 min on March 31, and is less on earlier dates. Our errors in estimating latitude and longitude may amount to 10 deg in some cases.

Accurate orbital data will ultimately be supplied to us by the Vanguard Computing Center.

**Table I Receiving stations**

| | |
|---|---|
| Blossom Point, Md. | NRL |
| Fort Stewart, Ga. | NRL |
| Antigua, Br. W. Ind. | NRL |
| Havana, Cuba | NRL |
| San Diego, Calif. | NRL |
| Quito, Ecua. | NRL |
| Lima, Peru | NRL |
| Antofagasta, Chile | NRL |
| Santiago, Chile | NRL |
| Woomera, Aus. | NRL |
| Patrick Air Force Base, Fla. | JPL |
| Earthquake Valley, Calif. | JPL |
| Singapore | JPL |
| Ibadan, Nigeria | JPL |
| Temple City, Calif. | JPL |
| Pasadena, Calif. | JPL |

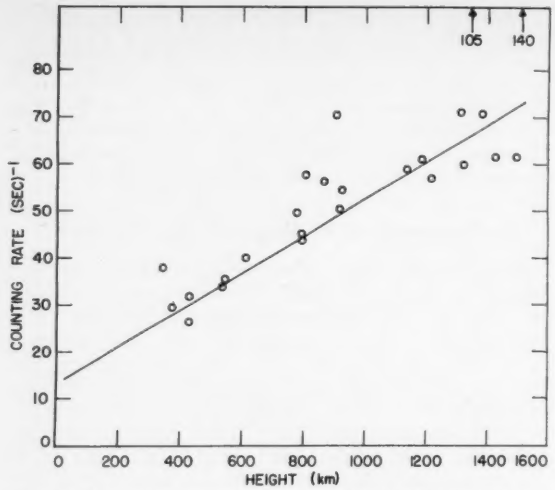


Fig. 3 Counting rate vs. height near California for 1958 $\alpha$

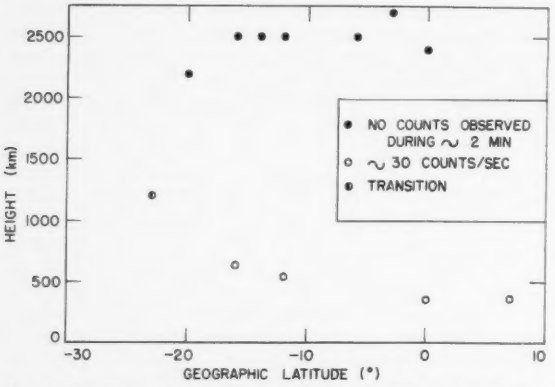


Fig. 4 Positions in altitude vs. latitude for telemetry of data from 1958 $\alpha$ over South America

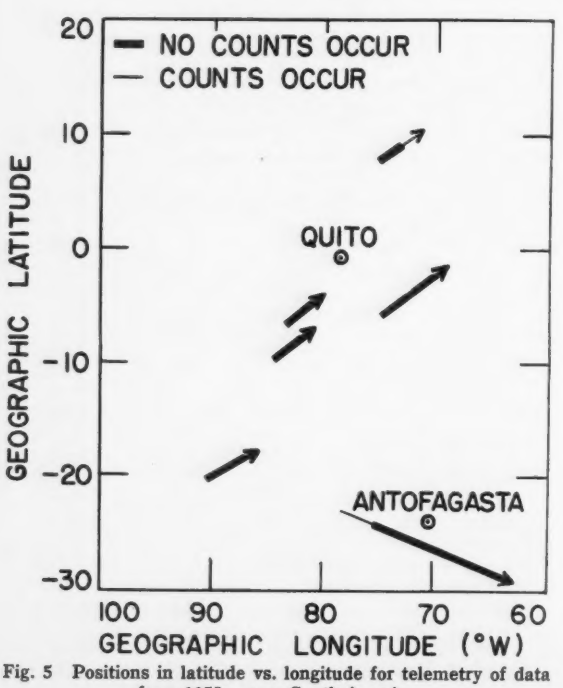


Fig. 5 Positions in latitude vs. longitude for telemetry of data from 1958 $\alpha$ over South America

We discuss first the data obtained from 1958 $\alpha$.

Fig. 3 is a plot of height against counting rate near the California coast. All of the passes recorded by JPL stations in California are included in this graph. There is some variation in latitude, which presumably accounts for some of the scatter of the points. In addition, as explained above, the orbital data are not yet known with good accuracy, and this presumably contributes significantly to the scatter. A linear extrapolation down to a height of 100 km yields a value of omnidirectional intensity of 1.22 $(cm^2\text{-}sec)^{-1}$, in adequate agreement with values we have previously obtained from rocket flights, considering the crudity of the extrapolation. The data shown in this figure were nearly all taken before Feb. 11.

The data obtained by the NRL stations in South America during the first two weeks of February are altogether different from those just discussed. The passes fall into two classes. In the first case, one obtains a counting rate of about 30/sec, a roughly reasonable value. In the second case, the telemetered signal fails to show a single scaler output pulse during the approximately 2 min of clean signal. This represents an input rate to the scaler of less than about 0.1/sec. There are, in addition, a few cases showing a strong change in counting rate during the pass.

For reasons discussed in section 3, we believe that the extremely low output rate of the scaler is caused by very intense radiation which "jams" the geiger tube so that it puts out pulses of such low height that they are below the threshold of the counting circuits. Laboratory tests show that this first happens for the present equipment when the radiation reaches such an intensity that a counter of the same effective dimensions and efficiency as the present geiger counter but with a zero dead time would produce 35,000 counts/sec.

Fig. 4 is a plot of height vs. geographic latitude in the vicinity of 75 W longitude. The positions of 1958 $\alpha$ during reception of its telemetering signal by various of the NRL stations are marked. A code designates the kind of information received. It is at once evident that the extremely low counting rates observed all occur at a high altitude, while the more or less normal rates occur at a low altitude. Transitional cases occur at a low altitude. Transitional cases occur at intermediate altitudes.

Quite similar behavior is observed near Singapore, and probably also Ibadan. In these two cases no thorough study has been made, mostly because of the lack of trajectory data for the dates on which extremely low telemetered counting rates occur. In the one case at Singapore where such a rate occurred on a date for which orbital data were available, the extremely low counting rate observed occurred at an altitude of about 2000 km.

Fig. 5 is a plot of geographic latitude vs. geographic longitude for various orbits. Only the high altitude cases are plotted on this figure. The fact that the segments of data do not correspond to positions of closest approach to the interrogating stations is due to our so far inaccurate knowledge of the trajectory.

These data already suggest a picture of the geophysical phenomenon being measured. The data from 1958 $\gamma$ are much more explicit. Fig. 6 is a plot of the scaler output as a function of time as given by the tape recorder readout for the pass ending near San Diego on March 28, 1748 UT. Since the tape recorder can only record one scaler output pulse each second (see section 1) the maximum indication on the tape recorder output corresponds to 128 counts/sec for the geiger tube output rate. (Our scaling factor is 128 in this case.) It is evident from the figure that reasonable counting rates occur near the two ends of the pass. These ends correspond to the most northern latitudes and the lowest heights above the earth. The section where the counting rate indication is zero corresponds to a portion of the magnetic tape where no tuning fork pulses were missing, and hence no scaler output pulses occurred. This condition lasted 15 min, and 128 pulses were fed to the scaler during this time. This is an

average counting rate for the interval of 0.14/sec, to be compared with the usual cosmic ray rate for a geiger tube of this sort of about 50/sec. The counter goes through the transition from putting out essentially no counts to putting out a great many very quickly, and we presume that most of the 128 counts observed during this 15 min interval occurred near the ends of the interval. There is, of course, no real evidence for this.

As discussed in detail in the next section, we believe that if we had had a detector with zero dead time, and a storage mechanism of unlimited capacity, Fig. 6 would begin where it does now, and at about 13 min would have begun rising rapidly to a peak near 25 min at which point the counting rate would have been greater than 35,000 counts/sec. After this time, the rate would gradually have subsided, returning finally to about the value actually recorded near the end of the pass.

Fig. 7 is a plot of geographic latitude vs. geographic longitude of those orbits for which the tape recorder readout data have so far been analyzed. We have simply identified the transition points between portions of the record where no tuning fork pulses are missing, all tuning fork pulses are missing, or some tuning fork pulses are missing. These three different kinds of regions are identified on the graph as >15,000/sec, 128 to 15,000, and <128, respectively. The dashed portions of the various curves represent regions where the identification as to counting rate range is uncertain. Since these passes all occurred during March 28 through March 31, the orbit did not have time to precess appreciably. Since perigee was near the most northern latitude, a given latitude corresponds closely to a given altitude. It is evident that at high altitudes and low latitudes, mostly in a certain range of longitude, the counting rate is very high. Near perigee the counting rate is low. Elsewhere intermediate counting rates occur. Possible interpretations of this result will be discussed in section 3.

## 3 Interpretation of Observed Data

We now propose to justify our claim that when essentially no scaler output pulses occur, the apparatus is, in fact, exposed to very intense radiation.

Three possibilities are immediately evident. The apparatus may have some simple malfunction. This possibility can immediately be rejected except for the scalers, geiger tubes, and geiger tube voltage supplies, since the subsequent treatment of the information is completely different in the 1958 $\alpha$ and 1958 $\gamma$. Some effect of temperature seems the only reasonable possibility here. The temperature of the geiger tube was measured in 1958 $\gamma$ and telemetered on the continuously operating transmitter. The observed temperatures range from zero to about 15 C. As discussed in section 1, the operating range of the circuitry is $-15$ to 85 C. In addition, the frequencies of the continuously telemetering channels which carried the cosmic ray information are significantly temperature sensitive. These showed that no extreme temperatures occurred at the location of the corresponding subcarrier generators.

Another possibility might be that the satellite passed through regions which very few cosmic rays could reach. This is extremely unlikely. A magnetic field of the order of one gauss extending over thousands of kilometers and remaining unbelievably free of local irregularities would be required to exclude a sufficient fraction of the cosmic radiation.

The possibility that we firmly believe is correct is that the geiger tube encountered such intense radiation that dead time effects reduced the counting rate essentially to zero. In order to explore this possibility, we have carried out the following experiments.

A spare flight unit for 1958 $\alpha$ was placed in an X-ray beam which was hardened by a $\frac{3}{8}$ in. thick, brass absorber. The voltage on the X-ray tube was varied between 50 and 90

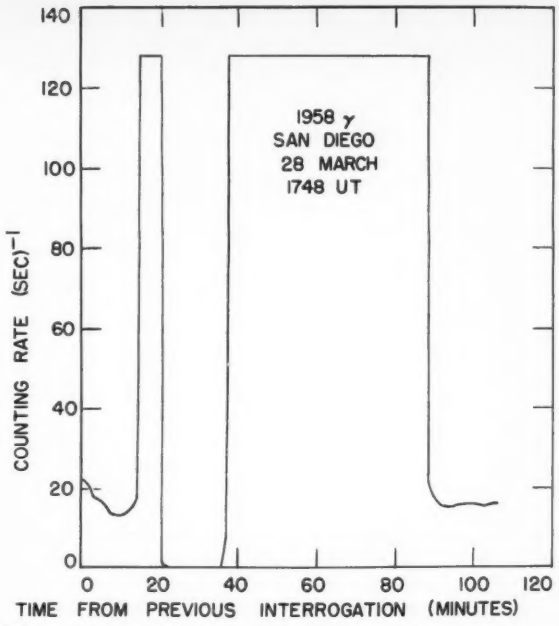


Fig. 6 A sample of the results of a tape recorder readout near San Diego on March 28, 1748 UT

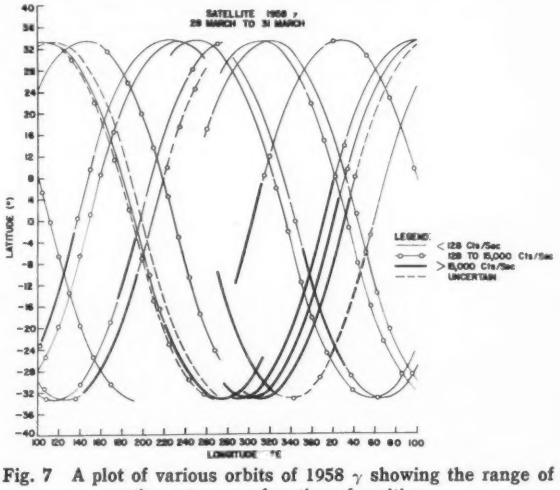


Fig. 7 A plot of various orbits of 1958 $\gamma$ showing the range of counting rates as a function of position

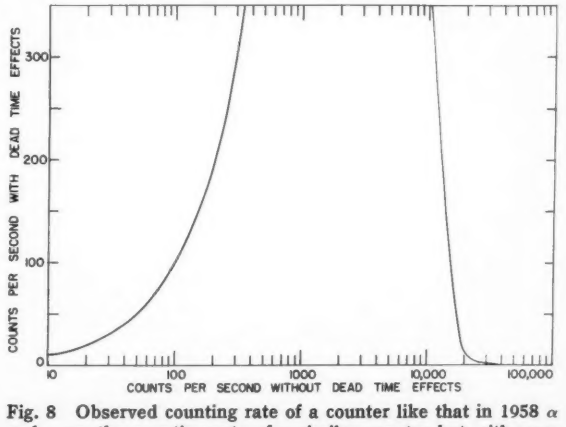


Fig. 8 Observed counting rate of a counter like that in 1958 $\alpha$ and $\gamma$ vs. the counting rate of a similar counter but with zero dead time

kev to vary the flux over a wide range. The counting rate was measured with and without lead shields which permitted only part of the beam to reach the geiger tube. In this manner the counting rates with and without the dead time effects were determined. As shown in Fig. 8, the dead time effects are negligible up to highest rates which can be handled by the telemetering systems. At high fluxes few of the pulses from the geiger tube have sufficient amplitude to operate the scaling circuit, and the counting rate returns to the range which can be telemetered. At very high fluxes no pulses have sufficient amplitude, and the counting rate is zero.

An ion chamber placed in the position of the satellite apparatus measured an intensity of 60 milliroentgens per hr at the minimum flux required to reduce the counting rate to zero. The ionization produced by different energy X-rays or by charged particles producing this effect would of course be different from this measurement. The X-rays used for this measurement had energies in the range 50 to 90 kev.

We have little concrete evidence concerning the nature of this radiation. Apparently, however, it is not electromagnetic. It makes its effects felt through the 1.5 g/cm$^2$ of absorber which constitute the hull of the satellite and the walls of the counter. Photons with such energy should then be seen down to the lowest altitudes our equipment reaches. The radiation can presumably be either protons or electrons. If it is electrons, we then are probably detecting bremsstralung formed in the satellite shell.

### 4 Implications

Any reasonable identification of this radiation strongly suggests several geophysical consequences. It is unlikely that the particles have several Bev of energy each. Then in order to reach such low heights through the geomagnetic field they must at least initially be associated with plasmas which seriously perturb the magnetic field at an earth radius or so. We presume that this plasma is closely related to geomagnetic storms and aurorae.

Secondly, at heights only a little above 1000 km, there is still some atmosphere. Crude quantitative estimates suggest that the energy loss in this residual atmosphere of the radiation we detect may contribute significantly, if not dominantly, to the heating of the high atmosphere. In addition to considering this heating effect, it will be important to calculate, on various assumptions as to the nature of the radiation, the amount of visible light, radio noise, and ionization produced.

Finally, there are obvious biological implications of these results. As discussed in section 3, if photons are being detected directly by the geiger tube, and if these photons are in the energy range 50 to 90 kev, then the radiation field inside the satellite corresponds to about 0.06 r/hr. The maximum permissible dose for human beings is 0.3 r/week. Other assumptions as to the nature of the radiation would obviously lead to different results.


### Acknowledgments

We owe a large debt of gratitude to many individuals and agencies. We are indebted to the Jet Propulsion Laboratory at Pasadena, Calif., for the high speed rocket cluster and for assembly of the satellite payload. The Army Ballistic Missile Agency at Huntsville, Ala., supplied the booster stage and conducted the launching. Project Vanguard of the Naval Research Laboratory assisted in the early design phases of the instrumentation. They also set up and operated the minitrack tracking and telemetering stations, with cooperation and assistance from the countries in which the stations are located. They supplied us with orbital information for both satellites. The Jet Propulsion Laboratory set up the microlock stations for telemetry reception and operated all of them except those at Ibadan and Singapore. These last two were operated by students at University College, Ibadan, and the University of Maylaya, Singapore, as a part of the British IGY effort.


# Flame Stabilization in the Boundary Layer of Heated Plates


RICHARD W. ZIEMER[1] and ALI BULENT CAMBEL[2]

Gas Dynamics Laboratory, Northwestern University, Evanston, Ill.



**This paper describes studies conducted with flames stabilized in the boundary layer of a heated flat plate. A graphical analysis of boundary layer flame stabilization is proposed and is verified by an experimental investigation of propane-air flames. The free stream flow was laminar with a turbulence intensity of 0.4 per cent, and the approach mixture velocity was 25 and 50 ft per sec. The maximum Reynolds number encountered, based on the length of the heated plate, was 122,000. Surface temperatures up to 2025 R were investigated.**


### Introduction

IN TURBOJET afterburners and ramjets, it is necessary to anchor the flame and prevent it from being blown out by the high velocity gases. One method which has been suggested is the stabilization of the flame on a high temperature surface. Such a surface may have the form of a circular cylinder or a flat plate, aligned parallel with the flow. The phenomenon whereby a flame anchors itself within the boundary layer of the surface as a result of boundary layer configuration and surface temperature is called boundary layer flame stabilization. No flow separation occurs, and, in addition, the surface upon which the stabilizing boundary layer is created need not obstruct the flow stream. No turbulence is created by the body other than that from the transition from the laminar to the turbulent regime.

### Previous Investigations

Probably the use of heated bodies to stabilize flames was first proposed in 1950 by Tsien (1)[3] who suggested a flameholder in the shape of a streamlined body. Such an airfoil would first be internally heated until combustion was initiated. Once the flame was started, it would be stabilized on


Presented at the ARS Semi-Annual Meeting, San Francisco, Calif., June 10–13, 1957.


[1] Now member of Technical Staff, Aeronautical Research Laboratory, The Ramo-Wooldridge Corp. Member, ARS.

[2] Professor and Chairman, Department of Mechanical Engineering. Fellow, ARS.

[3] Numbers in parentheses indicate References at end of paper.

the surface of the streamlined body. Thus, the portion of the airfoil downstream of the flame front would be heated by the hot gases. By lengthening the portion of the airfoil exposed to the hot gases, the temperature at the front of the airfoil could be raised, and the approach mixture velocity could be increased delaying blow-off.

Gross (2) studied boundary layer flame stabilization of premixed propane-air flames on thin flat plates as well as on symmetrical airfoils. He determined maximum blowout velocities for flames stabilized in the boundary layer or in the wake at the trailing edge of the plate.

A theoretical analysis of flames stabilized on a flat plate of constant temperature was made by Dooley (3) who formulated the differential equations for laminar boundary layer flow in which heat is released by chemical reaction. These equations were solved by mathematical iteration for any nonfractional order of reaction. Applying the solution of a first order combustion reaction, the stabilization performance for azomethane flames was calculated.

Gilbert, Haddock and Metzler (4) studied high heat release rates from the combustion of propane-air mixtures in a combustion chamber consisting of an electrical heating element mounted concentrically inside a steel tube. They observed that a flame front became stabilized on the heated rod and that its position in the chamber shifted as the mixture velocity, the equivalence ratio and the energy input to the heating element were varied.

Hottel, Toong and Martin (5) examined the stability of lean propane-air flames in the boundary layer on a water cooled rod. For a given coolant temperature, they correlated the Blasius velocity gradient at the rod surface with the propane-air ratio.

Toong (6) studied the incipient ignition of ethanol-air mixtures flowing over a hot surface. He made qualitative theoretical predictions of incipient ignition from boundary layer theory and correlated these experimentally. Finally, in a more recent study, Toong (7) studied the mechanism of flame stabilization by boundary layer theory.

## Proposed Model

In this paper boundary layer flame stabilization by hot surfaces is explained by the hypothetical model shown in Fig. 1. The proposed model consists of a flat plate over which a combustible mixture flows steadily, and a laminar boundary layer is created. A flame propagates upstream through the boundary layer on the plate until the upstream position is reached where the boundary layer is sufficiently thin to quench any further penetration of the flame, and the flame front becomes stabilized at this position.

If the flowing fluid is a combustible mixture, it has associated with it a finite velocity of laminar flame propagation. Since the fluid velocity tends to vanish as the surface is approached, there will be a region near the surface where the flame velocity exceeds the mixture flow velocity. If a flame is initiated in this region, the flame can propagate upstream through the combustible mixture. On the other hand, the surface of the plate acts as a heat sink as well as an absorber of active chemical radicals, thereby inhibiting the combustion reaction in a layer of the mixture adjacent to the surface. In this layer, near solid surface, there exists a zone devoid of flame which is called the dead space.[4] Smaller in depth, the dead space lies within the boundary layer. A flame propagating in the boundary layer region can occur no closer

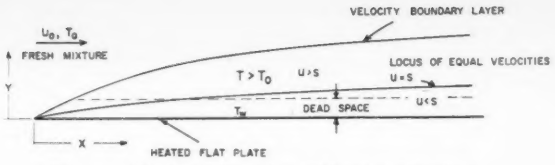


**Fig. 1a Model configuration without combustion**

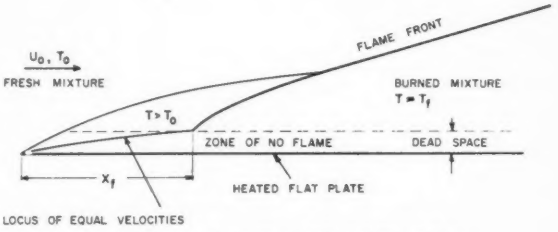


**Fig. 1b Model configuration with stabilized flame**

to the surface than the dead space distance. As the flame propagates upstream, the boundary layer through which it travels becomes thinner as the leading edge of the plate is approached. The flame traveling through the boundary layer can move upstream only as long as the flame velocity exceeds the fluid velocity at a distance from the surface greater than the dead space. The distance normal to the surface at which the mixture velocity is equal to the flame velocity of the mixture is an important parameter, because above this locus of equal velocities the fluid velocity is greater than the flame velocity, and hence any flame in this region would be carried downstream. Below the locus of equal velocities, the flame velocity exceeds the fluid velocity, and any flame in this region would propagate upstream parallel to the direction of flow. From the physics of the phenomena, it may be predicted that the limiting upstream position of the flame front should correspond to the location along the plate where the locus of equal velocity intersects the dead space, because at this position quenching will prevent the flame from penetrating any further upstream. The flame front should stabilize here and propagate into the fresh mixture.

When the surface temperature is raised by external or internal heat addition, several important changes take place. The flame velocity in the boundary layer will increase because of the higher local mixture temperature. The boundary layer thickness will increase because, with increased heat transfer from the surface to the boundary layer, the rate of boundary layer growth is more rapid. The dead space thickness will decrease, because as the surface temperature increases less quenching occurs. All of these changes associated with higher surface temperatures allow stabilization at a higher free stream velocity. For a given surface temperature, the boundary layer thickness may also be increased by lengthening the heated plate, thereby permitting flames to be stabilized at higher mixture velocities.

## Graphical Solution

It will be shown in this paper that it is possible to determine the position of the stabilized flame on a flat plate if the locus of equal velocities and the depth of the dead space can be specified for the desired conditions of surface temperature distribution and free stream velocity.

In summary, the graphical solution is based upon two basic combustion properties, the laminar flame velocity and the dead space distance. The analysis does not require a knowledge of the steps of the chemical reaction, the order of the reaction, or values of the activation energy, the diffusion coefficient or the frequency factor, which often are not known.

[4] The dead space is defined as the depth within which the surface extinguishes the flame (8). Immediately above the dead space is a zone in which the combustion reaction is inhibited, resulting in a decrease of the laminar flame velocity. The depth at which the velocity of flame propagation is 99 per cent of the velocity at an infinite depth of combustible mixture and which includes the dead space, is defined here, as quenching distance. Although this definition is an arbitrary one, it is based on the precedent used in defining boundary layer thickness.

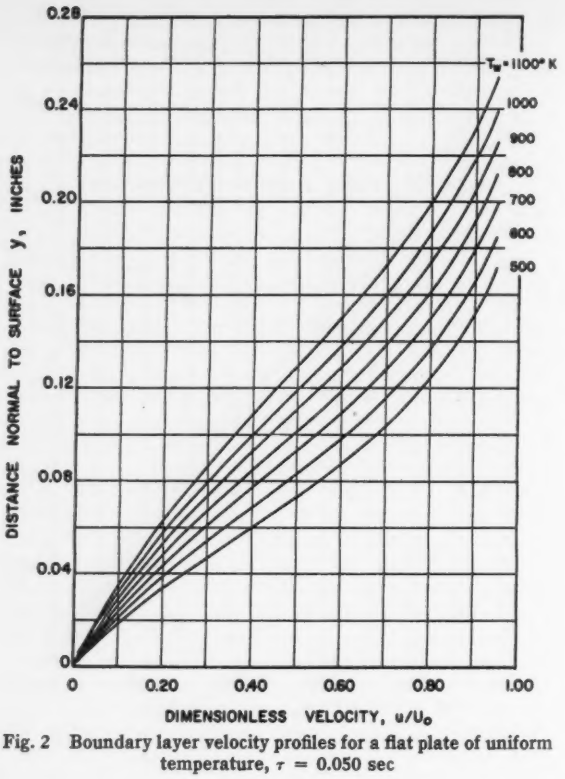


Fig. 2 Boundary layer velocity profiles for a flat plate of uniform temperature, $\tau = 0.050$ sec

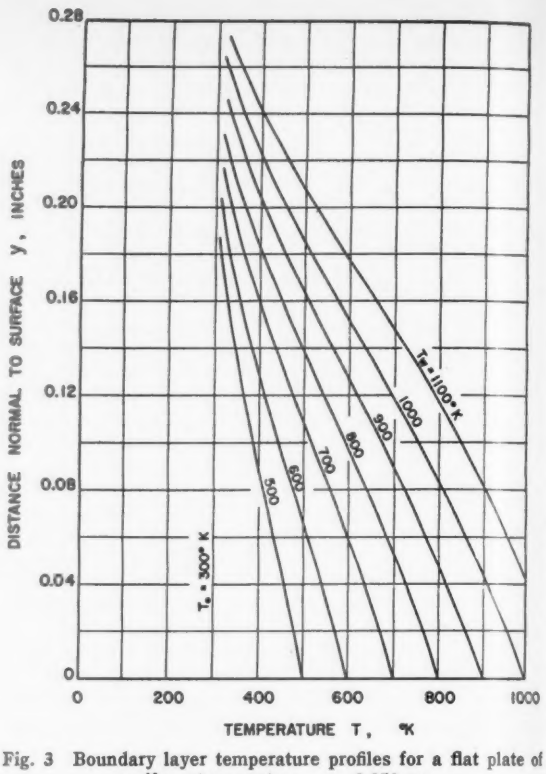


Fig. 3 Boundary layer temperature profiles for a flat plate of uniform temperature, $\tau = 0.050$ sec

In developing the graphical solution, the following assumptions are made:

1 No appreciable chemical reaction occurs upstream of the flame front.

2 The boundary layer temperature profile and the boundary layer velocity profile upstream of the flame front are not appreciably affected by the flame.

3 The mixture viscosity varies with the static temperature as defined in (8).

4 The curvature of the flame front within the quenching zone can be neglected.

5 The specific heat of the mixture is a constant.

The advantage of the proposed method is that the following assumptions, common to numerical solutions, need not be made:

1 The surface has a particular temperature distribution.

2 The Prandtl number equals the Schmidt number, and both are equal to unity.

3 The chemical kinetics is expressed by the Arrhenius reaction rate equation or some similar relation.

4 The order of the combustion reaction is nonfractional.

5 The average molecular weight of the mixture is constant.

The proposed graphical construction requires knowledge of the following functions:

1 The variation of temperature and velocity in the fluid boundary layer along the plate surface.

2 The variation of the laminar flame velocity with mixture temperature.

3 The variation of the depth of the dead space with plate surface temperature.

The methods of developing the graphical functions and the manipulations required to obtain the final solution of the analysis will be exemplified through consideration of a stoichiometric propane-air mixture for various plate temperatures, and for an initial mixture temperature of 300 K. A uniform temperature distribution along the plate will be assumed, although this assumption is not necessary to obtain a solution of the problem. First, each of the three previously listed graphical functions will be determined, and a discussion of the necessary assumptions and approximations will be undertaken. Then, the technique of utilizing the functions to predict the flame stabilization performance will be presented.

### Velocity and Temperature Profiles

The first functions of the illustrative solution to be calculated are the fluid boundary layer velocity and temperature profiles. These may be determined analytically by the general boundary layer solution of Chapman and Rubesin (9). Their solution applies to a laminar compressible boundary layer on a flat plate having an arbitrary temperature distribution. For a stoichiometric mixture of propane and air, the fuel represents only 4 per cent of the mixture by volume, and hence it is assumed that the fluid mechanic properties of the combustible mixture are the same as for air. The determination of the fluid boundary layer profiles by the above method does not take into consideration any chemical change in the fluid, and it is assumed that the degree of chemical reaction within the combustible mixture is negligible between the plate leading edge and the flame front. This is a valid assumption, because Linnett (10) has shown that the thickness of the reaction zone in laminar combustion is of the order of one millimeter, and hence is small compared to the length of surface being considered.

The boundary layer temperature and velocity profiles were calculated, using the solution of Chapman and Rubesin, for plates of uniform temperature distribution in the range of temperatures from 500 to 1100 K at increments of 100 deg. The profiles were computed for several values of the ratio $\tau = x/U_o$. It is then necessary to plot the distance $y$ versus the dimensionless velocity $u/U_o$ and the fluid temperature $T$, respectively, for different values of $\tau$ and $T_w$. In this study, values of $\tau$ between 0.001 and 0.100 sec were selected because they represent practical values of plate lengths for the particular mixture velocities encountered. In Figs. 2 and 3, a typical set is shown for $\tau = 0.050$ sec. Similar curves were

plotted for other values of $\tau$ but they are not shown. The use of the computed boundary layer profiles will be described later.

### Laminar Flame Velocity

The second graphical function, namely the variation of the laminar flame velocity with mixture temperature is required next. At a given pressure and for a given combustible mixture, the velocity of laminar flame propagation is a function of the mixture temperature, and this relation is readily obtained from experimental investigations.

In addition to being a function of the mixture temperature, the local laminar flame velocity is influenced by the quenching effect of a solid surface (8). However, it can be shown that this effect may be neglected in the analysis. Consider, for example, the flame velocity profile for a laminar flame front traveling through a quiescent isothermal mixture over a solid surface. The reduction of the flame velocity in the region within the quenching distance but above the dead space causes the moving flame front to be curved rearward. Since the flame front travels as a whole and since the displacement, parallel to the surface, of the flame front within the quenching distance is small compared to the length of the flat plate, the flame front can be considered to have the same effect as a plane flame front extending toward the surface to the border of the dead space. The resulting uniform flame velocity profiles are assumed to vanish discontinuously at the border of the dead space. A similar situation exists if the mixture is flowing across the surface and the flame front is fixed relative to the plate. Consequently, the flame velocity can be considered as a function of the local mixture temperature only, and the inhibiting effect of quenching above the dead space can be neglected. The latter assumption greatly simplifies the solution of the theoretical analysis.

For the illustrative solution, the variation of flame velocity with mixture temperature for a stoichiometric propane-air mixture is required. Experimental data from Dugger (11, 12) are plotted in Fig. 4. Since both sets of flame velocity data coincide up to a temperature of 600 K, it is reasonable to assume that the curve for the maximum flame velocity adequately represents the flame velocity variation for an equivalence ratio of unity in the range of 600 to 1000 K. This relation is the second graphical function which is required for the proposed solution

### Dead Space

The third function required for the proposed analysis is the relation between the depth of the dead space and the plate surface temperature. Values for the dead space distance for various surface temperatures are best obtained from experimental measurements. The dead space distance is closely related to the quenching distance, and, according to Lewis and von Elbe (8) and Wohl et al. (13), the dead space depth should be about one half of the quenching distance. Moreover, it has been shown by Friedman and Johnston (16) that the composition of the quenching surface has no measurable effect. Because in this study the quenching distance above a single flat plate is required, the values of quenching distance as commonly measured between parallel plates are halved, and hence the dead space distance above a single surface is approximately one fourth of the quenching distance for parallel plates.

When experimental data are lacking or available data must be extrapolated to a higher range of temperature, semitheoretical or empirical equations may be used. Potter and Berlad (14, 15) have derived equations for the flame quenching distance $d$ in terms of the temperature. Their empirical equation reads

$$s_o d = 1.206 \times 10^{-5} T_o T_f \text{ cm}^2/\text{sec}$$

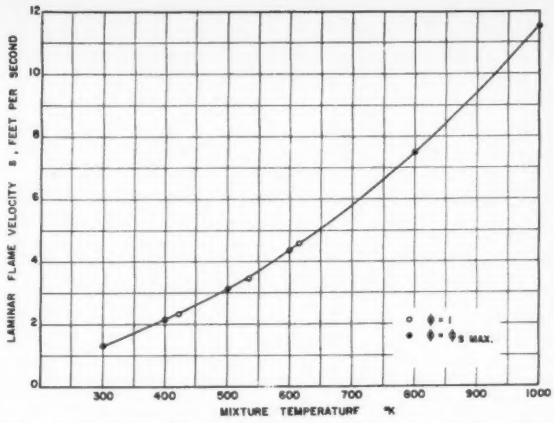


Fig. 4 Variation of laminar flame velocity with mixture temperature for propane and air

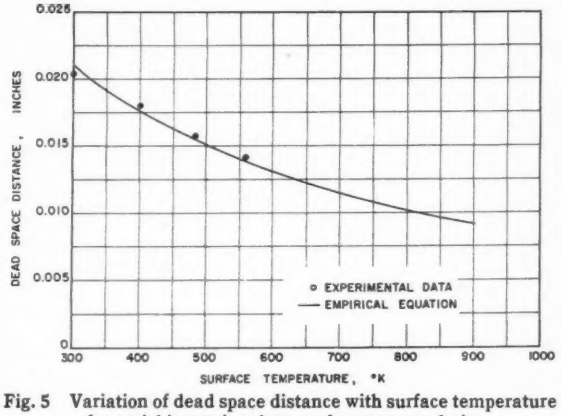


Fig. 5 Variation of dead space distance with surface temperature for stoichiometric mixture of propane and air

where

$s_o$ = burning velocity
$T_o$ = mixture temperature and also the surface temperature
$T_f$ = adiabatic flame temperature

The equation applies to stoichiometric hydrocarbon-oxygen-nitrogen flames at one atmosphere pressure. Since burning velocities are generally known for a wide range of temperatures, the quenching distances may be calculated for intermediate and high temperature surfaces.

For the problem under consideration, the variation of the dead space distance with surface temperature for a stoichiometric propane-air mixture is required. Such a relation may be partially derived from the experimental values of quenching distance for a stoichiometric propane-air mixture reported by Friedman and Johnston (16). The dead space distance, however, must be known for temperatures considerably above the range tested by Friedman and Johnston. Therefore, Potter and Berlad's expression for quenching distance based on the burning velocity is used to obtain the dead space distance in the range of surface temperatures from 560 to 1000 K. This is shown in Fig. 5. This curve is the third graphical function required for the graphical solution.

The basic graphical functions have been developed and the graphical solution may now be obtained. The next step of the solution is to determine the locus of equal fluid velocity and flame velocity. The boundary layer fluid temperature profiles have been plotted in Fig. 3, and since the relation between the fluid temperature and the laminar flame velocity is known from Fig. 4, a flame velocity profile can be con-

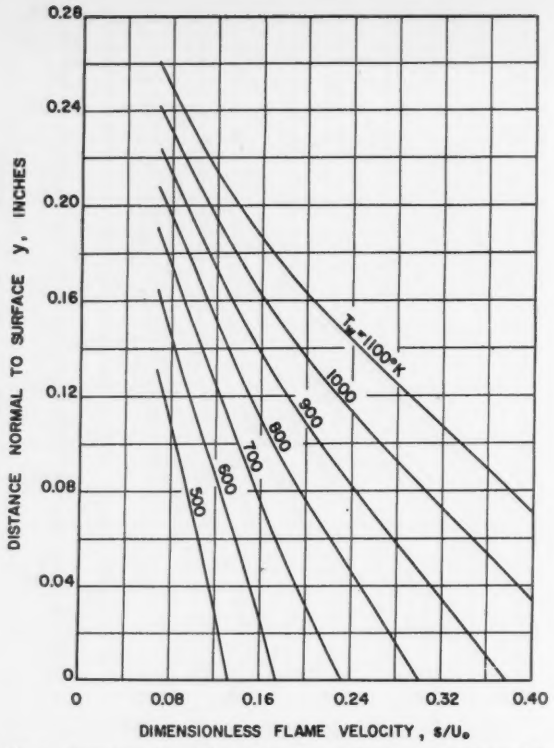


Fig. 6 Boundary layer flame velocity profiles for a stoichiometric propane-air mixture and for a flat plate of uniform temperature, $\tau = 0.050$ sec, $U_o = 25$ ft/sec

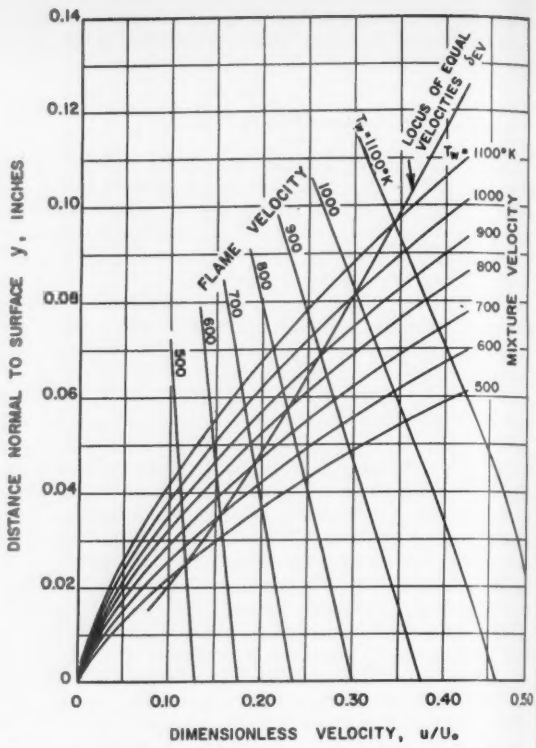


Fig. 7 Superposition of mixture velocity and flame velocity profiles, $\tau = 0.050$ sec, $U_o = 25$ ft/sec

structed, corresponding to each particular fluid temperature profile. In other words, at every point in the fluid boundary layer, the local fluid temperature defines a corresponding local flame velocity. A plot of typical flame velocity profiles is shown in Fig. 6.

After the flame velocity profiles throughout the boundary layer are known, each is superimposed graphically upon the corresponding fluid velocity profile. The intersection of the two profiles defines the point of equal velocities. This is shown in Fig. 7 for one particular value of $\tau$. However, similar curves for the other values of $\tau$ must be constructed so that the locus of equal velocities throughout the boundary layer can be determined. When this has been done for a sufficient number of points to define a curve, the resulting curve is plotted, as in Fig. 8, and the graphical relation between the dead space depth and the surface temperature is superimposed. The intersection of the locus of equal velocities for each value of $T_w$ with the curve of the dead space distance, represents the location in the boundary layer where conditions are satisfactory for a flame front to become stabilized.

The resulting performance map, defined by the graphical solution, is plotted in Fig. 9 for two mixture velocities.

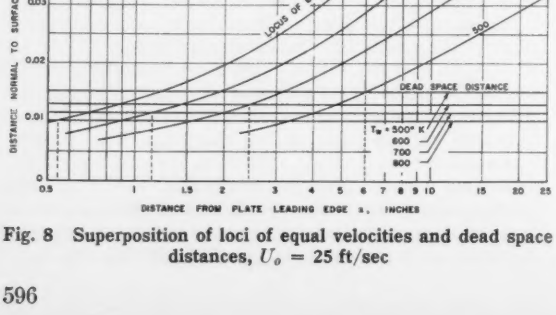


Fig. 8 Superposition of loci of equal velocities and dead space distances, $U_o = 25$ ft/sec

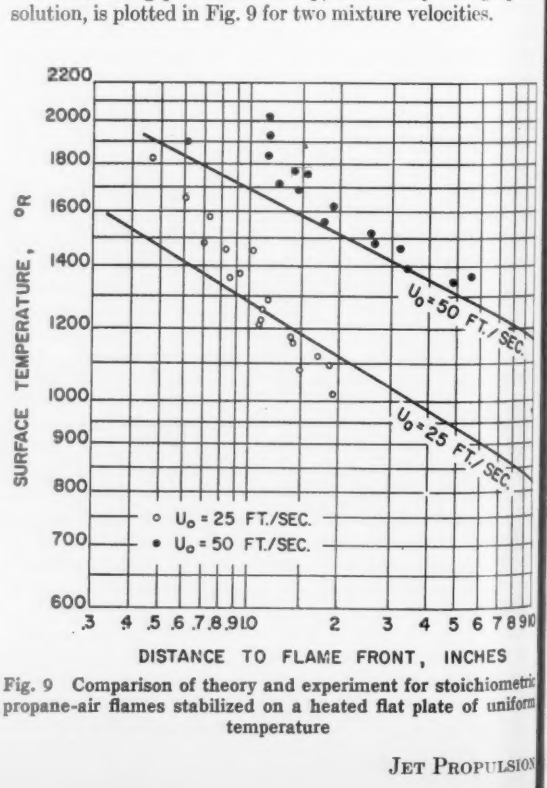


Fig. 9 Comparison of theory and experiment for stoichiometric propane-air flames stabilized on a heated flat plate of uniform temperature

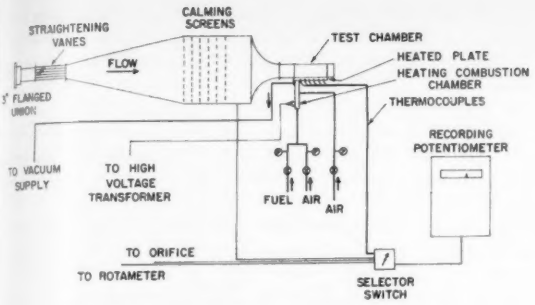


Fig. 10 Schematic diagram of test apparatus

## Experimental Work

In order to verify the solution of the graphical analysis, the stabilization of propane-air flames in the boundary layer of a heated flat plate was investigated experimentally. All the experimental data were obtained for constant mixture approach velocities of 25 and 50 ft per sec and for a range of plate temperatures from 1000 to 2000 R. The flame stabilization performance was measured as the variation of the distance from the flat plate leading edge to the stabilized flame front with change in the plate temperature for a constant mixture velocity. The experimental results for stoichiometric propane-air mixtures are plotted in Fig. 9, and superimposed upon the theoretical performance curves predicted by the graphical analysis.

The experimental apparatus was designed to provide a heated flat plate with a uniform temperature distribution upon which premixed propane-air flames could be stabilized. A description of the experimental equipment and procedure follows.

### Equipment

The experimental investigation was performed in a $2^1/_2$ by $2^1/_2$ in. cross-sectional test chamber. A schematic diagram of the test equipment is shown in Fig. 10. The test chamber, shown in Fig. 11, had vertical glass walls of Vycor plate glass, making it possible to observe the combustion process in the chamber. The horizontal chamber floor consisted of a heated plate of 5 in. length, upon which the flames were stabilized. The heated section of the floor of the test chamber simulated a flat plate in a semi-infinite flow field.

The heated plate was made from $\frac{1}{4}$ in. thick stainless steel. Heat transfer fins were formed on the bottom side by milling diagonal grooves to a depth of $\frac{1}{8}$ in., and the plate was heated by passing hot gases along the underside. The hot gases were obtained by the combustion of premixed propane and air in an auxilliary vertical combustor mounted below the test chamber. A horizontal rectangular duct carried the hot gases along the bottom of the heated plate parallel to the direction of the mixture flow in the test chamber. Control of the hot gas temperature was obtained by regulation of the propane and primary air flow rates and by the addition and regulation of secondary air.

The boundary layer profile of a flat plate was obtained by removing the boundary layer previously formed on the upstream portion of the test chamber floor by applying suction to a transverse slot at the leading edge of the heated plate. The boundary thickness was measured with a probe.

In order to reduce the turbulence level in the test chamber, the propane-air mixture was passed through straightening vanes, a diffuser, six turbulence screens of 200 mesh wire cloth, a calming chamber and then a converging nozzle with a 23 to 1 contraction ratio before entering the test chamber. The free stream turbulence intensity in the test chamber was determined by hot film anemometry and was found to be approximately 0.4 per cent. The mixture was not preheated and was at a temperature of approximately 535 R for all tests. Commercial grade propane having an analysis of 95 per cent to 98 per cent propane with 2 per cent to 5 per cent other saturated hydrocarbons was used in the experimentation. The velocity profiles in the test chamber were found to be flat to within $\frac{1}{8}$ in. from the floor of the chamber at velocities of 26.6 and 50.7 ft per sec. At $\frac{1}{16}$ in. from the surface, the velocity was 95 per cent or greater of the free stream value. The distance from the leading edge of the plate to the flame front was determined photographically by scaling. The photographs were taken with an exposure of $\frac{1}{2}$ sec at f 4.5.

### Test Procedure

The tests of flame stabilization characteristics on a heated flat plate were performed according to the following procedure.

The main air flow rate was first adjusted so that, when the proper amount of fuel was added to the air a predetermined mixture ratio and the desired free stream velocity would occur in the test chamber. The boundary layer suction was initiated and set to the required flow rate for the mixture velocity. The air and fuel for the heating combustion chamber were turned on and ignited by a high voltage spark. The secondary air was then turned on to dilute and reduce the temperature of the combustion gases. The fuel and secondary air were adjusted to give the desired uniform plate temperature. The next steps of the procedure were carried out in rapid succession. The propane was turned on to a predetermined flow rate which would give the desired equivalence ratio. The mixture was then ignited by a high voltage spark jumping between the chamber floor and a stainless steel rod which was positioned just inside the chamber exit. If conditions were favorable for the stabilization of a flame on the heated surface, the flame would travel upstream from the spark rod near the chamber exit to a position on the heated plate. If conditions were not satisfactory for stabilization of a flame on the plate, the flame would be stabilized only by the spark discharge. If the flame became stabilized on the heated plate, (which would occur within a fraction of a second after the igniting spark was turned on) the flame was quickly photographed through the glass walls of the test chamber. The fuel was then shut off, extinguishing the flame. The flames were allowed to remain in the combustion chamber only long enough to be photographed. This procedure prevented the flame from changing the plate temperature appreciably. This test procedure was repeated for a series of tests within a range of plate temperatures of 1010 to 2025 R, for approach mixture velocities of 25 or 50 ft per sec and for various mixture ratios within the stable combustion limits.

The time rate of change of the plate temperature, at a posi-

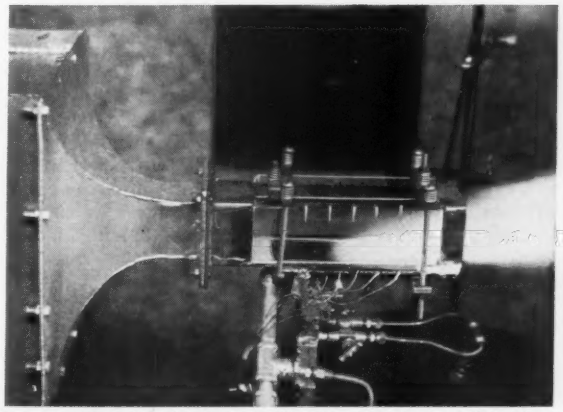

Fig. 11 Test chamber in operation showing flame stabilized on heated flat plate

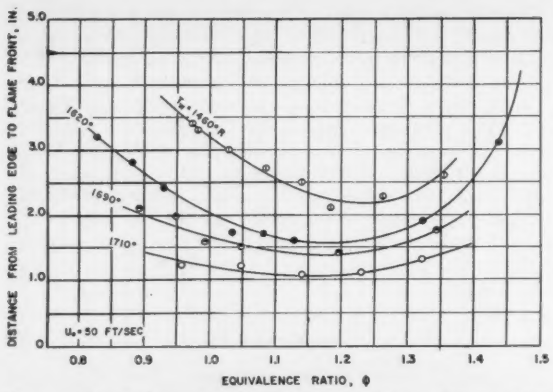


**Fig. 12 Effect of propane-air equivalence ratio on distance from plate leading edge to stabilized flame front**

**Fig. 13 Typical schlieren picture of propane-air flame stabilized on a heated flat plate, $U_o$ = 34 ft/sec, $T_w$ = 1020 F, $\phi$ = 0.902. Flow from left to right**

tion approximately an inch downstream from the flame front, due to the presence of the flame, was found to be of the order of 5 R per sec at a plate temperature of 1460 R. Because the period of time during which combustion occurred in the test chamber was very short namely, about 2 or 3 sec, the plate temperature did not change appreciably during each test.

## Experimental Observations

In addition to obtaining data for the stabilization performance of propane-air flames on the heated plate, the experimental investigation allowed observation of several characteristics of boundary layer flame stabilization. Specifically, it was observed that the position of the stabilized flame on the heated plate was affected by the fuel-air ratio of the flowing mixture. Also, a characteristic oscillation of the stabilized flame front was noted in all the tests.

Although less pronounced at higher plate temperatures, the equivalence ratio of the approach mixture had a considerable effect on the position of the stabilized flame for any given plate temperature and approach velocity. The variation of flame attachment with equivalence ratio is shown in Fig. 12 for free stream velocity of 50 ft per sec. It may be noted that the minima of the curves consistently fall within the range of equivalence ratios of 1.15 to 1.25. This phenomen is in agreement with the experimental results of Gross (2) and Gilbert, Haddock and Metzler (4) in which the maximum blow-off velocities for a given stabilizing surface occurred at equivalence ratios of about 1.25.

The effect of the equivalence ratio can be explained by the facts that the minimum required heated length would tend to occur at equivalence ratios at which the flame velocity is a maximum, and that the flame velocity, according to the experimental work of Dugger (11), peaks at an equivalence ratio of about 1.1. Moreover, the dead space distance derived from the quenching distance measured by Friedman and Johnston (16) exhibits a minimum value at an equivalence ratio of approximately 1.1. Since a shorter heated length is required to stabilize a flame as the quenching distance is reduced, the heated length would tend to be a minimum for a mixture having the minimum quenching distance. In addition, Zukoski (17) has found that for propane-air mixtures under laminar conditions preferential diffusion causes the mixture at the flame interface to be leaner than the free stream. Thus, the mixture in the flame region is actually leaner than the overall equivalence ratio, causing performance to peak at an even richer mixture. All of these factors in turn tend to allow the flame to be stabilized with a minimum heated length with fuel rich mixtures.

Observation of the stabilized flame front showed an oscillatory motion to exist. The flame front appeared as a blur to the eye, but the downstream position was somewhat more discernible, because here the flame front momentarily stopped before reversing the direction of travel. Such oscillation of the flame front is characteristic of boundary layer flame stabilization and had already been observed by Dooley and by Gross. Dooley reported that the oscillation is more pronounced if the heated surface has a slightly negative temperature gradient, i.e., the temperature decreases downstream along the body. In the experiments described in this paper, it was observed that flames stabilized on the portion of the plate having a small positive temperature gradient were stable and exhibited little oscillation.

In an attempt to gain an insight into this oscillatory phenomenon, high speed schlieren motion pictures were taken, and frame by frame analysis of the film was made. For a free stream velocity of 32 ft per sec and an equivalence ratio of 0.902, the frequency of individual cycles varied from 14 to 30 cycles per sec and appeared to be a random variation. The amplitude of the oscillation varied from $\frac{1}{2}$ in. to 2 in. and did not seem to correlate in any way with the frequency of the cycle. The ratio of the average upstream velocity of the flame front to the average of the downstream velocity of the flame front varied from 0.5 to 2.0 and did not seem to be influenced by the frequency. The magnitude of this ratio appeared to be random within the extremes. These observations are in disagreement with those of Gross who reported the upstream movement of the flame front to be four times as fast as the downstream motion.

The proposed model for boundary layer flame stabilization may be used as a basis to hypothesize a cause of the flame oscillations. Since, according to the proposed model, the point of stabilization is defined by the intersection of two curves, with very nearly equal slopes at the point of intersection, it is probable that the oscillation is a hunting motion of the flame tip moving along the boundary layer in a range where approximate conditions for the stabilization of the flame exist. If the stabilizing surface has a negative temperature gradient, the curves intersect at a greater angle. Physically, this means that the conditions necessary for the stabilization of a flame are more localized and definite. This should reduce the distance along which conditions may be favorable for the flame and reduce the flame oscillation. This effect is in agreement with experimental observations by Dooley.

Also it was observed that the rate of flame spreading across the test chamber was low. This would be expected, since there is no obstruction in the stream to generate turbulence as does a bluff body flameholder. The flame spreading results from essentially laminar flame propagation into the free stream from the flame tip stabilized in the boundary layer. This is indicated by high speed flash schlieren pictures, of which Fig. 13 is typical. The flash duration was approximately 7 microsec. Viewing the slightly wrinkled flame sheet from the side causes it to appear on the photograph as a cluster of lines. The boundary layer suction slot is located at the left edge of the photograph.

Under laminar conditions, the travel of the flame into the unburned mixture is relatively slow. However, in most practical applications of flame stabilization in high speed streams, the turbulence of the approach mixture would cause the rate of flame propagation across the combustion chamber to increase. On the other hand, the rapid flame spreading associated with bluff body flameholders would not normally be attained with boundary layer flame stabilization.


### Acknowledgments

These studies were made possible by the generous aid of the General Electric Company, Aircraft Gas Turbine Division. The authors appreciate the assistance of the Armour Research Foundation and the Technological Institute of Northwestern University. Special thanks are extended the members of the Gas Dynamics Laboratory and the staff of the Mechanical Engineering Department.


### References


1 Tsien, H., "Instruction and Research at the Daniel and Florence Guggenheim Jet Propulsion Center," JET PROPULSION, no. 81, June 1950, p. 62.

2 Gross, R. A., "Boundary Layer Flame Stabilization," JET PROPULSION, vol. 25, no. 6, June 1955, p. 288.

3 Dooley, D. A., California Institute of Technology Ph.D. Dissertation, Aug. 1956.

4 Gilbert, M., Haddock, G. and Metzler, A., "A Study of Combustion in a Flowing Gas," NACA TN 1037, 1946.

5 Hottel, H. C., Toong, T. Y. and Martin, J. J., "Flame Stabilization in a Boundary Layer," JET PROPULSION, vol. 27, no. 1, Jan. 1957, p. 28.

6 Toong, T. Y., "Ignition and Combustion in a Laminar Boundary Layer Over a Hot Surface," Sixth Symposium (International) on Combustion, New Haven, Conn., Aug. 19–24, 1956.

7 Toong, T. Y., "Flame Stabilization in Boundary Layers," 12th Meeting AGARD Combustion and Propulsion Panel, Washington, D. C., Nov. 18–26, 1957.

8 Lewis, B. and von Elbe, G., "Theory of Ignition, Quenching and Stabilization of Flames of Non-turbulent Gas Mixtures," Third Symposium on Combustion and Flame and Explosion Phenomena, Williams and Wilkins Co., Baltimore, 1949, p. 68.

9 Chapman, D. R. and Rubesin, M. W., "Temperature and Velocity Profiles in the Compressible Laminar Boundary Layer with Arbitrary Distribution of Surface Temperature," *Journal of the Aeronautical Sciences*, vol. 16, no. 9, Sept. 1949, pp. 547–565.

10 Linnett, J. W., "Some Experimental Results Relating to Laminar Flame Propagation," Selected Combustion Problems, AGARD-NATO, Butterworth Scientific Publications, London, 1954, pp. 95–106.

11 Dugger, G. L., "Effect of Initial Mixture Temperature on Flame Speed of Methane-Air, Propane-Air and Ethylene-Air Mixtures," NACA Report 1061, 1952.

12 Dugger, G. L., Weast, R. C. and Heimel, S., "Flame Velocity and Preflame Reaction in Heated Propane-Air Mixtures," *Industrial and Engineering Chemistry*, vol. 47, Jan. 1955, p. 114.

13 Wohl, K., Shore, L., von Rosenberg, H. and Weil, C. W., "Quenching, Flash-Back, Blow-Off—Theory and Experiment," Fourth Symposium (International) on Combustion, Williams and Wilkins Co., Baltimore, 1953, p. 68.

14 Potter, A. E., Jr. and Berlad, A. L., "A Thermal Equation for Flame Quenching," NACA TN 3398, 1955.

15 Potter, A. E., Jr. and Berlad, A. L., "A Relation of Burning Velocity and Quenching Distance," NACA TN 3882, 1956.

16 Friedman, R. and Johnston, W. C., "The Wall-Quenching of Laminar Flames as a Function of Pressure, Temperature, and Air-Fuel Ratio," *Journal of Applied Physics*, vol. 21, no. 8, Aug. 1950, pp. 791–795.

17 Zukoski, E. E., "Flame Stabilization on Bluff Bodies at Low and Intermediate Reynolds Numbers," Jet Propulsion Laboratory, Calif. Institute of Technology, Report no. 20-75, June 1954, pp. 9–12.


# Erosive Burning of a Colloidal Solid Propellant


JEAN A. VANDENKERCKHOVE[1]

Institut d'Aeronautique de l'Université de Bruxelles, Brussels, Belgium



**An attempt is made to obtain a physical understanding of erosive burning of a solid propellant, taking into account the flame structure. At low pressure the burning rate of a double base propellant is entirely determined by the heat transfer within the fizz zone with no heat exchanged from the high temperature flame zone. Therefore it has been assumed that erosive burning is due to the effects of turbulence within the fizz zone, the threshold velocity corresponding to the moment when incipient turbulence reaches the boundary of the fizz zone. By so doing it has been possible to calculate an erosion coefficient in close agreement with the experimental values.**


## Introduction and Basic Assumptions

THE burning rate of a solid propellant is increased by the presence of a flow parallel to the burning surface. The study of experimental data suggests, moreover, that the phenomenon takes place only when the flow mean velocity $U$ is greater than a so-called "threshold velocity" $U_{tv}$. (The existence of the threshold velocity is not clearly established.) In the present paper, an attempt is made to obtain a physical understanding of erosive burning, assuming the existence of the threshold velocity.


Received Jan. 7, 1958.


[1] Assistant. Consultant of the Poudreries Reunies de Belgique.

[2] Numbers in parentheses indicate References at end of paper.

In this problem in which aerodynamics, heat exchanges and chemical kinetics are simultaneously involved, it has been possible to show the influence of various parameters and even, despite numerous drastic assumptions, to find numerical results in accordance with the experimental values. The study of the combustion of a double base propellant is in itself a fairly difficult problem involving very complex theories.

The present paper is restricted to double base propellants burning at low pressure. The numerical values used in the example are the results of elaborate calculations made by Rice and Ginell (1)[2] for the HES. 4016 propellant.

## Basic Assumption in Solid Propellant Combustion

During combustion, the solid is transformed into a gas by chemical reactions (see Geckler (2)). Even if the transformation occurs through the formation of an intermediate liquid phase, there exists a certain position, called the burning surface, where gas is being formed. The mechanism of the solid-phase decomposition is considered by the majority of authors as the rate-controlling step of propellant burning, and the gas is being formed at a rate

$$m = KB \exp\left(-\frac{E}{RT_s}\right) \quad \ldots\ldots\ldots\ldots [1]$$

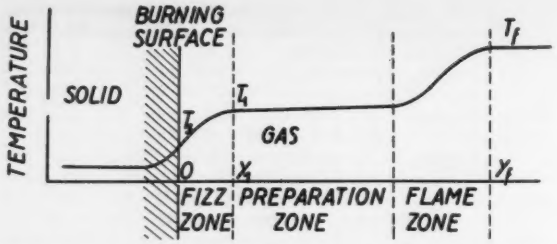


**Fig. 1 Representation of the flame of a double base propellant burning at fairly low pressure**

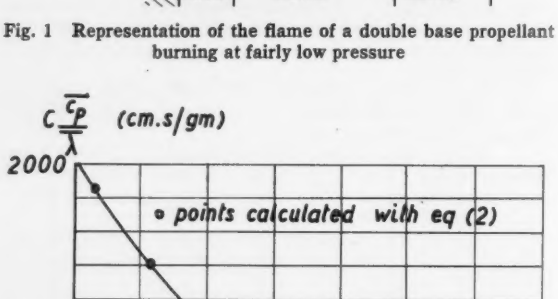


**Fig. 2 Plot of $C\bar{c}_p/\bar{\lambda}$ vs. the thickness $y_1$ of the fizz zone. The values used in calculating this curve correspond to the numerical example in this paper**

where $K$ is a constant, $B$ the frequency factor, $E$ the activation energy, $m$ the mass rate of burning per unit area ($m = r\,\rho_p$), $R$ the universal gas constant and $T_s$ the temperature of the gas at the burning surface.

The reaction occurring in the solid phase would have increased the temperature at the burning surface to a value $T_s'$, but actually a temperature $T_s$ greater than $T_s'$ is obtained there because heat is conducted back to the solid from the gas. The essential theoretical problem, according to this view, is to discover how $T_s$ depends upon the gas phase reactions and behavior.

We have assumed that the problem of combustion without erosion has been satisfactorily solved (see (1, 2)). Therefore the purpose of this study of erosive burning is to establish the influence of a flow parallel to the burning surface on the temperature $T_s$.

Fig. 1 represents a model of the flame of a double base propellant, satisfactory from both the experimental and theoretical points of view. After the solid phase decomposition, the gas phase reactions can be divided in three parts: Close to the burning surface, some exothermic reactions take place in the fizz zone. Then, in the preparation zone, activated products are formed without heat production. Finally, when a sufficient concentration of activated products is achieved, the final reaction occurs in the combustion zone at the end of which the isobaric combustion temperature is obtained.

At pressures between 20 and 80 atm, the thickness of the preparation zone is much greater than the thickness of the other zones, and the heat transfered from the flame zone into the fizz zone can be neglected. Therefore the temperature $T_1$ at the end of the fizz zone is approximately equal to the temperature $T_1'$ obtained without any heat exchange across the preparation zone, and temperature $T_s$ can be calculated considering only the heat exchange across the fizz zone.

This picture is probably fairly accurate when limited to the case of an end-burning strand where the gas flow is laminar and one-dimensional, directed normally away from the burning surface. In the more complex case of an important velocity parallel to the surface, one can raise the question of the validity of this model. We have assumed that the presence of a strong velocity gradient parallel to the burning surface (boundary layer) does not alter the picture appreciably in the laminar sublayer where all transport of heat or chemical species is accomplished by movements on a molecular scale. However, in the turbulent layer where the eddies play an important role in the transport, it is clear that the picture of separate zones does not hold anymore. Meanwhile one can expect that the flame structure still holds in the transition sublayer where turbulence is not yet fully developed and where the dimensions of the eddies are much smaller than the thickness of a zone.

## Conduction Equation Across the Fizz Zone Without Erosion

At a distance $y_1$ from the burning surface, the fizz zone reaction is completed, and therefore the temperature $T_1'$ is achieved if no heat is transferred back from the flame zone. A certain heat release pattern must be assumed in the fizz zone. Following Rice and Ginell (1) it was supposed that the heat evolved in the fizz zone is all released at the same distance $y_1$. Meanwhile provision must be made for diffusion and for distributed heat sources by means of a coefficient $C$. Therefore the equation giving the actual temperature $T_s$ of the burning surface can be written

$$\frac{T_s - T_s'}{T_1' - T_s'} = \exp\left(-mC\frac{\bar{c}_p}{\bar{\lambda}}\,y_1\right) \qquad [2]$$

Where $\bar{c}_p$ is the mean specific heat at constant pressure, and $\bar{\lambda}$ the mean thermal conductivity across the fizz zone, $m$ being the mass burning rate.

For a given propellant the quantities $T_s$, $T_s'$, $T_1'$, $m$, $\bar{c}_p$, $\bar{\lambda}$ and $y_1$ can be computed as functions of one independent variable, the pressure, for instance. Therefore the pressure dependent value of $C$ can be deduced from Equation [2].

Actually it is much simpler to consider as a whole the group $C\bar{c}_p/\bar{\lambda}$, and for our present purpose it is useful to plot that term against $y_1$ from the results obtained by Rice and Ginell for HES. 4016 (see Fig. 2).

## Conduction Equation Across the Fizz Zone With Erosion

In the presence of erosion due to the flow parallel to the burning surface, turbulence takes place in the combustion zone, increasing the thermal conductivity at each point by a factor taking into account the turbulence level at that point. Therefore the rate of heat transfer increases together with the temperature $T_s$ at the burning surface and the mass burning rate $m$, when the thickness of the combustion zone shrinks.

Indicating the values of $T_s$ and $m$ without erosion by $T_{so}$ and $m_o$, Equation [1] can be written

$$\frac{m}{m_o} = \exp\frac{E}{R}\left(\frac{1}{T_{so}} - \frac{1}{T_s}\right) \qquad [3]$$

Within the fizz zone the temperature $T_1'$ is achieved at a point $y_1' < y_1$ where the fizz zone reactions are possibly not yet completed. The conduction equation can be written directly between that point $y_1'$ and the burning surface, across a region in which the flow is still completely laminar

$$\frac{T_s - T_s'}{T_1' - T_s'} = \exp\left[-m_o \exp\frac{E}{R}\left(\frac{1}{T_{so}} - \frac{1}{T_s}\right) C\frac{\bar{c}_p}{\bar{\lambda}}\,y_1'\right] \qquad [4]$$

From Equation [4] the value of $T_s$ and consequently of $m/m_o$ can be obtained for each value of $y_1' < y_1$ if the proper value of $C$ or $C\,\bar{c}_p/\bar{\lambda}$ is used.

Equation [4] is valid in the laminar sublayer, since the presence of a velocity gradient perpendicular to the burning surface can hardly be expected to have a significant influence on the temperature distribution. That assumption is corroborated by the fact that no variation of the temperature distribution (no erosion) seems to exist below the threshold velocity, which can be viewed as the velocity at which the incipient turbulence penetrates into the fizz zone.

A difficulty arises with the choice of the proper value of $C\,\bar{c}_p/\bar{\lambda}$ to be used in the laminar sublayer between the burning surface and $y_1'$ if the outer part of the fizz zone is in this turbulent region. The value of $C\,\bar{c}_p/\bar{\lambda}$ taken at the point $y_1$ without erosion would be too small and would not account for the increase in the temperature level and for the associated shrinkage of the fizz zone. It therefore seems reasonable to use the value of $C\,\bar{c}_p/\bar{\lambda}$ corresponding to $y_1'$ in Fig. 2. That assumption is probably fairly accurate just above the threshold velocity but may be questionable at much higher velocity.

## Relation Between $y_1'$ and $U$

The dependence of the erosion ratio $m/m_o$ upon the distance $y_1'$ at which the temperature $T_1'$ is achieved, for a given pressure, will be of little help without a relation between that distance $y_1'$ and the mean flow velocity $U$ parallel to the burning surface.

The present study will be restricted to circular channels of radius $r$. The flow pattern across the channel can be expected to be somewhat similar to the flow inside a tube where the thickness of the laminar sublayer close to the wall decreases when $U$ increases. Moreover, above the threshold velocity for which the Reynolds number of the flow is well above the one corresponding to the transition, it seems reasonable to assume that, despite the presence of the flame, the flow pattern quantitatively follows the well-known relation giving the mean flow velocity $U$ in terms of the so-called friction velocity $u_x$ (rough pipe)

$$U = u_x \left( 1.75 + 5.75 \log_{10} \frac{r\,u_x}{\nu} \right) \qquad [5]$$

where $\nu = \mu/\rho$ is the cinematic viscosity.

That approximation has also been used by Corner (3) and may be explained by the fact that, near the threshold velocity $U_{tv}$, the velocity perpendicular to the burning surface represents only 2 or 3 per cent of the mean flow velocity $U$. On the other hand, in the laminar sublayer, the flow pattern is entirely determined by the viscous stresses. Therefore, neglecting the velocity component perpendicular to the burning surface, it can be written, by analogy with the classical flow in a tube

$$y^* = \frac{u_x y}{\nu} \qquad [6]$$

where $y^*$ is the so-called friction distance parameter and $y$ the distance from the burning surface. Equation [6] defines the laminar sublayer up to a critical value of the friction distance parameter $y_{cr}^*$ which is characteristic of the problem and represents the point where incipient turbulence appears. Above that limit, an increase in heat transfer is observed due to turbulence.

A normal approach will therefore be to work out completely the problem again with a variable thermal conductivity at each point $y$, taking into account the turbulence level related to the value of the mean flow velocity $U$. Such a method would lead to very elaborate calculations, as has been recognized by Geckler. We have tried to simplify the problem by assuming that erosive burning is only related to the flow behavior inside the fizz zone. It is obvious that such an approach is valid only when, without erosion, the heat flux reaching the fizz zone from the flame zone is negligible (approximately below 80 kg/cm²).

Moreover, we have supposed, as a working assumption, that inside the fizz zone, the temperature $T_1'$ is obtained at the limit of the laminar sublayer defined by the critical value $y_{cr}^*$ of the friction distance parameter. In the neighborhood of the threshold velocity, the increase of the temperature level of the fizz zone is fairly small ($T_1' \simeq T_1$), and turbulence is not yet fully developed at the beginning of the preparation zone. The influence of the turbulence is not only to increase the thermal conductivity by transporting hot gases toward the burning surface. Hitherto unreacted products are also transported back in the process in such a manner that they will react closer to the surface. Our working assumption seems to be a fair approximation, close to the threshold velocity.

In the theory of flow in tubes, the critical value of the friction distance parameter is about 5, but in the present case a lower value can be expected due to the flow perpendicular to the burning surface and to the strong temperature gradient. Therefore Equation [6] can be written

$$y_{cr}^* = \frac{u_x y_1'}{\nu} \qquad [7]$$

where $y_1'$ is the distance at which we have assumed that the temperature $T_1'$ is achieved.

The three unknowns to be determined are $U$, $u_x$ and $y_{cr}^*$, and it is therefore necessary, in addition to Equations [5, 7], to find a third condition. The use of the experimental value of $U_{tv}$ corresponding to $y_1' = y_1$ gives that third condition and allows the computation of $y_{cr}^*$. As expected, in the following example, we found $y_{cr}^* = 2.85 < 5$.

## Computation of the Erosive Constant $k_u$

We are now in a position to compute the erosive constant $k_u$ defined, for $U$ greater than $U_{tv}$, by

$$\frac{m}{m_o} = 1 + k_u(U - U_{tv}) \qquad [8]$$

Consistent with the experimental data, the value of $k_u$ will be slightly dependent upon the value of the term $(U - U_{tv})$ with its maximum when $(U - U_{tv})$ is approaching zero.

The sequence of the computation is the following:

1 For different values of $y_1' < y_1$, compute from Equations [3 and 4] the corresponding values of the mass burning ratio $m/m_o$, using the value of $C\,\bar{c}_p/\bar{\lambda}$ corresponding to $y_1'$.

2 For a given value of $U_{tv}$ known from experiments, compute from Equations [6 and 7] for $y_1' = y_1$ the corresponding value of $u_x$ and of the critical distance parameter $y_{cr}^*$.

3 Use that critical value in the same equation for the computation of the $u_x$ and of the $U$ corresponding to various $y_1'$ smaller than $y_1$.

4 Finally from Equation [8] compute the values of the erosion coefficient $k_u$.

## Numerical Example

From Rice and Ginell the characteristics of the HES. 4016 propellant can be summarized

$T_s' = 700$ K
$T_1' = 1400$ K
$E/R = 8000$ K
$\nu = 7.05/p$ cm²/sec ($p$ is the pressure given in atm)

The results of these computations in the fizz zone are given in the first four columns of Table 1. We have also indicated the corresponding values of $C\bar{c}_p/\bar{\lambda}$ calculated from

Equation [2] from which Fig. 2 has been established. (The calculations are quite sensitive to the way these three points have been connected graphically.) The values of $C\bar{c}_p/\bar{\lambda}$ are in fairly good accord with the value of $\bar{c}_p/\bar{\lambda} = 1140$ cm sec/gm estimated separately. See Table 1.

**Table 1**

| $p$ atm | $T_s$ K | $m_o$ gm/cm² sec | $y_1$ cm | $C\,\bar{c}_p/\bar{\lambda}$ cm sec/gm |
|---|---|---|---|---|
| 42 | 770 | 0.42 | 0.0063 | 455 |
| 22 | 840 | 1.01 | 0.00114 | 1400 |
| 82 | 910 | 2.10 | 0.00031 | 1850 |

Let us now compute the erosion coefficients $k_u$ vs. $U$ for the pressure of 22 atm assuming, in accordance with experimental results mentioned by Wimpress (4) and Green (5) for J.P.N. Ballistite, that $U_{tv} = 180$ m/sec. (J.P.N. is a propellant similar to HES. 4016.) We took $r = 1.45$ cm (where $r$ = radius of the port area). See Table 2.

**Table 2**

| $y_1'$ cm | $C\bar{c}_p/\bar{\lambda}$ cm sec/gm | $T_s$ K | $m/m_o$ | $u_x$ cm/sec | $U$ m/sec | $k_u$ sec/m |
|---|---|---|---|---|---|---|
| 0.0010 | 1468 | 845.3 | 1.062 | 912 | 205.3 | 0.00245 |
| 0.0008 | 1570 | 855.5 | 1.188 | 1140 | 263.5 | 0.00225 |
| 0.0006 | 1680 | 870.0 | 1.390 | 1520 | 362.0 | 0.00214 |

The curve $m/m_o$ vs. $U$ is given in Fig. 3. It corresponds fairly well with the experimental curve given by Wimpress and Green for J.P.N. (5). These authors have found $k_u = 0.00219$ sec/m just above the threshold velocity. The correlation given by Geckler (2) and based on Green's data, gives $k_u = 0.00163$ sec/m.

At greater pressure (82 atm) we have found, using the same value of the threshold velocity, a slightly greater erosion coefficient (about 0.003 sec/m). Such an increase seems to be in accordance with the data given by Green. The study of the experimental and theoretical results suggests also an influence of the pressure and possibly of the radius of the port area upon the value of threshold velocity $U_{tv}$, but the problem is not yet sufficiently advanced to allow definite conclusions to be drawn.

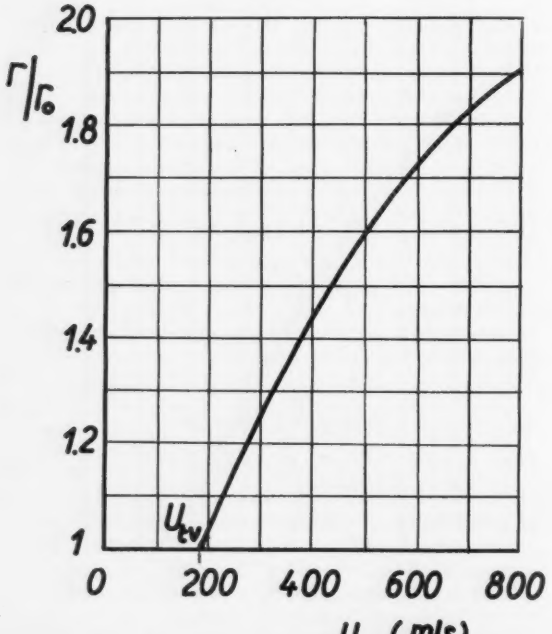


**Fig. 3 Erosion ratio $r/r_0$ vs. mean flow velocity $U$**

## Conclusions

Despite numerous drastic assumptions, the quantitative results obtained are in fairly good agreement with the experimental data. Although some of the assumptions may be questionable, the physical picture of the erosive process taking into account the various zones of the flame represents a frontal attack upon a highly complex problem. The proposed method provides a physical explanation of the computations made by Corner (3) who has assumed that the heat exchanges inside the flame zone can be characterized by the particular value of the thermal conductivity at the end of the fizz zone. (See also Geckler (2).) However Corner does not take into account the possible existence of the threshold velocity and assumes that the rate-controlling process of the combustion is in the gas phase.

Lenoir and Robillard (6) have also studied the problem of erosion neglecting the threshold velocity but assuming that the rate-controlling process of the combustion is the solid phase decomposition. According to them, the erosion is due solely to the convective heat transfer between the burning surface and the mean flow, and is governed by the same equations as a normal heat transfer problem including transpiration from the walls (as a matter of fact our method may be somewhat improved by the use of the boundary layer equations with transpiration). In our opinion such an approach is oversimplified since the temperature gradients, close to the burning surface, are mainly imposed by the chemical reactions inside the flame, the flow pattern having only a second order influence. Moreover their good numerical agreement has been obtained by matching the equations with the experimental data in order to determine the values of the constants involved.

A last attempt to study the erosive combustion has been made by Tavernier and Boisson (7). Their theoretical treatment assumes that the rate-controlling process of the combustion is in the gas phase and is therefore in opposition to the theory generally accepted.

Meanwhile they have found an erosion coefficient about twice greater than the one obtained by Green with a similar propellant. In our opinion, that interesting discrepancy can be explained by the experimental technique used. While Green measured the erosion of the main propellant grain in the chamber, Tavernier and Boisson used two grains, the main grain supplying the flow and the test sample on which erosion is measured being situated at the entrance of the nozzle and therefore being subjected to a higher turbulence.

By assuming that the erosion is normally due to a process entirely localized in the fizz zone, our study enables one to understand why the presence of instabilities can determine burning rates much higher than those that can normally be expected due to erosion alone. Indeed, with an abnormal degree of turbulence, hot products from the flame zone may reach the fizz zone, correspondingly increasing the burning rate. That explanation is supported by the fact that, in a liquid propellant rocket, the temperature of the walls is strongly increased by instabilities (see (8)).

The present theory is limited to double base propellants burning at fairly low pressures because we have been able only in that case to carry out quantitative calculations. Meanwhile, the fact that, after the disappearance of the dark layer of the flame, the pressure dependent burning rate law remains unchanged up to a much higher pressure suggests that the heat transfer toward the fizz zone remains small.

Therefore our method may possibly still hold above 80 atm.

On the other hand, proposed theories for composite propellant burning also allow for the decomposition of the flame into separate zones, and possibly the treatment may also be extended in that case if suitable characteristics of the different zones can be obtained.

### References


1 Rice, O. K. and Ginell, R., "Theory of Burning of Double-Base Rocket Powders," *Journal of Physical Chemistry*, vol. 54, 1950, pp. 885–917.

2 Geckler, R. D., "The Mechanism of Combustion of Solid Propellants," Selected Combustion Problems, Combustion Colloquium, Cambridge University, England, Butterworths Scientific Publications, 1954.

3 Corner, L., "Theory of the Interior Ballistics of Guns," Wiley, 1950.

4 Wimpress, R. N., "Internal Ballistics of Solid Fuel Rockets," McGraw-Hill, New York, 1950.

5 Green, L., "Erosive Burning of Some Composite Propellants," JET PROPULSION, vol. 24, Jan.-Feb. 1954, pp. 9–15.

6 Lenoir, J. M. and Robillard, G., "A Mathematical Method to Predict the Effects of Erosive Burning in Solid Propellant Rockets," Sixth Symposium on Combustion, Reinhold, 1957, pp. 663–667.

7 Tavernier, P. and Boisson, J., "Combustion Erosive des Poudres Colloidales," Laboratoire de Balistique de Sevran France (unpublished).

8 Ross, C. C. and Datner, P. P., "Combustion Instability in Liquid Propellant Rocket Motors," Selected Combustion Problems, AGARD, Butterworths Scientific Publications, 1954.


# Supersonic Aerodynamic Experiments Using Very High Temperature Air Wind Tunnels[1]


D. E. BLOXSOM Jr.[2]

Rhodes and Bloxsom, Canoga Park, Calif.



**Air at temperatures up to 9000 K and pressures to 40,000 psi has been expanded in a deLaval supersonic nozzle. Experimental measurements of the air pressure indicated that the air was substantially in equilibrium during the entire isentropic expansion. After the supersonic jet was expanded to one atmosphere ambient pressure, flow patterns around various models were studied as to self luminosity of the flow, equilibrium state of the air, drag coefficients, and laminar flow stagnation heat transfer coefficients. The experimental drag and heat transfer coefficients agreed with commonly accepted theories in the field. Heat power inputs up to 363,000 w/cm² in the nozzle throat produced varying amounts of erosion of the throat material. This erosion is presented with the corresponding wall vaporization theory.**


### Nomenclature

$a$ = speed of sound, cm/sec
$\alpha$ = acceleration, cm/sec²
$A$ = surface area, cm²
$C_v$ = gas specific heat at constant volume
$C_D$ = drag coefficient
$C_w$ = specific heat of solid wall, joules/gm K
$C_L$ = specific heat of liquid wall material, joules/gm K
$d^*$ = diameter of sonic flow throat, cm
$d_s$ = shock detachment distance, cm
$F$ = force, dynes
$\Delta H$ = gas enthalpy difference between stagnation and wall conditions, joules/gm
$K_H$ = Stanton number
$m$ = mass, gm
$m_w$ = mass of wall material, gm
$\mu$ = gas viscosity, poise
$Q$ = heat, joules
$Q_m$ = latent heat of melting of wall, joules/gm K
$Q_v$ = latent heat of vaporization of wall, joules/gm K
$\dot{q}_e$ = equilibrium heat transfer coefficient, w/cm²
$\bar{\dot{q}}_e$ = average equilibrium heat transfer coefficient, w/cm²
$\dot{q}_{BB}$ = black body heat transfer coefficient, w/cm²
$\dot{q}_{SF}$ = forced convection heat transfer coefficient, w/cm²
$\bar{\dot{q}}_{ne}$ = nonequilibrium heat transfer coefficient, w/cm²
$R$ = sphere radius, cm
$R_o$ = gas constant
$Re$ = Reynolds number based on throat diameter
$\rho$ = density, gm/cm³
$\rho_w$ = wall density, gm/cm³
$S$ = displacement, cm
$T$ = temperature, K
$T_w$ = initial wall temperature, K
$T_m$ = melting temperature of wall, K
$T_v$ = vaporization temperature of wall, K
$t$ = time, sec
$u$ = velocity, cm/sec
$y$ = erosion distance, cm

subscript $w$ refers to wall conditions
superscript * refers to sonic flow conditions


Received Feb. 12, 1958.


[1] This work was performed by Aro, Inc. at the Arnold Engineering Development Center for the USAF. The opinions expressed here are the author's and do not necessarily represent the views of the USAF and Aro, Inc.

[2] Partner.

### Introduction

AERONAUTICAL and astronautical engineers at present need to measure aerodynamic parameters at elevated temperatures. These air temperatures are produced by high velocity flight in the earth's atmosphere. This high stagnation air temperature is plotted against flight Mach number in the isothermal stratosphere in Fig. 1. This figure was computed with the aid of the real gas air equation of state (1).[3] Fig. 1 shows that temperatures up to 10,000 K will be encountered at earth satellite velocities. In addition to the high temperature requirement, high stagnation pressure is required for wind tunnel operation due to the high total pressure drop encountered in very high Mach number steady flow isentropic air expansions. In order to meet these requirements, a method of heating air by means of condenser electrical sparks was developed by the United States Air Force at the Arnold Engineering Development Center (AEDC) at Tullahoma,

[3] Numbers in parentheses indicate References at end of paper.

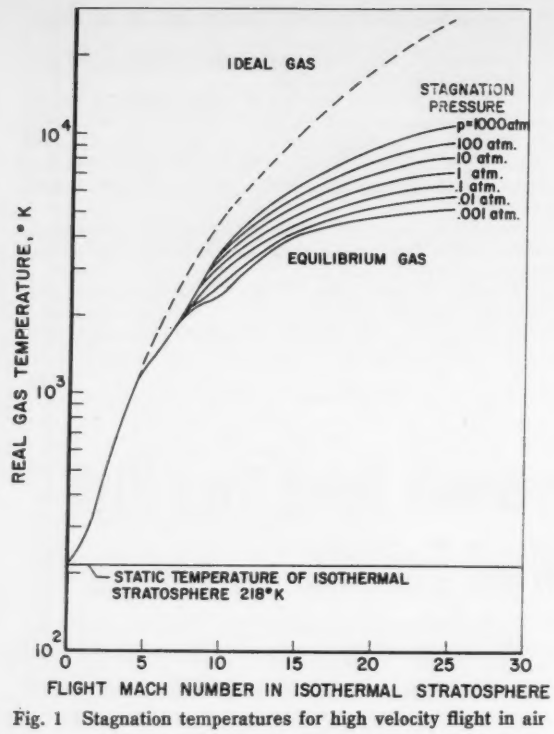


Fig. 1 Stagnation temperatures for high velocity flight in air

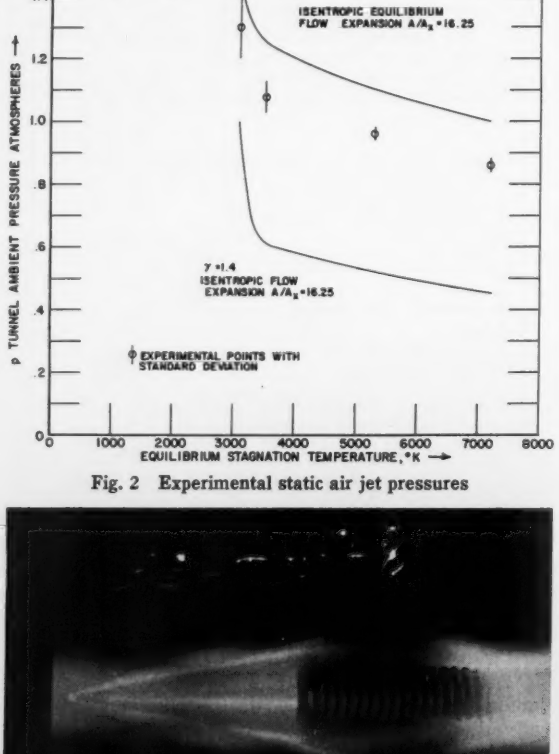
ISENTROPIC EQUILIBRIUM FLOW EXPANSION A/A* =16.25
γ =1.4 ISENTROPIC FLOW EXPANSION A/A* =16.25
EXPERIMENTAL POINTS WITH STANDARD DEVIATION
p TUNNEL AMBIENT PRESSURE ATMOSPHERES
EQUILIBRIUM STAGNATION TEMPERATURE, °K

Fig. 2 Experimental static air jet pressures



Fig. 3. Direct luminosity photograph of 20 deg steel cone in Mach number 4 flow

Tenn. This technique is described in (2) which includes the technique of operation and impurity level experimentally obtained. Bomb 2, described in (2), enabled air heating to 5000 psi and 7200 K. Bomb 3, also described in (2), enabled air heating to 40,000 psi and 9000 K. The nozzles used for supersonic flow production opened out of the bombs.

## Supersonic Nozzle Air Expansion

These experiments were performed in bomb 2 (2).

The sudden rise of air pressure in the stagnation chamber of the wind tunnel blows a thin diaphragm at the wind tunnel throat. The air then rushes through the nozzle and starts the wind tunnel. The experimental tunnel starting times with a back pressure of 0.97 atmosphere and an area ratio of 16.2 were measured with a 14,000 frames/sec Fastax camera. The start of the heating pulse could be easily seen on the film, and the fully started flow appeared about 130 microsec later. The testing described below occurred in the next 500 microsec following the tunnel opening. The stagnation pressure dropped less than 10 per cent of maximum pressure in the testing time (2).

The static jet pressure was measured by inspection of the first few frames showing the jet. The area ratio of the nozzle is chosen so that the static jet pressure is close to atmospheric. The jet ambient pressure is usually slightly over the laboratory pressure (0.97 atmosphere), then matched, then slightly under the laboratory pressure as the stagnation pressure drops in bomb 2 as a function of time. The bomb pressure decreases due to heat transfer and mass flow out of the tunnel throat. As little as 2 per cent change in static pressure can be detected in the jet configuration of this hot air near the laboratory pressure matching point. Jet details were easily seen as changes in the self luminosity due to jet expansion waves and shock waves. The outline of the jet was not used in these observations, which were made on the jet interior. The data on this static pressure are given in Fig. 2. If the flow is completely in equilibrium, an isentropic real gas steady flow expansion can be made, using a Mollier chart for air (3). If the gas is completely out of equilibrium, except for the translational and rotational degrees of freedom, an isentropic flow expansion using $\gamma = 1.4$ can be made. Fig. 2 shows that the tunnel flow is almost in equilibrium.

Assuming the flow to be in equilibrium, the tunnel calibration ($\pm 15$ per cent) can be completed. The Mach number is around 4 for these experiments.

## Flow Visualization by Gas Luminosity

The heated gas is quite luminous. There are two types of luminosity. One, very brilliant, always occurs in the first 500 microsec of flow from the tunnel, even when the ambient temperature is less than 1000 K and no luminosity is expected. The second type of luminosity is fairly steady in time, to 20 millisec. For stagnation temperatures of 3000 K, this luminosity first appears in the boundary layer of blunt objects, such



Fig. 4 Direct luminosity photograph of 10 deg wedge in Mach number 4 flow (14,000 frames/sec). Air stagnation temperature: 3500 K. Jet ambient pressure: 1.0 atm

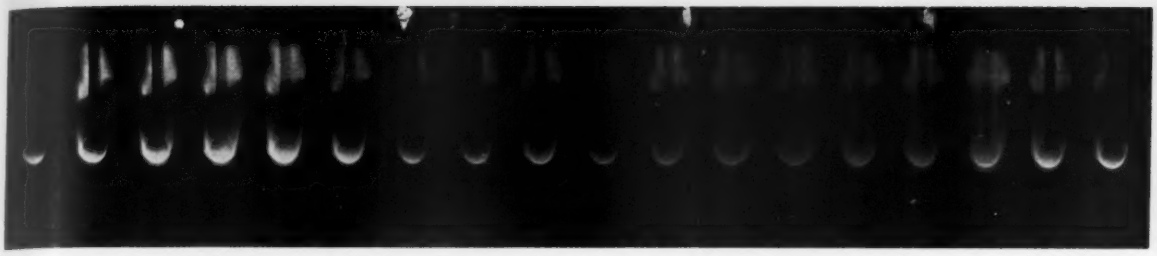

**Fig. 5 Direct luminosity photograph of ¼-in. steel sphere in Mach number 4 flow (14,000 frames/sec)**

as spheres. As the stagnation temperature increases, this luminosity then appears in the shock heated gas on blunt objects (3350 K) and then appears finally in the shock heated gas of slender bodies (to 7200 K). This is probably the true gas luminosity. The first type of transient luminosity is probably due to the dying down of the active nitrogen metastable atomic states excited by the heating spark. Reference (4) shows that the active nitrogen will not affect aerodynamic supersonic flow parameters significantly. Fig. 3 is a remarkably clear time integrated photograph taken in the nitrogen afterglow. Shock waves and expansion waves can be clearly seen around the 20 deg cone.

Shock waves can also be easily seen in Fig. 4, which shows the development of a hot boundary layer on the upper surface of the 10 deg wedge. At low temperatures, this luminosity layer looks like a normal boundary layer. At high temperatures, however, the luminous layer gets very thick. It is not obvious why this luminous layer is so large at high temperatures. The luminous layer decreases in size aft of the wedge due to expansion waves in the jet.

## Equilibrium Studies of Laminar Sphere Flow

When ¼-in. steel spheres were placed in the flow, it was possible to determine shock detachment distances by means of the 14,000 frames/sec Fastax camera. This camera was aimed perpendicular to the jet as is shown in Fig. 8. An f-2 lens permitted reasonable exposures by means of the self luminosity of the flow. Fig. 5 shows such a Fastax camera frame of a sphere at 3550 K stagnation temperature. The shock wave, boundary layer, boundary layer separation and shock detachment distance may be clearly seen. The flow separates on all spheres used in this report at an angle of about 73 deg measured from the stagnation point. This flow separation is characteristic of laminar flow in the boundary layer. Recovered spheres were melted only to this angle, the rest of the sphere being intact. These shock detachment distances are plotted in Fig. 6. That the shock detachment distance would be sensitive to equilibrium state was first suggested by Schwartz and Eckerman (5). Their formula for Mach number 4 for the shock detachment distance is given also in (5), page 170. The values for $C_v/R_o = 3/2$ (monatomic gas) and $C_v/R_o = 5/2$ are plotted in Fig. 6. Two other curves are plotted in Fig. 6. One, entitled "Tunnel Flow in Equilibrium, Sphere Flow Out of Equilibrium" uses the $C_v/R_o$ characteristic of the equilibrium ambient tunnel flow; whereas the curve entitled "Tunnel Flow and Sphere Flow in Equilibrium" uses the value of $C_v/R_o$ characteristic of complete equilibrium sphere flow conditions. The experimental data of Fig. 6 indicate that only translational and rotational degrees of freedom are activated in the sphere flow.

The air equilibrium data discussed in this paper do not disagree with Logan's published data (6). Logan has collected theoretical and experimental relaxation times for dissociation at 1 amagat[4] density for air, oxygen and nitrogen, using shock tube techniques. AVCO Research Laboratory has also reported on air dissociation rates in this temperature region, using radiation shock tube techniques (15). These data are summarized in Fig. 7. The stagnation gas is in equilibrium by the time the pressure is measured (in 100 microsec), since the characteristic gas holding time referenced to 1 amagat density is over 1 millisec. The tunnel gas is marginal in equilibrium, as it has about 16 microsec to achieve equilibrium. The sphere flow is completely out of equilibrium, as it has a characteristic time of only $10^{-8}$ sec to achieve equilibrium. Hence, the experimental equilibrium data of this report are not in conflict with previous theoretical and experimental determinations of the relaxation time of air. In reduction to 1 amagat density, the relaxation times for air were assumed to scale according to the following law

$$t \propto \rho^{-1.5}$$

Data is currently available (15) which indicates the air dissociation density dependence is $\tau \propto \rho^{-0.87}$. The density correction of Fig. 7 is small on the sphere data, however.

## Drag Coefficients of Spheres in Laminar Flow

In order to demonstrate the feasibility of measuring forces in a blowdown tunnel of millisec time duration, a steel sphere ⅛ in. in diameter was mounted ballistically in the tunnel, as shown in Fig. 8. A small wire was used to suspend the sphere in the center of the wind tunnel. While the wind tunnel was running, the sphere moved from position 1 to position 2 in 500 microsec, due to the drag forces on the sphere. Gravitational force during this time was negligible compared with the drag force.

By matching seven displacement points, obtained by the 14,000 frames/sec Fastax camera, with a curve of the type

$$S = ut + \tfrac{1}{2}\alpha t^2$$

is is possible to determine the accelerations to 3 per cent.

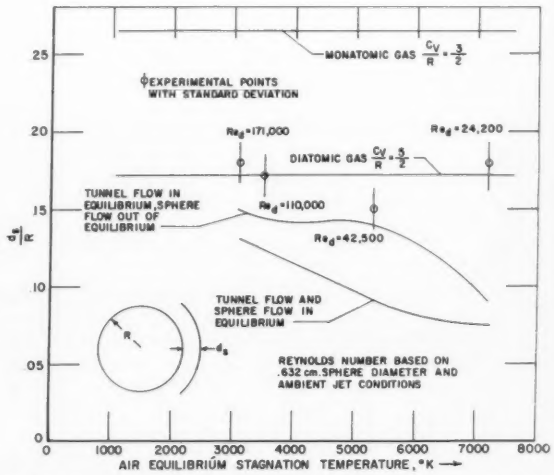


**Fig. 6 Experimental shock detachment distances on ¼-in. steel sphere**

[4] 1 amagat is the density at 300 K and 1 atmosphere pressure.

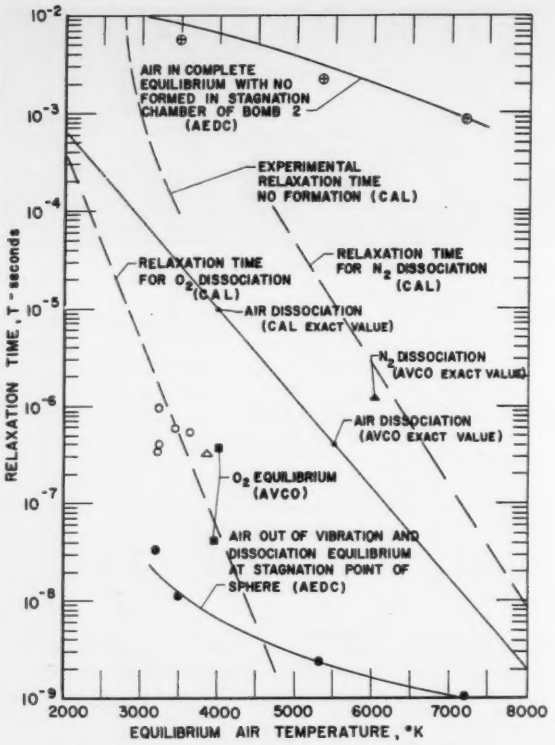
AIR IN COMPLETE EQUILIBRIUM WITH NO FORMED IN STAGNATION CHAMBER OF BOMB 2 (AEDC)
EXPERIMENTAL RELAXATION TIME NO FORMATION (CAL)
RELAXATION TIME FOR $O_2$ DISSOCIATION (CAL)
RELAXATION TIME FOR $N_2$ DISSOCIATION (CAL)
AIR DISSOCIATION (CAL EXACT VALUE)
$N_2$ DISSOCIATION (AVCO EXACT VALUE)
AIR DISSOCIATION (AVCO EXACT VALUE)
$O_2$ EQUILIBRIUM (AVCO)
AIR OUT OF VIBRATION AND DISSOCIATION EQUILIBRIUM AT STAGNATION POINT OF SPHERE (AEDC)
RELAXATION TIME, τ - seconds
EQUILIBRIUM AIR TEMPERATURE, °K
(NOTE: ALL RELAXATION TIMES REFERENCED TO 1 AMAGAT DENSITY)
● ⊕ DATA FROM AEDC AIR △ RESLER, CORNELL, AIR
○ GLICK AND WURSTER, CAL $O_2$ EXACT VALUES

Fig. 7 Experimental relaxation times

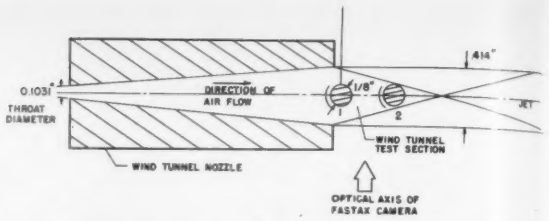


Fig. 8 Wind tunnel nozzle with ballistically slung sphere

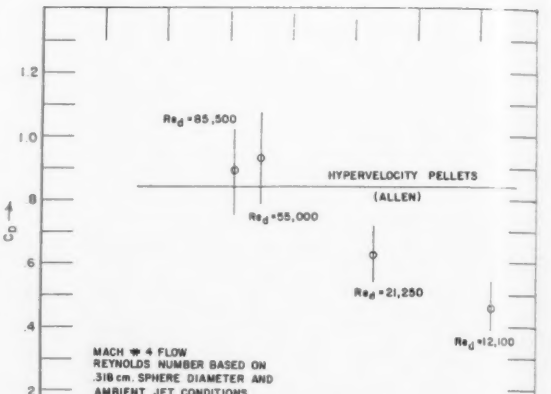
$Re_d$ = 85,500
$Re_d$ = 55,000
$Re_d$ = 21,250
$Re_d$ = 12,100
HYPERVELOCITY PELLETS (ALLEN)
$C_D$
MACH # 4 FLOW
REYNOLDS NUMBER BASED ON .318 cm. SPHERE DIAMETER AND AMBIENT JET CONDITIONS
EXPERIMENTAL DATA WITH STANDARD DEVIATION
AIR STAGNATION TEMPERATURE, °K

Fig. 9 Experimental drag coefficients of spheres

Therefore, the forces are determined to the same accuracy

$$F = m\alpha$$

and with the help of the tunnel calibration, a drag coefficient may be obtained based on the projected sphere area

$$C_D = F/\tfrac{1}{2}\rho u^2 A$$

These drag coefficients, plotted in Fig. 9, are only accurate to 15 per cent due to uncertainties in the tunnel calibration. Fair agreement is obtained with the values of drag coefficients for hypervelocity pellets, in this velocity and Reynolds number range, as given by Allen (7).

Associated with the curve matching technique was an initial velocity about one quarter to one half the final velocity as the sphere left the test section. This means that the starting processes put a force about five to ten times the steady drag force on the sphere for 50 microsec. This ballistic technique looks promising, even at very low drag forces, as nylon models may be used with correspondingly higher accelerations.

The dynamic force $\frac{1}{2}\rho u^2 A$ changed about 48 per cent as the sphere moved in the source flow test section. For greater accuracy an axisymmetric Foelsch (8) type nozzle should be used. This nozzle produces a parallel and uniform jet with suitable hypersonic boundary layer corrections.

## Laminar Flow Heat Transfer Coefficients

One of the most important types of information to come from work on high temperature tunnels is realistic heat transfer coefficients, defined as average heat transferred per unit area per unit time

$$\bar{q}_e = \frac{Q}{At} \frac{\text{w}}{\text{cm}^2}$$

Our method of measuring the heat transfer coefficients experimentally involves the melting of models.[5] This technique has been used successfully at 19 w/cm² (9). We use this technique to measure heat transfer coefficients in this tunnel by the melting of solid steel models. The steel cones exposed to the hot flow eroded to a surface of minimum heat transfer for a 20 deg cone. This technique can be used to find such minimum heat transfer surfaces for any configuration. For scaling purposes, the mode of heat transfer, laminar skin friction, turbulent skin friction or radiation must be duplicated.

When a steel model of 0.003-in. radius hemispherical tip is placed in the flow, the model acts as a heat sink for about 500 microsec. Then suddenly the tip erodes, spreading high luminosity in the flow around the tip. Melted and vaporized material can be seen to flow away from the tip. This melting time can be read to 70 microsec on the Fastax pictures. The amount of melted material can also be seen by means of the model's change in shape in the frame that the melting occurs. Knowing this mass we compute

$$Q = m_w[C_w(T_m - T_w) + q_m] \text{ joules}$$

[5] This early crude technique was intended to indicate feasibility of heat transfer measurement only; more refined techniques are found in (12).

About 5 micrograms were melted in this time, requiring about 4 millijoules of heat. Since the surface area exposed to the laminar flow is known to be $365 \times 10^{-6}$ cm², an average heat transfer coefficient may be computed. This average heat transfer coefficient is plotted in Fig. 10.

Lees has published a theory on laminar heat transfer over spheres at hypersonic flight speeds (10). The stagnation point heat transfer for equilibrium flow is given in (10). The average sphere equilibrium heat transfer for laminar flow can be computed from the heat transfer rate distribution as

$$\bar{q}_e = 0.4\ \dot{q}_e$$

Using the tunnel calibration and sphere radius, the average heat transfer equilibrium coefficients can be computed. These computed values are plotted in Fig. 10 as "Lees' Equilibrium Limit."

According to the rate processes given by Lees, the maximum difference for a given flight speed in surface heat transfer rate between the equilibrium and completely out of equilibrium flow with a catalytic wall is given by

$$\bar{q}_{ne} = 1.3\ \dot{q}_e$$

This is also plotted in Fig. 10 as "Lees' Nonequilibrium Limit." It will be seen that there is very good agreement between the theory and the experimental data. The maximum possible black body radiation is also plotted to show that this form of heat transfer is not important in this case.

Observation of the models in the flow indicate that the flow is separating about 85 deg from the stagnation point and hence is laminar.

Further work on the theory of stagnation point heat transfer in dissociated air has been done by Fay and Riddell (11). This work indicates that Lees' values are slightly low. Further experimental work in this field has been done by Rose and Stark (12). The heat transfer coefficients of Fig. 10 agreed with the published data in (12).

## Wind Tunnel Throat Erosion

If bomb 3 (2) is converted into a wind tunnel, heat power rates over 100,000 w/cm² are obtained in the sonic flow throat. A picture of this bomb running as a Mach number 5 wind tunnel is given as Fig. 11. The throat is cooled by the vaporization of the throat material. The total energy input into the throat is given by

$$Q = At\dot{q}_e = Ay\rho[C_w(T_m - T_w) + C_L(T_v - T_m) + Q_m + Q_v] \text{ joules}$$

This equation assumes one-dimensional heat transfer and neglects the unsteady heat conduction through the unmelted wall. If the values from Table 1 are used in the above equation, it will be seen that the latent heat of vaporization is much greater than the other terms of the wall heat equation combined.

If oxidation occurs at the point of vaporization, the oxidation process will produce heat at a rate in excess of the cooling by vaporization, since all these oxidation processes are exothermic. This would make the vaporization heat sink capabilities of various substances useless. However, we will show below that oxidation close to the surface does not occur in the boundary layer in this particular wind tunnel throat. This oxidation undoubtedly occurs in wakes or supersonic portions of a wind tunnel, whose throat is eroding in this manner (13).

**Table 1 Properties of wall materials**

| Material | Carbon | Tungsten | Molybdenum | Units |
|---|---|---|---|---|
| $K$ | 0.24 | 1.99 | 1.45 | joules/K-cm sec |
| $C_w$ | 1.90 | 0.163 | 0.314 | joules/gm K |
| $T_w$ | 300 | 300 | 300 | K |
| $T_m$ | Sublimes | 3670 | 2920 | K |
| $T_v$ | at 3950 | 6227 | 5103 | K |
| $Q_m$ | ... | ... | ... | joules/gm |
| $Q_v$ | 59,800 | 4605 | 6823 | joules/gm |
| $\rho Q_v$ | 134,600 | 87,360 | 69,400 | joules/cm³ |

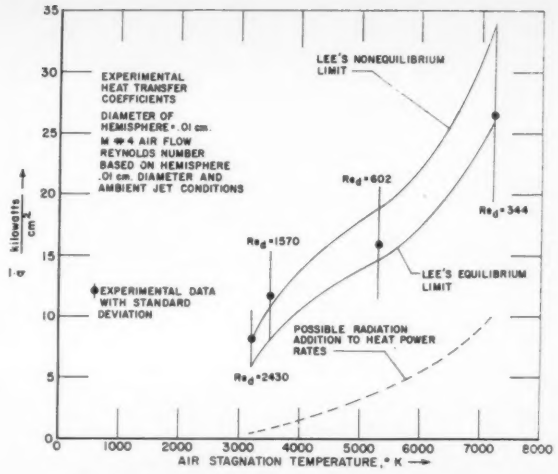
EXPERIMENTAL HEAT TRANSFER COEFFICIENTS
DIAMETER OF HEMISPHERE = .01 cm.
M = 4 AIR FLOW
REYNOLDS NUMBER BASED ON HEMISPHERE .01 cm. DIAMETER AND AMBIENT JET CONDITIONS
LEE'S NONEQUILIBRIUM LIMIT
LEE'S EQUILIBRIUM LIMIT
EXPERIMENTAL DATA WITH STANDARD DEVIATION
POSSIBLE RADIATION ADDITION TO HEAT POWER RATES
Re_d = 602
Re_d = 344
Re_d = 1570
Re_d = 2430
kilowatts / cm² / σ
AIR STAGNATION TEMPERATURE, ° K

Fig. 10 Experimental heat transfer coefficients

Fig. 11 Mach number 5 flow. Air stagnation temperature: 9000 K. Air stagnation pressure: 40,000 psi. Jet ambient pressure: 1 atm

The steady state heat vaporization condition will only be reached after a certain amount of time—the time required to heat the surface to the melting point (14). This time is

$$t = \frac{\pi}{4} K \rho_w C_w \frac{T_m^2}{\dot{q}^2}$$

Using Table 1, we obtain for $\dot{q}_e = 363{,}000$ w/cm²

carbon $t = 0.098 \times 10^{-3}$ sec

tungsten $t = 0.49 \times 10^{-3}$ sec

molybdenum $t = 0.24 \times 10^{-3}$ sec

The characteristic testing time in the wind tunnel is 0.00227 sec.

After the time required to melt the wall, the wall is cooled by the vaporization of its surface, and the heat balance equa-

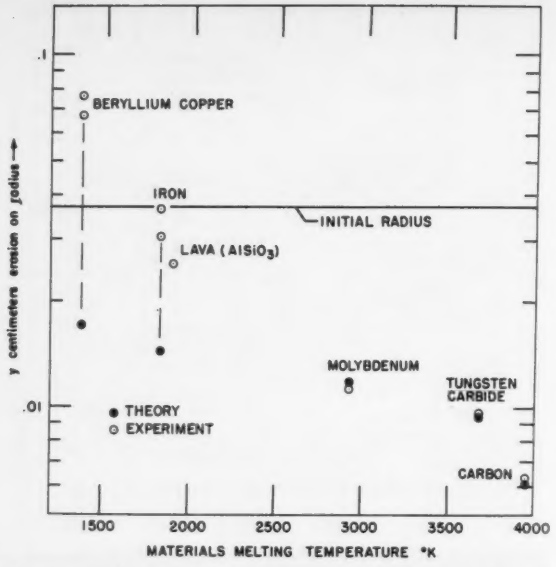


**Fig. 12 Sonic throat erosion by means of high temperature air flow**

tion may be approximated for our heat power input regime

$$y\rho Q_v = t\dot{q}_e \text{ joules/cm}^2$$

The following conditions are obtained in the sonic wind tunnel throat of diameter $d^*$ (as computed from real air isentropic expansion from measured stagnation conditions)

$\mu^* = 3.61 \times 10^{-3}$ poise
$d^* = 0.0762$ cm
$T_{stag.}^* = 9000$ K
$\rho^* = 0.0501$ gm/cm$^3$
$a^* = 2.13 \times 10^5$ cm/sec
$(\Delta H)^* = 19{,}000$ joules/gm
$Re^* = 5.2 \times 10^5$ (based on tunnel throat diameter)

This leads, by Reynolds' analogy for turbulent flow, to a Stanton number of $0.0016 = K_H$ (Prandtl number 1), for smooth walled pipes. This is probably a minimum Stanton number for this kind of flow. Three small corrections which all raise the heat transfer rate are:

1 As the gas is black, the heat input rate per unit area for black body radiation is

$$\dot{q}_{BB} = \sigma T^4 = 5.67 \times 10^{-12}(9000)^4 = 37{,}600 \text{ w/cm}^2$$

2 Due to the fact that we only have three diameters of pipe flow, the inlet heat transfer rate is about 20 per cent higher over these three diameters.

3 Oxidation can change the heat input rate, raising it by as much as a factor of three for some materials; however, it does not occur here, as will be shown.

The expected heat input rate for the minimum Stanton number is

$$\dot{q}_{SF} = K_H\rho^* u^*(\Delta H)^* = 3.25 \times 10^5 \text{ w/cm}^2$$

Adding the black body radiation

$$\dot{q}_e = \dot{q}_{BB} + \dot{q}_{SF} = 363{,}000 \text{ w/cm}^2$$

This is taken as a minimum total.

The bomb has been observed to run for at least 0.020 sec in supersonic flow. However, the primary heat transfer occurs in the first 5 millisec (observed by means of Fastax camera). If we assume a characteristic running time of 0.00227 sec, we get a constant expected energy input to all tested throat materials of 823 joules/cm$^2$ = $\dot{q}_e t$.

The quantity $\rho Q_v$ is governed by the material and is called the volumetric heat of vaporization. For our materials, this quantity is tabulated in Tables 1 and 2.

Expected values of $y$ as radius enlargement of initial radius = 0.038 cm throat are found in Fig. 12.

Graphite, tungsten carbide, molybdenum, lava ($AlSiO_3$), steel and beryllium copper were run in the sonic throat. These results are plotted in Fig. 12 along with the theory as worked out in the first part of this paper. Results are plotted as a function of melting temperature. The clear superiority of graphite over all other materials at 40,000 psi stagnation pressure seems to indicate that it is the preferred material for wind tunnel throat under these conditions.

The lava broke in pressure fracture. Improperly supported carbon also broke in pressure fracture. The other materials withstood the pressure but not the high heat power rate. If the melting point of the material gets much below 2500 K, the simple theory proposed above fails, due to the fact that the wall softens and the pressure blows the molten throat out in drops. This problem also occurs in electrical arc discharges at the electrodes, and it is recommended that such materials be avoided in this heat power range.

Since the experimental erosion of the best materials (graphite, tungsten carbide and molybdenum) followed the simple vaporization theory without oxidation, this is evidence that no additional heat input due to oxidation occurred in the sonic throat. If the wall had oxidized, the experimentally determined erosion depths would have varied with the differing heats of oxidation and not with the heats of vaporization as was determined.

## Conclusions

A series of typical aerodynamic experiments have been presented to demonstrate that data of interest to aeronautical engineers can be obtained in wind tunnels operating in millisec intervals.

Supersonic nozzles were constructed and tested by means of jet pressure observations, proving that the isentropic equilibrium flow computations are valid for such high temperature, high pressure nozzle expansions. The flow about models can be observed in the self luminosity of the air. The flow equilibrium studies that have been carried out agree with other experimental shock tube results. Drag and heat transfer coefficients have also been made. For spheres, these results agree with commonly accepted present theories in the field.

Throat erosion is a very serious problem in this type of wind tunnel, due to the high temperatures and high heat flux rates. An experimental study is presented which demonstrates theoretically and experimentally that tungsten and carbon throats are to be preferred if wall vaporization is the throat cooling technique.

## Acknowledgment

The author would like to acknowledge the assistance given him by the supporting facilities of the Arnold Engineering Development Center, especially the Gas Dynamics Facility.

**Table 2 Heat of vaporization and melting temperature**

| Material | Heat of Vaporization joules/cm$^3$ | Melting Temperature K |
|---|---|---|
| Graphite | 134,600 | 3950 |
| Tungsten | 87,360 | 3670 |
| Molybdenum | 69,400 | 2920 |
| Iron | 56,850 | 1835 |
| Copper | 48,070 | 1383 |

Without these facilities the work would not have been done. The author would especially like to acknowledge the assistance given him by B. V. Rhodes and R. Smelt, whose continual encouragement and ideas were most valuable.

### References

1 Hilsenrath, J. and Beckett, C. W., "Tables of Thermodynamic Properties of Argon-Free Air to 15,000°K," AEDC-TN-56-12, Sept. 1956.

2 Bloxsom, D. E., Jr., "Use of Capacitor Discharges to Produce High Temperature, High Pressure Air," JET PROPULSION, vol. 28, no. 9, Sept. 1958.

3 Feldman, S., "Hypersonic Gas Dynamic Charts for Equilibrium Air," AVCO Research Laboratory, Jan. 1957.

4 Benson, J. M., "Measurements of the Physical Properties of Active Nitrogen," *Journal of Applied Physics*, vol. 23, no. 7, July 1952, pp. 757–763.

5 Schwartz, R. N. and Eckerman, J., "Shock Location in Front of a Sphere as a Measure of Real Gas Effects," *Journal of Applied Physics*, vol. 27, no. 2, Feb. 1956, pp. 169–174.

6 Logan, J. G., "Relaxation Phenomena in Hypersonic Aerodynamics," IAS Preprint 728, Jan. 1957.

7 Allen, W. A., Rinehart, J. S. and White W. C., "Phenomena Associated with the Flight of Ultra-Speed Pellets," *Journal of Applied Physics*, vol. 23, no. 1, Jan. 1952, pp. 132,137.

8 Foelsch, J., "The Analytical Design of an Axially Symmetric Laval Nozzle for a Parallel and Uniform Jet," *Journal of the Aeronautical Sciences*, March 1949, pp. 161–188.

9 McLellan, C. H., "An Investigation of the Melting of Bodies Due to Aerodynamic Heating," *Trans. ASME*, July 1955, pp. 727–733.

10 Lees, L., "Laminar Heat Transfer over Blunt-Nosed Bodies at Hypersonic Flight Speeds," JET PROPULSION, vol. 26, 1956, pp. 259–269.

11 Fay, J. A. and Riddell, F. R., "Theory of Stagnation Point Heat Transfer in Dissociated Air," *Journal of the Aeronautical Sciences*, vol. 25, no. 2, Feb. 1958, pp. 73–85.

12 Rose, P. H. and Stark, W. I., "Stagnation Point Heat Transfer Measurements in Dissociated Air," *Journal of the Aeronautical Sciences*, vol. 25, no. 2, Feb. 1958, pp. 86–97.

13 White, W. C., "Suppression of A10 in the Wake of Ultra-speed Pellets," *Astrophysical Journal*, vol. 121, pp. 271–276.

14 Carslaw, H. S. and Jaeger, J. C., "Conduction of Heat in Solids," Clarendon Press, Oxford, 1947, p. 56.

15 Camac, M., Camm, J., Feldman, S., Keck, J. and Petty, C., "Chemical Relaxation in Air, Oxygen and Nitrogen," IAS Preprint no. 802, Jan. 27, 1958.

# Use of Capacitor Discharges to Produce High Temperature, High Pressure Air[1]

D. E. BLOXSOM Jr.[2]

Rhodes and Bloxsom, Canoga Park, Calif.

**An electrical spark gas discharge technique, using condensers, is described, which has been used to heat air to 9000 K and 40,000 psi at close to 100 per cent energy transfer efficiency. The heat losses from the air at near stagnation conditions have been measured. These heat losses restrict the holding time of the hot air to milliseconds in laboratory size apparatus. The impurities introduced into the air from the heating and electrode erosion have been experimentally measured, and these measurements are also presented. The total of these impurities is about 1 to 5 per cent of the total heated air mass. Other experiments are presented to show that the air is in equilibrium. Various theoretical explanations are given for the experiments.**

### Nomenclature

$A$ = surface area, cm²
$D$ = bomb diameter, cm
$H_0$ = specific enthalpy of air at stagnation temperature conditions, joules/gm
$H_W$ = specific enthalpy of air at wall temperature conditions, joules/gm
$I$ = current, amp
$K_H$ = Stanton Number
$m$ = mass, gm
$\mu$ = air viscosity, poise
$\bar{q}$ = average heat transfer coefficient, w/cm²
$\dot{q}_{BB}$ = black body heat transfer coefficient, w/cm²
$\dot{q}_{SF}$ = forced convection heat transfer coefficient, w/cm²
$Q_V$ = heat of vaporization, joules/gm
$\rho$ = air density, gm/cm³
$Re$ = Reynolds number of air
$\sigma$ = Prandtl number of air
$T$ = air temperature, K
$t$ = time, sec
$u$ = air velocity, cm/sec
$\Delta V$ = voltage change, at electrodes ~30 v

Received Feb. 12, 1958.

[1] This work was performed by Aro, Inc. at the Arnold Engineering Development Center for the USAF. The opinions expressed here are the author's and do not necessarily represent the views of the USAF and Aro, Inc.

[2] Partner.

## Introduction

PRECEDING work in high pressure, high temperature electric condenser discharges has been done by J. A. Anderson in the early 1920's (1, 2).[3] This work involved the sudden release of electrical energy stored originally in capacitors. The air heating technique described in this paper is similar to Anderson's technique except that the electrical explosion is confined in a closed bomb, and the data are taken by means of fast pressure probes. These modifications of Anderson's technique extend the time scale of the experiment to millisecond time intervals and make possible gas dynamic and heat transfer studies at these elevated air temperatures. Roth (3) has done work indicating very high air electrical heating efficiency from smaller ignition-type sparks.

## Air Heating by Capacitor Discharge

The spark heating of air considered here deals with a constant volume and constant density condition. No details of heating during spark growth are available from the instrumen-

[3] Numbers in parentheses indicate References at end of paper.

tation used, as the minimum time of response of the instrumentation was longer than the entire time of spark discharge.

The air was heated in a closed chamber called a bomb. Bomb 1 was a glass tube 18 in. long with an inside diameter of $\frac{1}{2}$ in. The bomb was used to heat air to a maximum pressure of 300 psi. Bomb 2 was 2 in. long with a 1.6 in. inside diameter. This bomb was made of steel and permitted holding of air pressures to 5000 psi. Bomb 3 was also fabricated of steel, with a $\frac{3}{4}$ in. inside diameter and was 1 in. long, which permitted holding of air pressures to 40,000 psi.

The procedure for using these bombs was to first fill the bomb with high pressure air at laboratory temperature. The high pressure air was restrained with a diaphragm and valves. Then, a bank of capacitors was discharged into the high pressure air in the bomb. A small wire was used to initiate the spark between the electrodes, as the gaps were too long to spark over. A low resistance spark gap, which could be triggered by external means, was used to permit 3 microsec high voltage rise across the tease wire. The usual discharge circuit for bombs 2 and 3 may be found in Fig. 1. The total discharge time of the circuit was 50 microsec. It is very important, for this type of electrical heating, to keep the discharge time of the electrical circuits small relative to the cooling time of the hot air.

As the air is heated to higher and higher specific enthalpies, more and more of the energy is transferred to other than

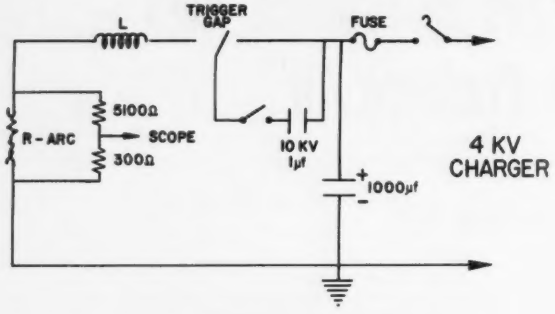


Fig. 1 Schematic of electric circuit for bombs 2 and 3

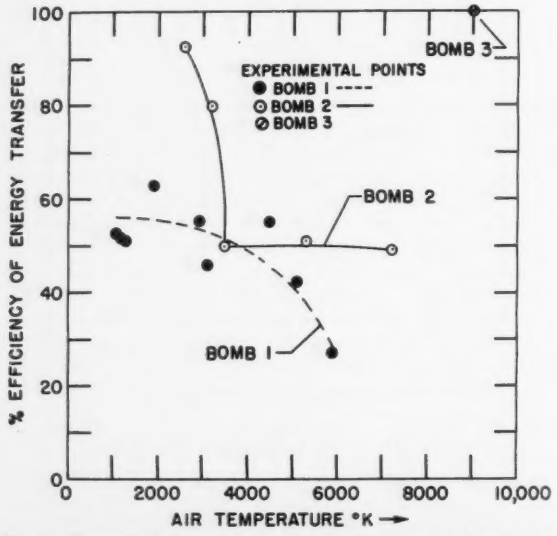


Fig. 2 Overall efficiency of energy transfer from condensers to usable air

translational degrees of freedom. The amount of this energy for thermodynamic equilibrium may be found in the equation of state for air (4). By means of these equations of state, the specific internal energy, specific enthalpy, etc., may be plotted as a function of density, pressure and temperature. If thermodynamic equilibrium is assumed, then knowledge of two of the three air parameters, pressure, temperature and density, permits the other to be computed. Since the bomb is closed, the density remains constant in the absence of large disturbances in the air. This density is measured by measuring the initial air pressure in the bombs at 300 K. Gas density is measured here in amagat units, the density of a gas at one atmosphere pressure and 300 K temperature—for air, one amagat is $1.17 \times 10^{-3}$ gm/cm$^3$.

The pressure rise in the air due to spark heating was measured by means of a pressure pickup in the bomb wall. This was an Electro Products Laboratory, Inc. Model 3700-C Pressograph capacitance pressure pickup with a critically damped rise time less than 100 microsec. The high current of the spark discharge produced a signal as large as the full pressure signal, but this inductive pickup was confined to the first 50 microsec of the pressure trace, i.e., the first half of the pickup's rise time. The pressure pickup was calibrated statically by means of registering oscilloscope deflections produced by dead weight pressure on the pickup. This calibration was made before and after a series of runs with a given pressure pickup. The calibrations agreed to within 5 per cent. The oscilloscope used in these experiments was the Tektronix 513D.

Using the equation of state for air from (4), equilibrium air temperatures were computed from the pressure data. Experiments involving the sudden cooling of the air ($10^6$ K/sec) in a short isentropic nozzle discharging into a cold air mass indicated that the air is in equilibrium in bomb 2 in a time less than 1 millisec. After 0.1 millisec, the pressure in the bombs was slowly decreasing due to heat transfer only. Finally, shock tube measurements of air equilibrium (5) indicate that the air is in equilibrium in essentially the time required for the pressure pickup to measure the pressure rise in the spark heated air. A comparison of these data is found in Fig. 7 of (6).

Using the equilibrium air internal energy indicated by the pressure and density measurements, an overall efficiency of energy transfer from the condensers to the air can be obtained. These data are found in Fig. 2.

It will be seen from Fig. 2 that overall efficiencies around 50 per cent of the initial capacitor energy are obtained. Voltage and current measurements of the electrical power delivered to the air spark were made as a function of time, using the circuit of Fig. 1. Care was taken not to introduce spurious signals into the measuring circuits during discharge by inductive loops responding to the 100,000 amp current of the spark discharge. To prevent these inductive loops, the resistance of the voltage circuit must be kept high, but not too high so as to prohibit high frequency performance with the distributed capacitance of the lines and oscilloscope plates. Around 5000 ohms are suitable for a circuit given in Fig. 1. The inductance of the current measuring device must be kept as low as possible. If an M-shaped foil loop is used as a resistor, properly insulated and supported, the inductive component of this current test resistor can be made as low as $10^{-11}$ henries. Both the current and voltage circuits had 0.01 microsec rise times to measure 50 microsec pulses. Proof that spurious signals were not entering the circuits was obtained by disconnecting the high signal lead but leaving the lead close by with its ground connected. Neither circuit had enough spurious pickup to trigger the oscilloscope, thus proving the spurious signals were below 5 per cent of the peak signals. A study of these current and voltage oscilloscope traces of the spark discharge indicated that almost the full condenser energy enters the ohmic spark resistance. Hence the lower efficiencies measured by the pressure pickup (Fig. 2) are the

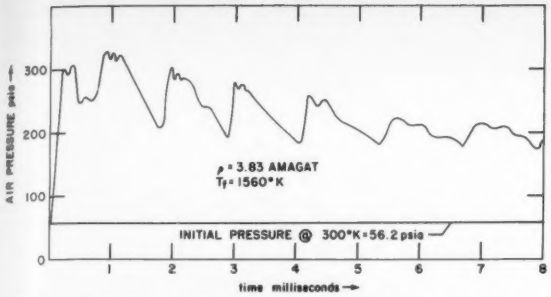


Fig. 3 Pressure vs. time oscillogram of air heat transfer in bomb 1

result of heat losses during the actual spark formation. No information concerning these losses is given in this paper, as the actual variable density high pressure spark formation could not be followed by the pressure instrumentation.

## Experimental Measurement of the Heat Losses

The pressure measurements indicated a slow drop in pressure with time. A typical example of these data is found in Fig. 3. The useful experimentation time in bombs 1–3 at high temperature is defined as the time for the pressure to drop to 0.90 of maximum pressure. This time is found in Fig. 4 as a function of temperature. Fig. 4 shows that at all temperatures there is about 0.5 millisec available for such hot air experimentation. The maximum time of electrical heating is 0.05 millisec.

From the drop in average air pressure with time, at constant air density, it is possible to compute a heat transfer coefficient for a given time interval

$$\bar{q} = \frac{Q}{At} \quad \ldots\ldots\ldots\ldots\ldots\ldots\ldots\ldots [1]$$

These heat power rates are found in Fig. 5 for bomb 1 heat losses, and in Fig. 6 for bombs 2 and 3.

The actual heat power loss mechanism is not known at the present time. The black body limit to radiation heat power loss is given by

$$\dot{q}_{BB} = 5.67 \times 10^{-12} T^4 \text{w/cm}^2 \quad \ldots\ldots\ldots\ldots [2]$$

This black body limit is plotted in Figs. 5 and 6.

Another possible mechanism of heat transfer from the hot air is forced convection. The heat power given by this mechanism is

$$\dot{q}_{SF} = K_H(H_0 - H_W)\rho u \text{ w/cm}^2 \quad \ldots\ldots\ldots\ldots [3]$$

These Stanton numbers have been measured by means of pipe flow friction factors and are given by Reynolds' analogy

$$K_H = 1/2\sigma^{-2/3} C_f \quad \ldots\ldots\ldots\ldots\ldots\ldots [4]$$

These Stanton numbers are a slowly varying function of the Reynolds numbers for turbulent flow

$$Re = \frac{\rho u D}{\mu} \quad \ldots\ldots\ldots\ldots\ldots\ldots [5]$$

The viscosity of high temperature air is not very well known. Viscosity values for air used here may be found in (7). The friction factors may be found in (8) as a function of Renolds number and pipe surface roughness.

In order to compute the forced convection heat transfer expected in the three bombs, the average air velocities must be experimentally measured as a function of time. All other parameters of the forced convection heat transfer Equation [3] are known from other measurements and computations from the average pressure oscilloscope traces (using an equilibrium equation of state).

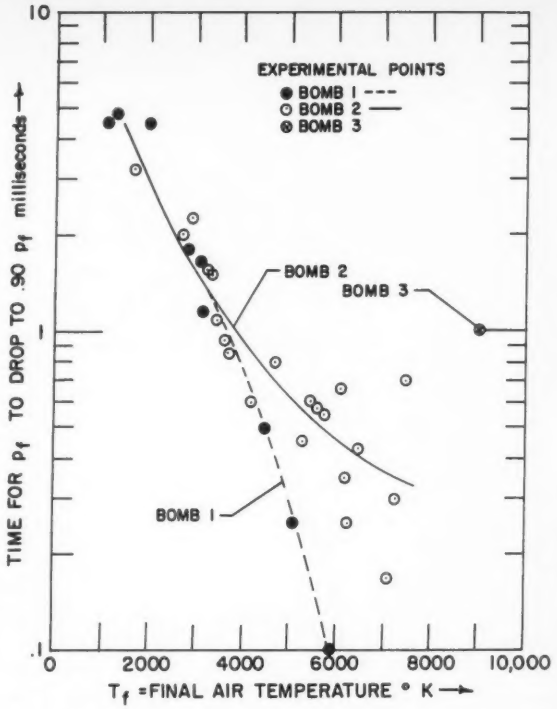


Fig. 4 Usable experimentation time at various peak temperatures in the 3 bombs

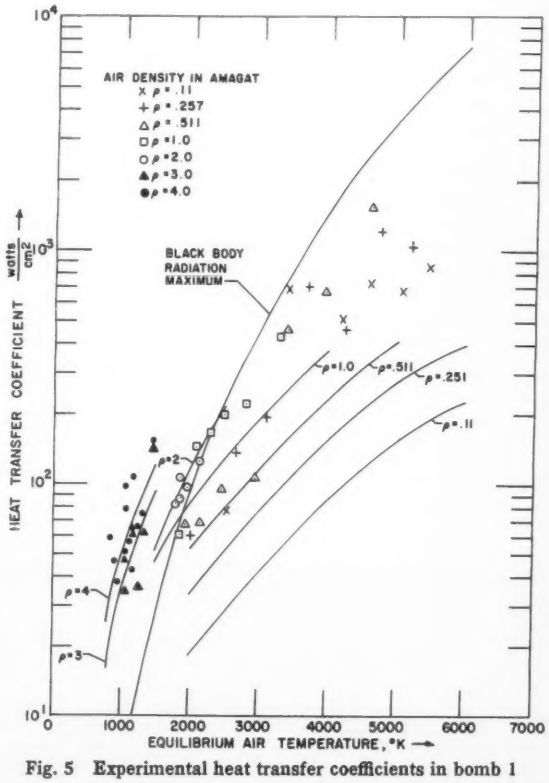


Fig. 5 Experimental heat transfer coefficients in bomb 1

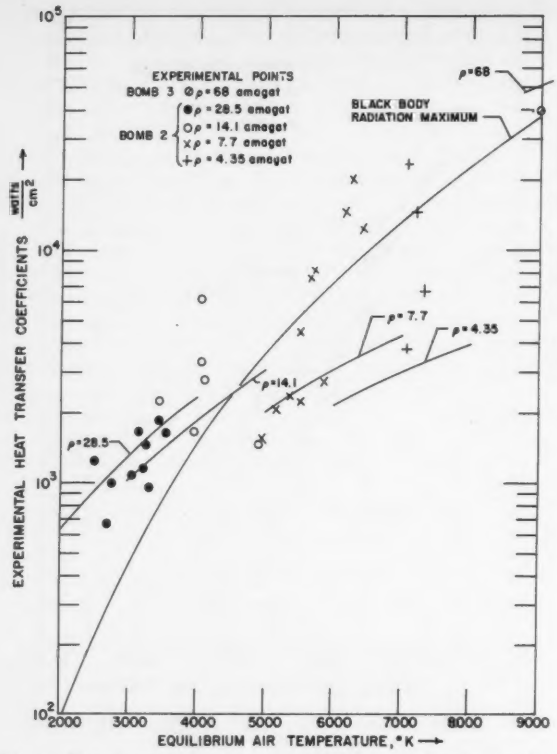


Fig. 6 Experimental heat transfer coefficients in bombs 2 and 3

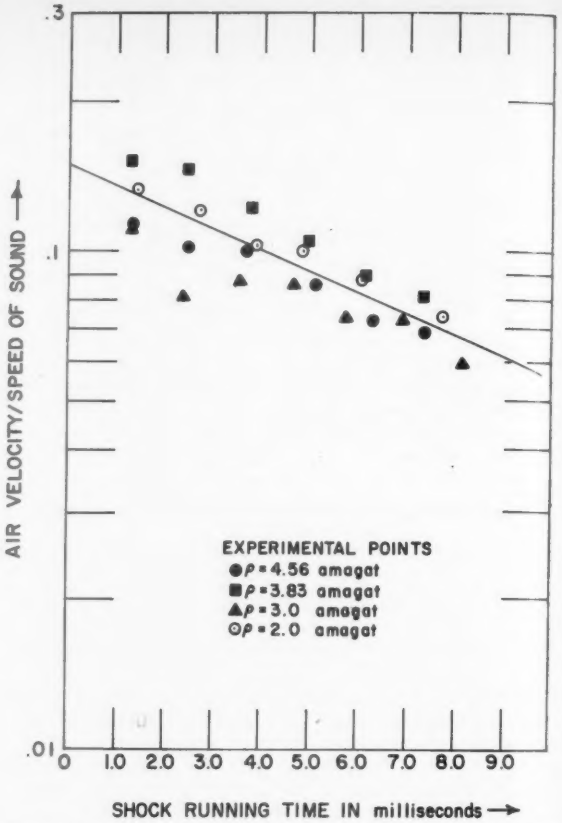


Fig. 7 Longitudinal air shock decay as a function of time in bomb 1

A measurement of the air velocities may be obtained from the actual pressure fluctuations measured at one end of bomb 1. A typical oscilloscope pressure trace is given in Fig. 3. The N-shaped wave imposed on the steady average pressure permits the Mach number of the near sonic shock to be uniquely determined. The air velocity driving this near sonic shock is also uniquely determined from the Mach number, since the speed of sound is known in the hot air. The air velocity-speed of sound ratio so determined as a function of time is found in Fig. 7. This shock wave decay is to be expected in the bombs due to the stability of weak shocks, near Mach number 1, in the time scale of the experiment. It must be emphasized that there was no net air flow out of bomb 1, since the shock wave simply moved the air around in the bomb. Additional optical evidence of the existence of the shock wave is found in a series of smear camera photographs, which record luminosity perpendicular to the bomb 1 axis as a function of time. A representative photograph is given in Fig. 8. The initial high intensity spark may be seen, and later, the glow of the hot gas cooling. The decaying shock wave is also easily seen as a sharp Z-shaped division between brighter and darker luminosity. Particle paths may also be seen moving in the tube. Gas temperature measurements from this shock wave velocity agree with the temperature measurements from the constant volume pressure rise to 10 per cent, so the gas temperature is believed accurate to this percentage.

Figs. 5 and 6 contain estimates of the forced convection heat transfer, using the measured air velocities of Fig. 7 and the turbulent flow smooth pipe friction factors of (8).

The experimental heat transfer coefficients of Figs. 5 and 6 seem to follow the turbulent flow forced convection theory for low temperatures and the black body radiation theory for high temperatures. It should be emphasized again, however, that additional experimentation is necessary to determine the heat transfer mechanism.

## Impurities

Impurities can come from several sources:

1 Condensable impurities due to vaporization of the tease wire and electrode surfaces. These impurities are found experimentally as dust in the flow gas.

2 Permanent gases eroded from the electrode shields, such as carbon dioxide.

3 Permanent impurities frozen into the air by high cooling rates, such as nitric oxide.

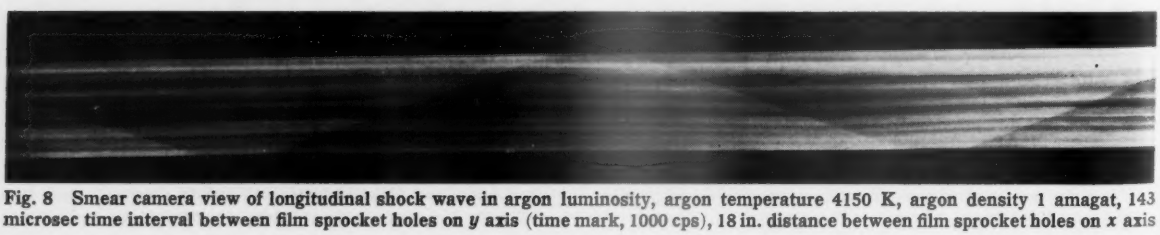

Fig. 8 Smear camera view of longitudinal shock wave in argon luminosity, argon temperature 4150 K, argon density 1 amagat, 143 microsec time interval between film sprocket holes on $y$ axis (time mark, 1000 cps), 18 in. distance between film sprocket holes on $x$ axis

**Table 1 Dust impurity measured in bomb 2**

| Initial temperature, K | Initial density, amagat | Dust mass, gm | Dust per cent of gas mass, based on mean dust mass | Expected dust per cent of gas mass from tease wire and electrode erosion |
|---|---|---|---|---|
| 7200 | 4.37 | 0.0391 | 5.9 | 4.6 |
| 5350 | 7.76 | 0.016 | 3.3 | 2.7 |
| 3550 | 14.6 | 0.0146 | 1.8 | 1.3 |
| 3200 | 28.2 | 0.0246 | 0.8 | 0.7 |

**Table 2 Composition of air samples after heating in bomb 2 and cooling at constant volume**

| Initial temperature, K | Initial density, amagat | Composition by volume percentage of $N_2$ | $O_2$ | $H_2O$ | A | $CO_2$ | NO |
|---|---|---|---|---|---|---|---|
| Air sample before heating, 300 K | 1 | 76.7 | 20.0 | 2.4 | 0.93 | 0.03 | no trace < 0.1 |
| 7200 | 4.37 | 78.1 | 19.0 | 0.9 | 0.96 | 0.41 | no trace <0.1 |
| 5350 | 7.76 | 79.1 | 18.7 | 0.5 | 0.95 | 0.74 | no trace <0.1 |
| 3500 | 14.6 | 81.3 | 15.1 | 0.5 | 0.95 | 2.14 | no trace <0.1 |
| 3100 | 28.2 | 80.8 | 15.1 | 0.6 | 0.95 | 2.50 | no trace <0.1 |

The mass of electrode material eroded from very high current arc electrodes is given by (9)

$$m = \frac{(\Delta V)It}{Q_v} \text{ gm} \quad \ldots\ldots\ldots\ldots\ldots\ldots [6]$$

The effects of the impurities of the vaporized tease wire and electrode surfaces were determined by collecting and weighing the dust after a closed bomb 2 run. In these runs, all openings into the bomb were closed, and the hot air permitted to cool by heat transfer to the cold walls. The cooled air did not change in density from the initial density before heating. These dust impurities, which were weighed with a chemical balance, are found in Table 1. The expected dust per cent of gas mass from the known weight of tease wire and electrode erosion (from Equation [6]) are also given in Table 1. The greater contribution came from the vaporized electrode. There is substantial agreement between the measured and expected dust impurities. The maximum dust impurity comes at low gas masses and amounts to about 6 per cent. Fastax camera pictures at 14,000 frames/sec indicated that it takes over 10 millisec for the dust impurities to diffuse from the electrodes into the body of the heated air and affect the hot air experiments.

The cooled gaseous products from the closed bomb 2 runs were then analyzed with a mass spectrometer (Model 20-610 Consolidated Engineering Corporation) to determine the composition of the air after spark heating. This technique will detect any impurity present as permanent gases. The results of the mass spectrometer analysis are found in Table 2. It will be seen that there is a rise in carbon dioxide level in the air, to a maximum of 2.5 per cent by volume. This mass spectrometer did not respond to small traces of nitric oxide.

According to equilibrium theory, some nitric oxide will be formed at the temperatures achieved in the hot air. Then if the air experiment involves cooling the air, the kinetics of the nitric oxide reaction (10) indicate that, at a finite cooling rate, a part of the nitric oxide will be frozen in and will remain as a permanent impurity.

Calculations of the equilibrium concentrations from Hirschfelder (11), of nitric oxide at high air temperatures, will be found in graphical form in Fig. 9. These theoretical results are compared with data showing the result of bubbling the cooled air through several water-collecting towers in series (Bubble Tower) and analyzing the nitric acid produced with a pH meter. The nitric oxide gas was also collected on other occasions by scrubbing with water (Scrubbing Tower). From the known pressure decay in the closed bomb, a rate of 6000 K/sec was measured at 2000 K, the most probable freeze-in temperature. The work of Steinmetz (10) indicates a yield of about 1.3 per cent at this rate, and the measured quantity of nitric oxide approximates this value. Using cooling rates of 500,000 K/sec, Hertzberg (12) reports that 51 per cent of Steinmetz's yield was realized.

The determination of temporary impurities was also made with the help of bomb 2. A question arises concerning the state of the air after sudden cooling (to $10^6$ K/sec). These

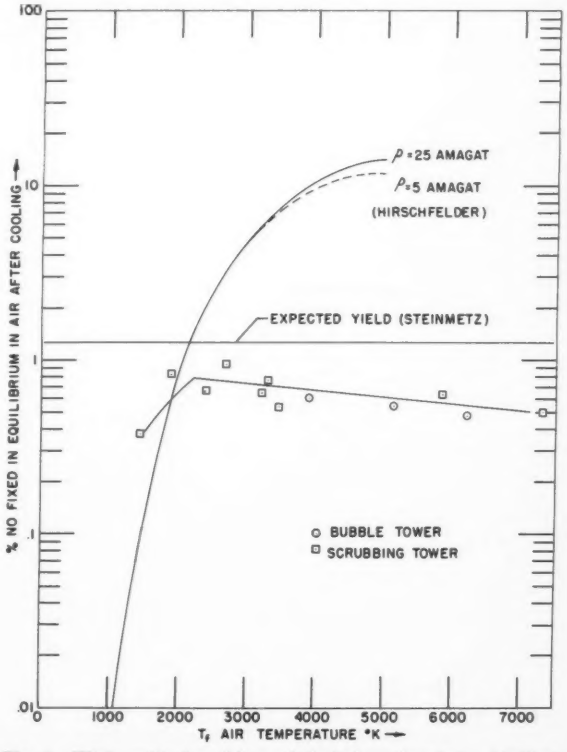


**Fig. 9 Nitric oxide found in cooled air from bomb 2. Cooling rate: 6000 K/sec at 2000 K**

**Table 3 Relaxation time upper limits and production of nitric oxide produced by $10^6$ K/sec cooling in bomb 2**

| Initial temperature, K | Initial density, amagat | Cooled gas temperature, K | Time to reach final pressure, millisec | Per cent nitric oxide by volume |
|---|---|---|---|---|
| 7200 | 4.37 | 1170 | 1 | 0.65 |
| 5350 | 7.76 | 579 | 1 | 0.67 |
| 3550 | 14.6 | 702 | 1 | 0.93 |
| 3200 | 28.2 | 507 | 3 | 0.89 |

data are important if rapid isentropic expansions are to be studied. To investigate this condition, the hot gas was dumped into a chamber with ten times the initial volume of hot gas and filled with cold gas (300 K) at the same density. The 0.1 millisec rise time pressure probe was used to record the pressure rise in the large chamber. Data resulting from tests of the cooled gas are presented in Table 3. Also shown is the time necessary to equilibrate the pressure to final pressure (of the large chamber heated gases) within 3 per cent, and the per cent of nitric oxide determined by water absorption. At this cooling rate, the expected yield of nitric oxide from (10) is 2.5 per cent, and Table 3 shows about one third this yield is achieved.

## Conclusions

A technique has been described by which any gas can be heated electrically in a constant volume and constant density process to temperatures up to 9000 K and pressures up to 40,000 psi. Overall heating efficiencies of air are as much as 100 per cent even at the highest temperatures. The natural cooling times of these gases in laboratory size vessels are on the order of milliseconds, permitting various gasdynamic experiments on this time scale. The possibilities of raising the gas temperature are only limited by the size of the electrical power supplies available as compared with the losses from the heated gases. Due to the fact that the heat power inputs to the electrodes are so high in these times, some impurity contaminates the heated gas. The impurity rises as the gas is held for longer times, appearing in various experiments in about 10 millisec. The design and use of these hot gas sources is then a compromise between sufficient testing time to perform a given experiment and the rise in impurity level due to the extreme temperature and heat power inputs.

## Acknowledgment

The author would like to acknowledge the assistance given him by the supporting facilities of the Arnold Engineering Development Center, especially the Gas Dynamics Facility. Without these facilities the work would not have been done. The author would especially like to acknowledge the assistance given him by B. V. Rhodes and R. Smelt, whose continual encouragement and ideas were most valuable.

## References

1 Anderson, J. A., "The Spectrum of Electrically Exploded Wires," *Astrophysical Journal*, vol. 51, 1920, pp. 37–48.

2 Anderson, J. A. and Smith, S., "General Characteristics of Electrically Exploded Wires," *Astrophysical Journal*, vol. 64, 1926, pp. 295–314.

3 Roth, W., Guest, P. G., von Elbe, G. and Lewis, B., "Heat Generation by Electric Sparks," *Journal of Chemical Physics*, vol. 19, Dec. 1951, pp. 1530–1535.

4 Hilsenrath, J. and Beckett, C. W., "Tables of Thermodynamic Properties of Argon-Free Air to 15,000°K," AEDC-TN-56-12, 1956.

5 Logan, J. G., "Relaxation Phenomena in Hypersonic Aerodynamics," Institute of Aeronautical Sciences Preprint no. 728, 1957.

6 Bloxsom, D. E., Jr., "Supersonic Aerodynamic Experiments Using Very High Temperature Air Wind Tunnels," JET PROPULSION, vol. 28, no. 9, Sept. 1958.

7 Hirschfelder, J. O., University of Wisconsin Report CF-1507, April 17, 1951 (Reproduced in Navord 1488, vol. 5, Table 1510.10).

8 Hall, N. A., "Thermodynamics of Fluid Flow," Prentice-Hall, New York, 1951.

9 Wilson, W. R., "High Current Arc Erosion of Electric Contact Materials," *Trans. AIEE*, vol. 74, part III, Aug. 1955, pp. 657–64.

10 Steinmetz, C. F., "Theoretical Study of Nitrogen Fixation by the Electric Arc," *Chemical and Metallurgical Engineering*, vol. 22, nos. 7, 8, 9 and 10, Feb. and March 1920.

11 Hirschfelder, J. O. and Curtis, C. F., "Thermodynamic Properties of Air III," N.R.L. Reports CM-472 and CM-518, NORD 9938, Dec. 1948.

12 Hertzberg, A., "The Application of the Shock Tube to the Study of the Problems of Hypersonic Flight," JET PROPULSION, vol. 26, no. 7, July 1956, p. 549.

# Measurement of Turbulent Heat Transfer Rates on the Aft Portion and Blunt Base of a Hemisphere Cylinder in the Shock Tube[1]

JOSEF RABINOWICZ[2]

California Institute of Technology, Pasadena, Calif.

**Turbulent heat transfer rates on the aft portion and on the blunt base of a hemisphere cylinder were measured in the $2\frac{7}{8} \times 2\frac{7}{8}$ in. GALCIT shock tube over a range of shock Mach numbers between 3.25 and 5.1 and initial pressures between 3 and 17 cm Hg. The local Reynolds numbers on the cylindrical afterbody varied between $3.5 \times 10^4$ and $3.0 \times 10^5$ per cm. A side support was used for the model to eliminate the disturbing effect of a rear sting support. The measured turbulent heat transfer rates on the cylindrical portion agreed very well with previous flat plate measurements for small temperature differences, although the ratio of stagnation to surface enthalpy varied between 3 to 8 in the present tests. Only a slight effect of this large variation in $h_s/h_w$ was detected in this range of local Mach numbers, i.e., $1.25 < M_e < 1.5$. The measured heat transfer rate on the base indicated that at the center of the base the heat transfer rate is comparable to that on the surface just ahead of the base, while the heat transfer rate falls off to one-half to one-third of this value toward the rim of the base. This unexpected distribution of heat transfer rate over the base, and particularly the high value at the center, shows the necessity for a careful study of wake phenomena.**

## Nomenclature

$C_H$ = Stanton number = $\dfrac{\dot{q}}{\rho_e u_e (h_{aw} - h_w)}$
$h$ = enthalpy, cal/gr
$M$ = Mach number
$Nu_x$ = Nusselt number = $C_H \cdot Pr \cdot Re_x$
$Re_x$ = Reynolds number = $\dfrac{\rho_e u_e \bar{x}}{\mu_e}$
$Pr$ = Prandtl number = $\dfrac{c_p \mu_e}{k_e}$
$R$ = body radius, cm
$p$ = pressure, cm Hg abs
$\dot{q}$ = heat transfer rate, cal/cm²/sec
$r$ = recovery factor
$u$ = velocity, cm/sec
$\delta$ = boundary layer thickness, cm
$\rho$ = density, gr/cm³
$\mu$ = viscosity coefficient, gr/cm-sec

*Subscripts*

$e$ = value at the outer edge of the boundary layer
1 = ahead of shock front
2 = behind shock front
$s$ = stagnation
$aw$ = recovery
$w$ = wall

Received Dec. 23, 1957.
[1] The work discussed in this paper was carried out under the sponsorship and with the financial support of the Office, Chief of Ordnance, and the Office of Ordnance Research, U. S. Army.
[2] Research Fellow, Guggenheim Aeronautical Laboratory.

## 1 Introduction

THE use of the shock tube to simulate various aspects of hypersonic flight is now widely accepted. Recent development of the film resistance thermometer has made possible accurate heat transfer studies in the extremely short testing times available in the shock tube. Measurements of laminar heat transfer rates at and near the stagnation region of a blunt-nosed body (1 and 2)[3] indicated a very good agreement with the equilibrium laminar boundar layer theory for hypersonic flight speeds as developed by Lees (3) and Rose and Riddell (4). The present work extends these measurements to the aft region of a blunt body, i.e., to the aft surface and to the model base. For reasons which will be explained in detail in section 3, it is very difficult to obtain undisturbed laminar boundary layer flow on the aft portion of a long model in the present straight section of the $2\frac{7}{8} \times 2\frac{7}{8}$ in. shock tube. Thus the work was confined to turbulent heat transfer studies.

Published experimental data on turbulent heat transfer rates with large temperature differences across the boundary layer are scarce. In a recent report, Libby and Cresci (5) compare their turbulent heat transfer rate data measured on a blunt-nosed body in a wind tunnel with several analyses and find the data to agree best with the local flat plate approximation. However, they suggest that their result should be substantiated at a higher stagnation enthalpy, since their wind tunnel tests were limited to ratios of stagnation enthalpy to surface enthalpy of 1.3 to 2.0. The shock tube enables us to realize much higher ratios of stagnation to surface enthalpy, and in the present work this ratio lies between 3 and 8. The results of the present investigation tend to confirm the previous conclusion of the validity of the flat plate analysis. This result, which is at first somewhat surprising, fits well into the overall trend indicating no startling or unexpected phenomena associated with high temperatures at ordinary pressures.

The heat transfer problem on a blunt base is considerably more difficult. Much experimental and theoretical work has been done on the base pressure problem from the point of view of an overall "mixing" analysis. However, the heat transfer rate probably depends also on local conditions, so that a knowledge of the flow field near the base surface is required before local heat transfer rates can be predicted. The measurement of base heat transfer rates in the shock tube is also complicated by the question of the time required to establish a steady wake behind a model. Thus the present experiment has two main objectives: (a) To determine whether time-independent heat transfer rates on a blunt base are established in the time interval available in the shock tube (about 400–600 $\mu$ sec). (b) To investigate heat transfer rates on a blunt base when the body is supported from the side, in order to eliminate the usual disturbing effect of a rear sting support.

[3] Numbers in parentheses indicate References at end of paper

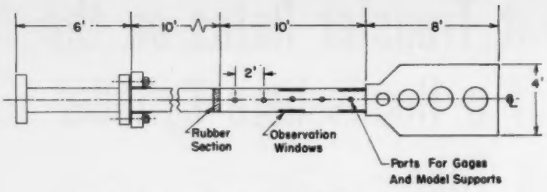


Fig. 1 $2^7/_8 \times 2^7/_8$ in. GALCIT shock tube

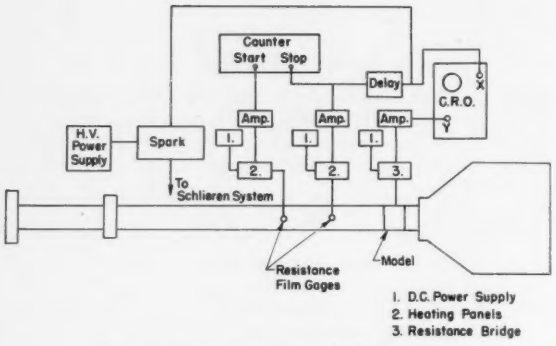


Fig. 2 Instrumentation block diagram

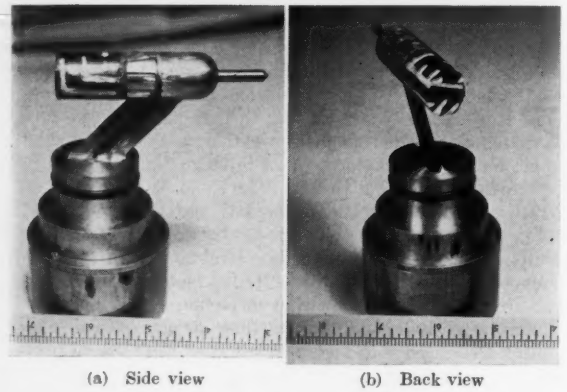

(a) Side view (b) Back view

Fig. 3 Hemisphere cylinder model

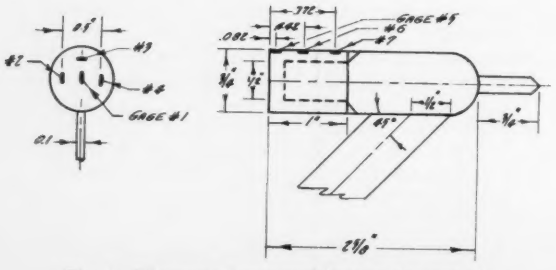


Fig. 4 Diagram of gage positions on the model

The shock tube and the instrumentation used in this investigation are described in (1); therefore, only a brief summary will be included in section 2. Section 3 presents the experimental results, including a discussion and indication of future work on this problem.

The author would like to thank Prof. L. Lees for suggesting the problem and for his many helpful discussions and suggestions.

## 2 Experimental Technique

### Shock Tube and Instrumentation

This investigation was performed in the $2^7_8 \times 2^7_8$ in. GALCIT shock tube (Fig. 1). Heat transfer rate and schlieren studies were carried out with the model placed at the 19-ft station of the straight section. The instrumentation block diagram is shown in Fig. 2 (see (1)). Shock speed is determined by measuring the time for the shock to travel between two monitoring stations spaced 2 ft apart. The heat transfer gages are used for detection, and the time is measured by the 7360 Berkeley counter. The schlieren spark is triggered through a time delay, which is activated by the downstream wave-speed monitoring gage.

The heat transfer gages are sputtered directly on the model. Their initial resistance was measured by a Wheatstone bridge and the current was measured by a milliammeter. The gage output is fed through a Tektronix 121 wide band amplifier to a 535 Tektronix oscilloscope, and the records are obtained by a polaroid camera.

The gages are calibrated for quantitative heat transfer measurements utilizing the method described in (1). The overall accuracy of the heat transfer instrumentation is about $\pm 5$ per cent as demonstrated in (1).

### The Hemisphere Cylinder Model

The model consists of a brass cylinder $\frac{3}{4}$ in. in diameter and $2\frac{5}{8}$ in. long, with a hemispherical nose. A $\frac{3}{16}$ in. spike $\frac{3}{4}$ in. long is attached to the nose in order to produce a separated region and thus insure a fully developed turbulent boundary layer upon reattachment of the flow to the cylinder surface (Fig. 3). The aft portion of the model consists of a hollow Pyrex glass "cup" $\frac{3}{4}$ in. in diameter and 1 in. long, which is waxed on the mating brass cylinder. The outside diameter of the glass and brass parts are matched to provide a continuous smooth surface, and the platinum film resistance gages are sputtered on the glass cup (Fig. 3). Four gages are positioned on the flat base—gage 1 at the center and gages 2, 3 and 4 on the circumference of a $\frac{1}{2}$ in. circle as shown in Fig. 4. Three additional gages are positioned on the cylindrical surface 0.082, 0.442 and 0.772 in., respectively, from the base, and are denoted as gages 5, 6 and 7 on Fig. 4.

The model is side-supported by a 45 deg swept-back, double wedge that is $\frac{3}{4}$ in. wide and 0.100 in. thick. This support enables schlieren observation of the aft part of the model and portions of the wake, and eliminates the need for a rear-sting.

The leads on the glass cup are provided by a thick layer of silver paint to which wires are soldered on the unexposed edge of the glass cup (Fig. 3). The wires are then led through machined grooves in the model surface, then along the side support to the outside of the shock tube. The cup is aligned so that gages 3, 5, 6 and 7 are opposite the wake of the side support in order to minimize the effect of this wake on the readings of these gages (Figs. 3 and 4).

## 3 Experimental Results

### Range of Experiments

A preliminary investigation was undertaken to determine the maximum size of the heat transfer model permitted by the blockage effects—specifically by the effect of the reflection

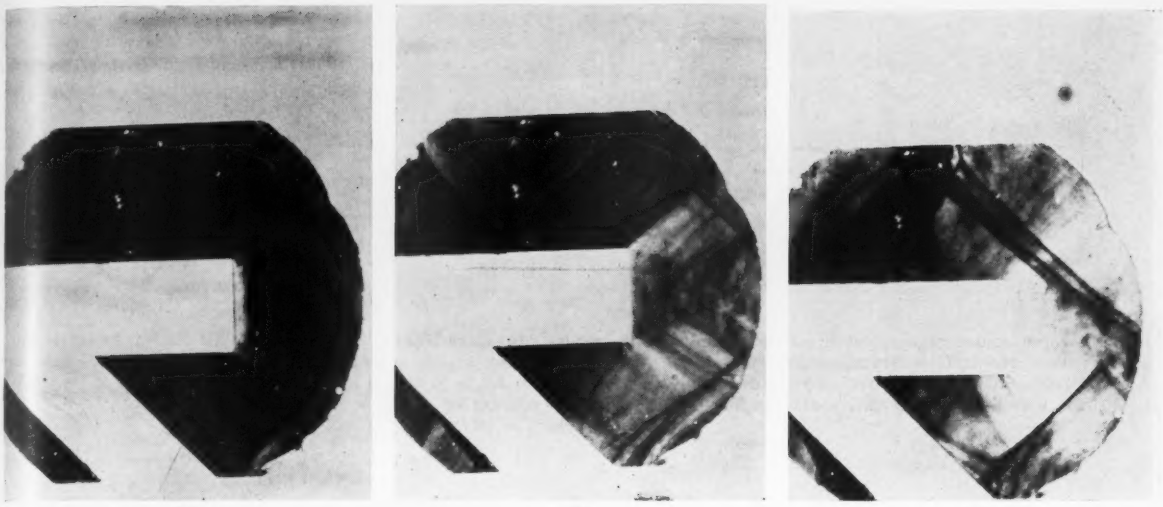

(a) (b) (c)

Fig. 5 **Schlieren studies of flow over the aft portion of the model.** (a) $M_s = 3.8$, $p_1 = 11.7$ cm Hg, $\Delta t = 40$ $\mu$ sec. (b) $M_s = 3.8$, $p_1 = 11.3$ cm Hg, $\Delta t = 140$ $\mu$ sec. (c) $M_s = 3.0$, $p_1 = 12.5$ cm Hg, $\Delta t = 360$ $\mu$ sec

by the bow shock wave from the shock tube wall. It was determined that a $\frac{3}{4}$ in. diam body can be accommodated in the $2\frac{7}{8} \times 2\frac{7}{8}$ in. section without choking the flow. For this model the ratio of blocked area to the tube cross section area is 0.07, including the projected area of the side support. However, the flow Mach number is only 1.3 to 2.0, which presents a more difficult problem so far as model length is concerned. The bow wave angle is relatively steep, and the first shock reflection from the shock tube wall reaches the model at a station between $\frac{3}{4}$ and $1\frac{1}{2}$ in., a measured from the model nose. Thus it is impractical to attempt to test a model which is shorter than the distance of the first shock reflection from the nose. The model was designed to extend about 1 in. behind the first shock reflection, thus anticipating a range of shock strengths within which the second shock reflection from the tube wall will be weak enough and will strike the wake far enough downstream of the base so as to have little or no effect on the wake structure and the base heat transfer rate.

The flow around the actual heat transfer model is shown in the schlieren photographs in Fig. 5. Figs. 5(a) and 5(b) show the developing flow at $\Delta t = 40$ $\mu$ sec and 140 $\mu$ sec, respectively, for a shock Mach number $M_s$ of 3.8. Fig. 5(c) shows the flow at $\Delta t = 350$ $\mu$ sec for $M_s = 3.0$. Fig. 5(b) indicates a fully developed wake and a relatively weak second reflection, while at the lower Mach number, Fig. 5(c), the flow is obviously choked. At high Mach number, $M_s > 4.5$, the reflected shocks again increase in strength, and a choking effect again appears. Thus the base heat rate measurements were limited to a narrow range of shock Mach numbers ($3.5 < M_s < 4.0$) because of the particular combination of flow Mach number and test section geometry. The initial pressures were varied between 3 and 17 cm Hg corresponding to Reynolds numbers/cm in the range $3.5 \times 10^4$ to $3 \times 10^5$. The lower limit is imposed by the minimum pressure required for a fully developed turbulent boundary layer, and the upper limit is set by structural considerations. The advantages of larger tube cross section dimensions and of higher flow Mach number are obvious. These considerations indicate the advantages of using an expansion nozzle as the test area for this type of investigation.

The limitations on the range of shock Mach numbers for the turbulent heat rate measurements on the cylindrical surface are not as severe, because the expansion around the shoulder limits the feedback from the wake. Good results are obtained for shock Mach numbers in the range 3.25 to 5.1.

The disturbance caused by the shock wave reflection on the model surface ahead of the heat transfer gages causes disturbances in the laminar boundary layer when one attempts to obtain laminar heat rate measurements. However, the effect is negligible for turbulent boundary layers, so the present investigation was confined to the turbulent case.

### Turbulent Heat Transfer Rate Measurements on the Cylindrical Surface

Representative gage outputs at various positions on the model are shown in Fig. 6. Fig. 6(d) is a record of gage 7 on the surface of the cylinder. Measured heat transfer rates from gages 5, 6 and 7 at $M_s = 5.8$ are shown in Fig. 7 as a function of initial pressure $p_1$. The lines drawn[4] show a relation $\dot{q} \sim p_1^{0.8}$. The heat transfer rate measured by gage 1 on the base is also shown for comparison. These base measurements will be discussed in the next section.

In Fig. 8 the heat transfer rates measured at the various locations on the cylindrical surface of the model are plotted as $\dot{q}/p_1^{0.8}$ vs. $M_s$ (were $p_1$ is measured in cm Hg abs and $\dot{q}$ is cal/cm$^2$/sec). For comparison the stagnation point heat transfer rate for $p_1 = 1$ cm Hg abs calculated for the equilibrium laminar boundary layer according to (3), is also shown. Turbulent heat transfer rates on the cylindrical afterbody are one quarter to one third of the laminar stagnation point heat transfer rate for comparable free stream conditions.

Turbulent heat transfer rates are generally expressed in terms of the Stanton number $C_H$ where

$$\dot{q} = \rho_e u_e C_H (h_{aw} - h_w) \quad [1]$$

Semi-empirical correlations of the available experimental data give

$$C_H = BRe^a Pr^b \quad [2]$$

where $a = -0.2$, $b = -\frac{2}{3}$, and $B$ depends on the local Mach number and the temperature (or enthalpy) ratio across the boundary layer. Also

$$h_{aw} = h_{se}\left[1 - (1 - r)\frac{u_e^2}{2h_{se}}\right]$$

[4] The actual Mach number varies between 3.5 and 4.0, and the heat transfer rates are normalized to $M_s = 3.8$ by the factor $[M/(M_s)]^3$.

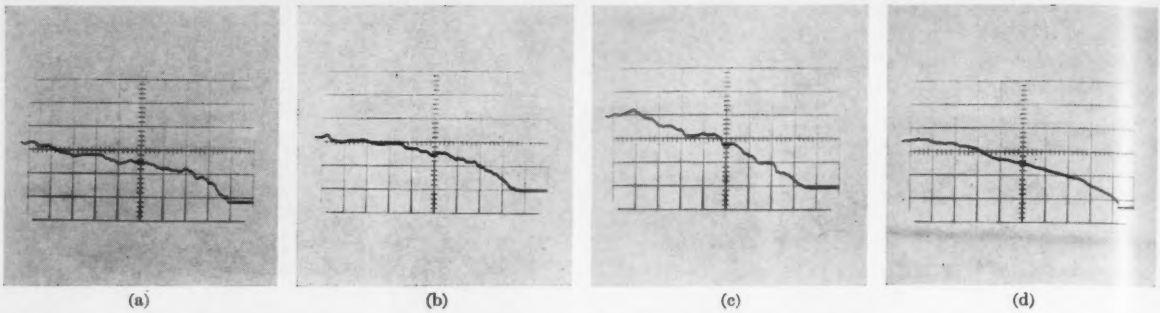


**Fig. 6 Representative gage output at various positions on the model.** (a) **Gage No. 1:** $M_s = 3.5$, $p_1 = 8.0$ cm Hg, sweep = 100 $\mu$ sec/div, $R_0 = 24.9\ \Omega$, $I_0 = 20$ ma, sensitivity = 10 mv/div. (b) Gage No. 3: $M_s = 3.6$, $p_1 = 6.6$ cm Hg, sweep = 100 $\mu$ sec div, $R_0 = 19.0\ \Omega$, $I_0 = 20$ ma, sensitivity = 5 mv/div. (c) Gage No. 4: $M_s = 3.5$, $p_1 = 6.9$ cm Hg, sweep = 100 $\mu$ sec/div, $R_0 = 20.5\ \Omega$, $I_0 = 20$ ma, sensitivity = 5 mv/div. (d) Gage No. 7: $M_s = 3.81$, $p_1 = 6.86$ cm Hg, sweep = 100 $\mu$ sec/div, $R_0 = 19.3\ \Omega$, $I_0 = 20$ ma, sensitivity = 10 mv/div

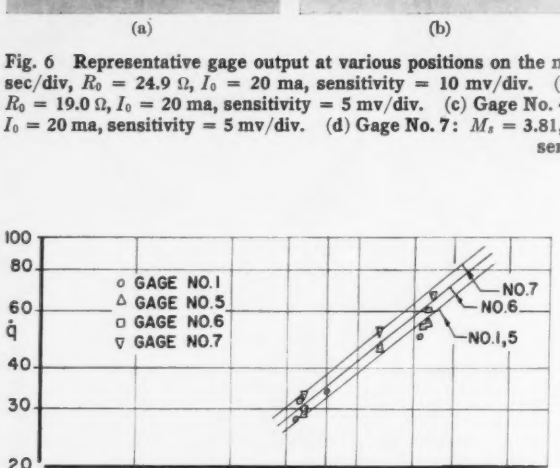


**Fig. 7 Turbulent heat transfer rate variation with pressure at $(\bar{M}_s) = 3.8$**

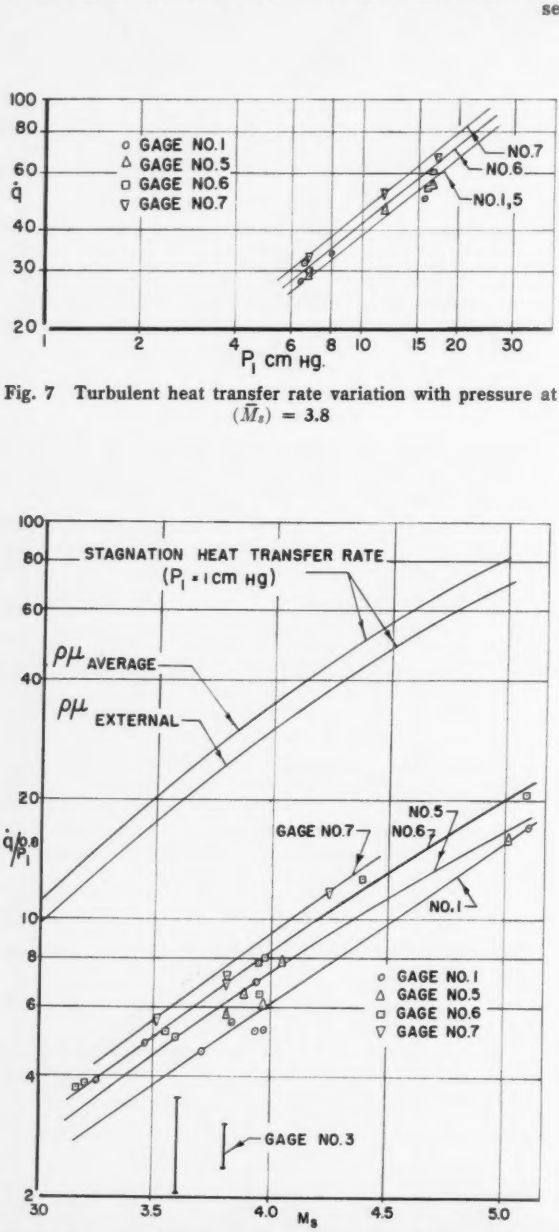


**Fig. 8 Turbulent heat transfer rate variation with shock Mach number**

where the recovery factor $r$ is approximately $Pr^{1/3}$; i.e., $r = 0.89$ for $Pr = 0.7$. According to Equations [1, 2]

$$\dot{q} = B(\rho u)_e^{0.8}\mu_e^{0.2}(Pr)^{-2/3}(h_{aw} - h_w)(\bar{x})^{-0.2} \quad [3]$$

where $\bar{x}$ is some effective length of run for the fully developed turbulent boundary layer. In other words in the present experiments the quantity $\dot{q}\bar{x}^{0.2}/p_1^{0.8}$ should be the same for all three gage locations at the same shock Mach number. This effective distance $\bar{x}$ is determined directly from the measured values of $\dot{q}$ and turns out to be remarkably constant for all three gages over the range $3 < M_s < 5.1$, with the following values: $\bar{x}_7 = 0.50$ in., $\bar{x}_6 = 0.82$ in., $\bar{x}_5 = 1.19$ in. within $\pm 5$ per cent.[5] In Fig. 9 the quantity $\dot{q}\bar{x}^{0.2}/p_1^{0.8}$ is plotted against shock Mach number; evidently the "spread" between the three gages shown in Fig. 8 is practically eliminated.

Previous measurements of turbulent heat transfer rates with zero pressure gradient are correlated very well by Equation [3], where $B = 0.03$ for $M_e \cong 0$ with $T_w/T_e \cong 1$; $B = 0.0266$ for $M_e = 0.87$, and $B = 0.021$ for $M_e = 1.62$, with $T_w/T_{aw} \cong 1$, i.e., small temperature differences. These data are obtained from (6, 7, 8, 9, 10) and are reproduced in Fig. 10. In order to compare the present results with this earlier

[5] This effective distance $\bar{x}$ for any gage is very nearly equal to the distance measured from the point on the model at which the bow shock reflected from the shock tube wall strikes the model surface (Fig. 5).

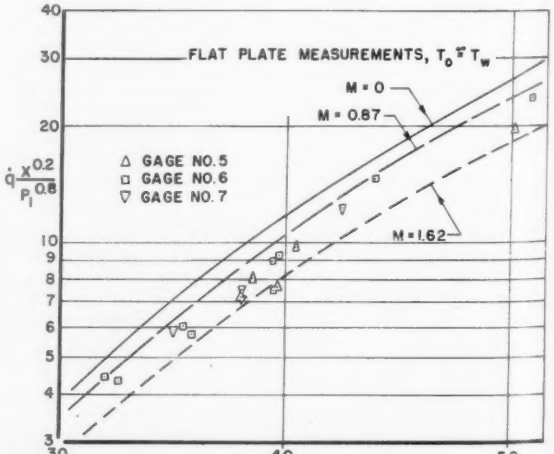


**Fig. 9 Comparison of turbulent heat transfer rate with flat plate measurements**

work the "external" flow quantities $(\rho u)_e$ and $\mu_e$ for the present experiments were computed by assuming a normal shock ahead of the model nose and an isentropic expansion along the body surface from the stagnation point to the free stream pressure $p_2$. The turbulent heat transfer data obtained in the shock tube agree remarkably well with the earlier data of (6, 7, 8) in which $T_w/T_{aw} \sim 1$. In Fig. 9 the curves representing the average of these data (obtained from Fig. 10) at Mach 0, 0.87 and 1.62 are shown. The shock tube data which correspond to local Mach numbers between 1.25 and 1.5 fall between the curves for $M = 0.87$ and $M = 1.62$. The remarkable fact here is that the corresponding ratio of stagnation to surface enthalpy increases from 3 to 8 in the present tests.

When one plots the data in the form $Nu_{\bar{x}}$ vs. $Re_{\bar{x}}$ disregarding the variation in enthalpy level (Fig. 11), the scatter in the data increases slightly as compared to Fig. 9. This scatter indicates a slight effect caused by the variation of $h_s/h_w$. One can conclude that in this Mach number range[6] the effect of enthalpy level is surprisingly small. This conclusion is in agreement with the previous results of Libby and Cresci (5).

The experiments of Libby and Cresci (5) can also be used to observe the effect of falling pressure gradients on turbulent heat transfer rates. These experiments were performed in a blowdown wind tunnel with varying stagnation pressures and temperatures during the run. In order to correlate the accumulated data, modified Reynolds and Nusselt numbers, based on stagnation conditions, were used. It is difficult without recomputing the data to obtain local heat transfer values. However, a comparison with flat plate analysis is presented in (5), from which the agreement with the local flat plate data can be examined.[7] The geometrical distance from the stagnation point has been used in evaluating the Reynolds and Nusselt numbers. This procedure is consistent with most turbulent boundary layer studies on flat plates. The fact that it seems to give good results in the case of an axially symmetric body with a falling pressure gradient is worth noting. Fig. 7 of (5) shows that the measured heat transfer rates fall within ±10 per cent of the curve described by Equation [6] of (5). Translating the particular definition of the modified Reynolds and Nusselt numbers into their conventional form results in the relation

$$Nu_x = 0.03(\rho'/\rho_e)^{0.8}(\mu'/\mu_e)^{0.2}(Pr)^{1/3}(Re_x)^{0.8} \quad [4]$$

where $\rho'$ and $\mu'$ are defined at reference conditions determined by the local pressure and reference enthalpy

$$h' = 0.5h_w + 0.22h_{s_e} + 0.28h_e \quad [5]$$

Now for the Libby and Cresci experiments $h_s/h_w$ varies between 1.3 and 1.7; thus $h' \cong h_e$. The local Mach number at the thermocouple positions in these experiments varied between 0.5 to 0.8. Thus one observes that these data agree with the flat plate data with no pressure gradients at the corresponding Mach numbers.

One can conclude from the collection of data presented here that for subsonic and low supersonic flow Mach numbers, the turbulent heat transfer rates seem to be to a surprising degree independent of falling pressure gradients, stagnation to wall enthalpy ratio, and radius of curvature when $\delta/R \ll 1$. The only appreciable effect is found to be the local Mach number, which is responsible for about 15 per cent reduction in the heat transfer coefficient by the increase of local Mach number from 0 to about 1.5.

[6] This result does not imply that the effect of $h_s/h_w$ is small also at high local Mach numbers.

[7] It may be that some of the scatter of the experimental results may be due to the correlation with respect to stagnation rather than local conditions. A replotting of the data in terms of the conventional local quantities would be very helpful in generalizing these data to other heat transfer applications.

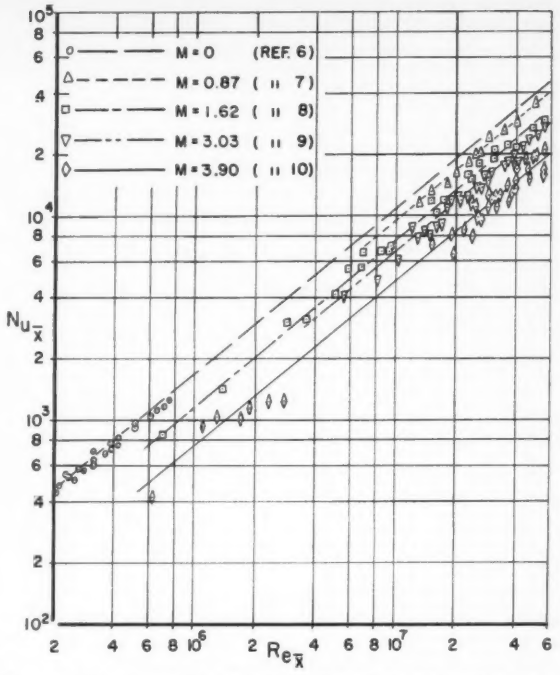


**Fig. 10 Measurements of turbulent heat transfer rates on a flat plate, $T_0 \cong T_w$ (6, 7, 8, 9, 10)**

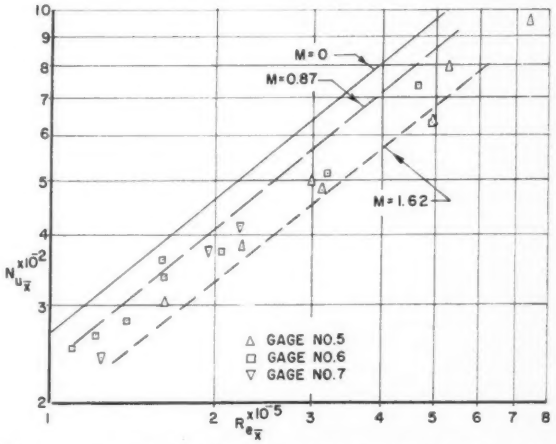


**Fig. 11 Comparison of the shock tube turbulent heat transfer rates with the flat plate results**

### Turbulent Base Heat Transfer Measurements

The arrangement of the four heat transfer gages on the blunt base is shown in Fig. 4, and representative outputs of gages 1, 3 and 4 are shown in Figs. 6(a), 6(b) and 6(c). The output of these gages is not as smooth as that of the surface gages 5, 6 and 7. However, the output of gages 1 and 3 indicates a steady heat transfer rate after a "building-up" period of about 100–150 $\mu$ sec. Gage 4 lies in the wake of the side support, and the output of this gage never gave a steady heat transfer rate. The comparison of the base heat rate at the center and at a location $\frac{1}{4}$ in. from center as measured with gages 1 and 3 is shown in Fig. 8. Gage 1 at the center of the base indicates a heat rate comparable with that of gage 5 on the surface just ahead of the base. At the gage 3 position the

heat rate is only one half to one third of this value. One should note that the output of gage 4 (though disturbed) is comparable to that of gage 3, which increases one's confidence in this result.

The experimental data indicate that a "steady" heat transfer rate is established after about 100–200 $\mu$ sec. However, the total testing time is about 400–600 $\mu$ sec, which may not be long enough to establish steady equilibrium wake flow such as may be experienced in a wind tunnel or in free flight. Until this question is settled the present base heat transfer data are considered to be preliminary and are reported mainly to call attention to this result and stimulate further thought and research into this effect. However, the fact that these measurements are repeatable, that the heat rate is steady and uniform with time after about 100–150 $\mu$ sec, and that the heat rate at the base center varies like $p_1^{0.8}$ may be used as arguments to indicate that these effects are real.

The unexpected distribution of heat transfer rate over the base, particularly the high value at the center of the base, shows the necessity for careful study of wake phenomena. One way to attack this problem is to perform similar experiments in the shock tube with a wide range of model sizes. If the observed effect is caused by the unsteady flow conditions, the size of the model should affect the results. Because of the limitation in size of the present shock tube, such a program could not be undertaken at this time. In order to shed more light on this problem, an investigation of base and wake flows is now under way in the GALCIT 5 in. continuous-flow hypersonic tunnel.

### References


1 Rabinowicz, J., "Aerodynamic Studies in the Shock Tube," GALCIT Hypersonic Research Memo. 38, June 1957.

2 Rose, P. H. and Stark, W. I., "Stagnation Point Heat Transfer Measurements in Dissociated Air," Avco Research Laboratory, Research Note 24, April 1957.

3 Lees, L., "Laminar Heat Transfer over Blunt-Nosed Bodies at Hypersonic Flight Speeds," JET PROPULSION, vol. 26, April 1956, pp. 259–269.

4 Rose, P. H. and Riddell, F. R., "An Investigation of Stagnation Point Heat Transfer in Dissociated Air," Heat Transfer and Fluid Mechanics Institute Meeting, June 19–21 ,1957.

5 Libby, P. A. and Cresci, R. J., "Evaluation of Several Hypersonic Turbulent Heat Transfer Analysis by Comparison with Experimental Data," Polytechnic Institute of Brooklyn, WADC TN 57-72, July 1957.

6 Pappas, C. C., "Measurement of Heat Transfer in the Turbulent Boundary Layer on a Flat Plate in Supersonic Flow and Comparison with Skin Friction Results," NACA TN 3222, June 1954.

7 Brevoort, M. J. and Rashis, B., "Turbulent Heat Transfer Measurements at a Mach Number of 0.87," NACA TN 3599, Dec. 1955.

8 Brevoort, M. J. and Rashis, B., "Turbulent Heat Transfer Measurements at a Mach Number of 1.62," NACA TN 3461, June 1955.

9 Brevoort, M. J. and Rashis, B., "Turbulent Heat Transfer Measurements at a Mach Number of 3.03," NACA TN 3303, Sept. 1954.

10 Brevoort, M. J., "Turbulent Heat Transfer Measurements at a Mach Number of 3.9," NACA TN 3734, July 1956.


# Technical Notes

## A Comparison of Turbojets and Ramjets for High Speed Flight


M. ARENS[1]

Israel Institute of Technology, Haifa, Israel


### Nomenclature

$F_n$ = thrust, lb
$f/a$ = fuel-air ratio
$g$ = gravitational acceleration
$P$ = total pressure
$p$ = static pressure
SFC = specific fuel consumption, lb/hr/lb
$T$ = total temperature
$V$ = velocity
$w$ = airflow, lb/sec
$\gamma$ = ratio of specific heats
$\eta$ = efficiency
$\pi$ = total pressure ratio
$\tau$ = ratio of total temperature to ambient temperature

*Subscripts*

$b$ = burner
$c$ = compressor
$e$ = nozzle exit
$n$ = nozzle entry
$o$ = ambient
$t$ = turbine
$T.J.$ = turbojet
$\lambda$ = turbine entry
$r$ = ram

THE relative advantage of ramjet powerplants over turbojet powerplants in high speed applications has taken on renewed significance with the rapidly increasing flight speed range of current airplanes. If we limit our attention to the propulsive performance of the two powerplants, in terms of thrust per pound of airflow or specific fuel consumption, it is possible to clearly delineate an area of superiority for each powerplant. Since current applications of turbojets to high speed vehicles require the use of an afterburner, the comparison is based on an afterburning turbojet, although the method can be applied to non-afterburning engines as well.

The specific fuel consumption of an air-breathing engine can be expressed as

$$\mathrm{SFC} = \frac{3600\, f/a}{F_n/w} \qquad [1]$$

If we assume that the effective combustion efficiency of the two-stage combustion process in the turbojet is equivalent to that of the ramjet combustion process, and neglect consideration of any air-leakage or bleed in the turbojet, then the fuel-air ratio to attain a desired nozzle entry temperature will be the same for both engines. Their relative superiority can therefore be measured in terms of thrust per pound of airflow

$$\frac{F_n}{w} = \frac{V_e - V_o}{g} \qquad [2]$$


Received April 4, 1958.


[1] Department of Aeronautical Engineering.

EDITOR'S NOTE: The Technical Notes and Technical Comments sections of JET PROPULSION are open to short manuscripts describing new developments or offering comments on papers previously published. Such manuscripts are published without editorial review, usually within two months of the date of receipt. Requirements as to style are the same as for regular contributions (see masthead page).

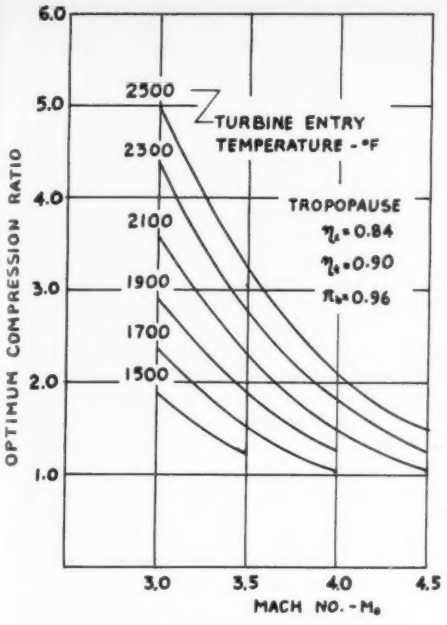


Fig. 1 Optimum turbojet compression ratio

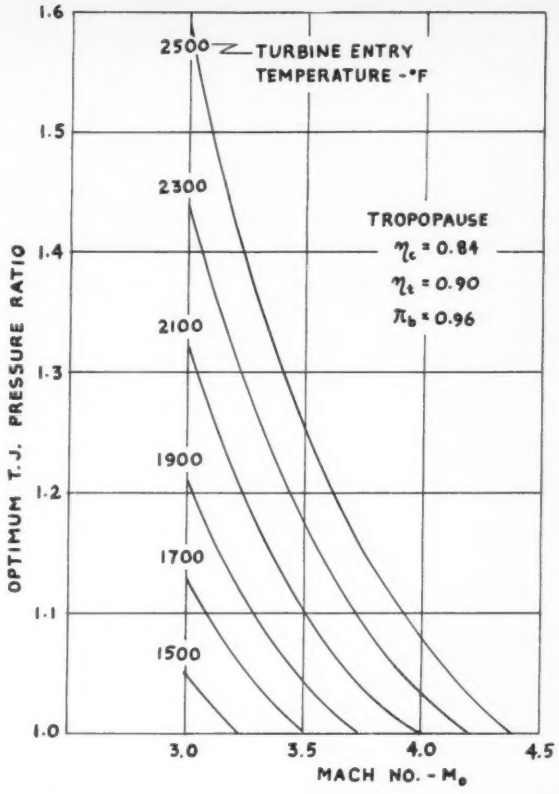


Fig. 2 Optimum turbojet gas generator pressure ratio

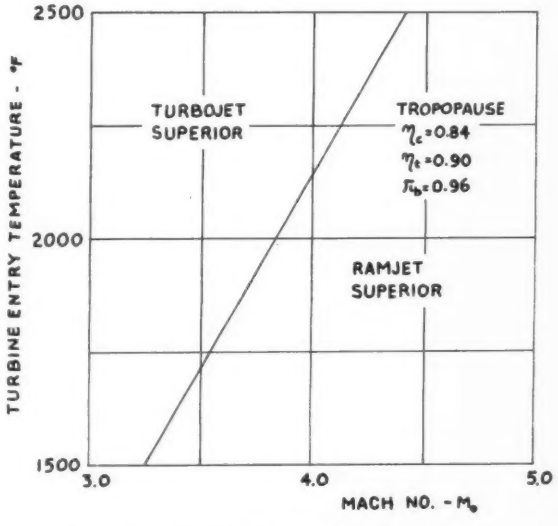


Fig. 3 Regions of turbojet and ramjet superiority

or in terms of nozzle exit velocity, since the powerplants are compared at the same flight speed. For a fully expanded nozzle[2]

$$V_e = \sqrt{\frac{2\gamma}{\gamma - 1} T_n \left[1 - \left(\frac{p_o}{P_n}\right)^{(\gamma-1)/\gamma}\right]} \quad \ldots\ldots [3]$$

and therefore, for any desired afterburner or ramjet temperature, the engine providing the highest nozzle pressure ratio is the more efficient. If it is assumed that the total pressure losses in the turbojet afterburner are equivalent to those of the ramjet combustion chamber, the requirement for turbojet superiority is

$$\pi_{T.J.} > 1 \quad \ldots\ldots [4]$$

or that the turbojet "gas generator" produce an increase in pressure.

It is obvious that for any flight speed and turbine-entry temperature there is an optimum compression ratio subject to assumed component efficiencies. Equation [5] gives the gas generator pressure ratio

$$\pi_{T.J.} = \pi_c \pi_b \pi_t \quad \ldots\ldots [5]$$

By introducing the equivalence of compressor and turbine work, as well as their respective efficiencies, one obtains

$$\pi_{T.J.} = \pi_c \pi_b \left[1 - \frac{\tau_r}{\tau_\lambda \eta_c \eta_t} (\pi_c^{(\gamma-1)/\gamma} - 1)\right]^{\gamma/(\gamma-1)} \quad \ldots [6]$$

The optimum compression ratio can then be found by differentiating Equation [6] with respect to $\pi_c$ and setting the result equal to zero

$$\frac{\partial \pi_{T.J.}}{\partial \pi_c} = \pi_b \left\{ \left[1 - \frac{\tau_r}{\tau_\lambda \eta_c \eta_t} (\pi_c^{(\gamma-1)/\gamma} - 1)\right]^{\gamma/(\gamma-1)} - \pi_c^{(\gamma-1)/\gamma} \frac{\tau_r}{\tau_\lambda \eta_c \eta_t} \left[1 - \frac{\tau_r}{\tau_\lambda \eta_c \eta_t} (\pi_c^{(\gamma-1)/\gamma} - 1)\right]^{1/(\gamma-1)} \right\} = 0 \ldots\ldots [7]$$

in which case the optimum compression ratio is

$$\partial \pi_c(\text{optimum}) = \frac{1}{(2)^{\gamma/(\gamma-1)}} \left(1 + \frac{\tau_\lambda \eta_c \eta_t}{\tau_r}\right)^{\gamma/(\gamma-1)} \quad \ldots\ldots [8]$$

and the condition for turbojet superiority is that Equation [6] be greater than one when the optimum compression ratio is used. Figs. 1 and 2 show the optimum compression ratio and gas generator pressure ratio as a function of flight speed and turbine-entry temperature, while Fig. 3 indicates the region of turbojet superiority. It may be concluded from Fig. 3 that the ramjet is the appropriate powerplant for a significant portion of the flight spectrum.

[2] Sutton, G. P., "Rocket Propulsion Elements," Wiley, 2nd edit., p. 53.

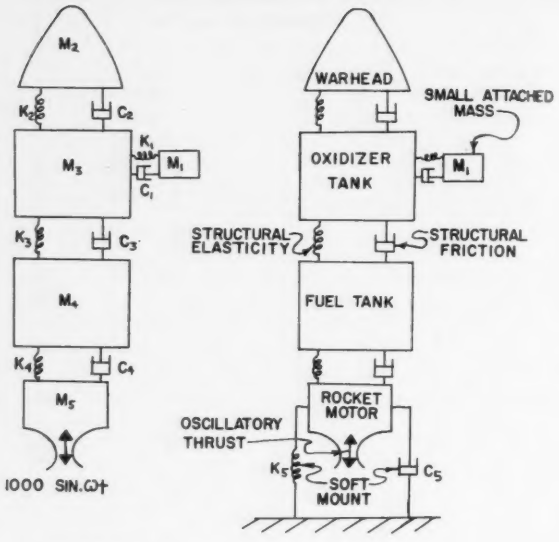


Fig. 1 Nomenclature

# Simulation of Free Flight Structural Characteristics by Captive Missile I. Computer Analysis

P. LIEBERMAN[1]

Armour Research Foundation, Chicago, Ill.

THE limitations of conventional test stands for preparing missiles to withstand the vibration environment of free flight are revealed by a computer study (1)[2] of a missile structure. A test stand mount that is soft and has a low damping characteristic is quantitatively shown to reduce the error between free and captive flight tests; however, structural considerations limit the degree of softness that can be obtained for a particular sized missile.

The purpose of this paper, which was inspired by a previous report by Lee and Miesse (3), is to determine the extent of difference between the vibration environment of missiles in captive and free flight tests during single frequency excitation and to suggest a method of obtaining captive test data that will accurately predict free flight performance. At present, until the nature of the vibration environment is better defined, the advantages of the classical steady-state vibration theory can be used. Although aerodynamic and rocket forces are random in nature, they are filtered by structural

Received April 11, 1958.

[1] Associate Research Engineer, Combustion Research Section.

[2] Numbers in parentheses indicate References at end of paper.

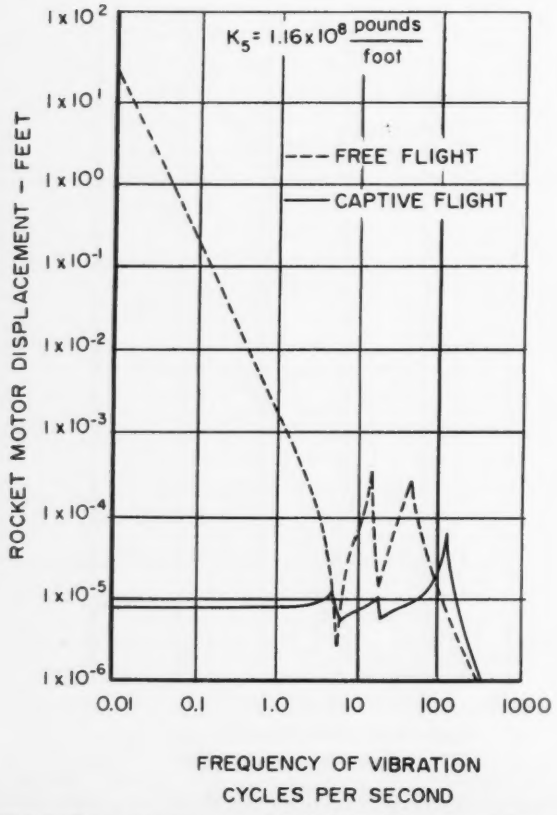


Fig. 2 Frequency response of typical missile in conventional test stand

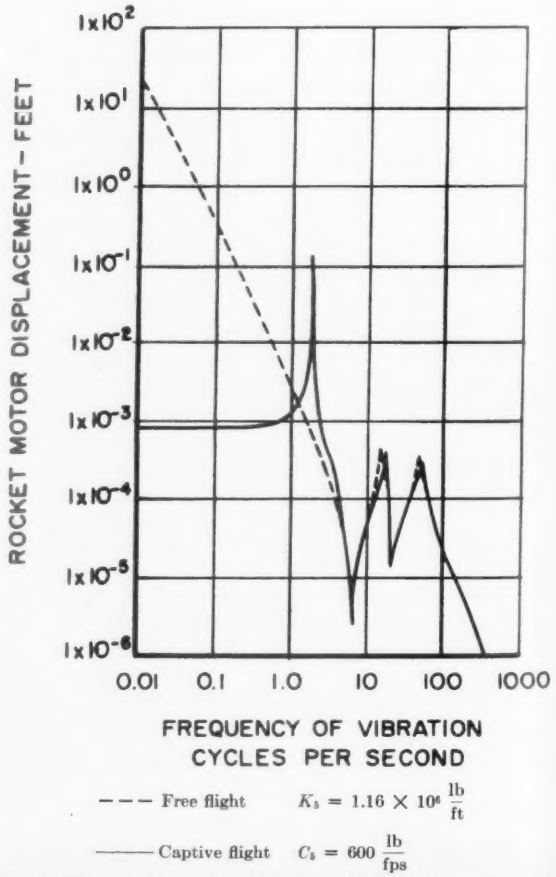


Fig. 3 Frequency response of typical missile in soft mount test stand

members and emerge as vibration confined to a narrow frequency band with an apparent fluctuating amplitude (2). Thus the classical single frequency excitation technique is valid for any degree of damping. Although the missile can vibrate in axial, bending and torsional modes, only the axial modes were considered. However, the test stand restraint resulting from an axial analysis is also applicable to the other degrees of freedom.

The variational portion of the rocket motor thrust causes a missile to vibrate as though it were a multimass spectrum interconnected by springs and dash-pots, as illustrated by Fig. 1. Restraint of the missile vibratory motion by a static test stand causes thrust energy to be reflected and absorbed in a manner which produces considerable difference between free flight and test stand frequency response.

A comparison of free flight and captive missile frequency response to an oscillatory force of 1000 lb amplitude is shown in Fig. 2, for which the spring constant of the stiff missile mounts was set up at $1.16 \times 10^8$ lb/ft. It is immediately apparent that missile mounts of this stiffness introduce considerable undertesting of the system, so that a missile which operates satisfactorily on the test stand is apt to experience violent destructive vibrations in free flight.

In an effort to avoid the errors shown by Fig. 2, various agencies have used nylon cord, cable and springs as means of restraint for small missiles in order to simulate the air cushion experienced in free flight. For large missiles, the steel torsion bar is thought to be a practical approach to soft mounting. The beneficial effects of soft mounting are vividly portrayed by Fig. 3, which assumes a spring constant of $1.16 \times 10^6$ lb/ft. For frequencies above 6 cps, it is apparent that the soft mount gives excellent simulation. If the missile vibrates at frequencies lower than 6 cps, however, then the high amplitudes must be restrained by auxillary damping and servo-control systems that will inhibit the simulation but save the test stand for future tests.

The soft mount test stand is adequate for a range of missile sizes, as well as under the condition of changing missile mass during firing. Fig. 4 shows that the placing of an IRBM-type missile on a soft mount test stand designed to be optimum for an ICBM-type missile, still permits acceptable simulation for the former. Another extreme condition occurs when the missile empties 85 per cent of its mass by ejecting propellant. As shown in Fig. 5, the soft mount designed for full tanks continues to yield adequate simulation at the end of the firing. Apparently the smaller missile masses on the flexible mount raise the missile stand resonant frequency; however, at the higher frequency, inertia reduces the amplitude discrepancy between free and captive frequency response.

As a result of this investigation, the following conclusions can be drawn:

1 Ground testing of missiles in conventional test stands is

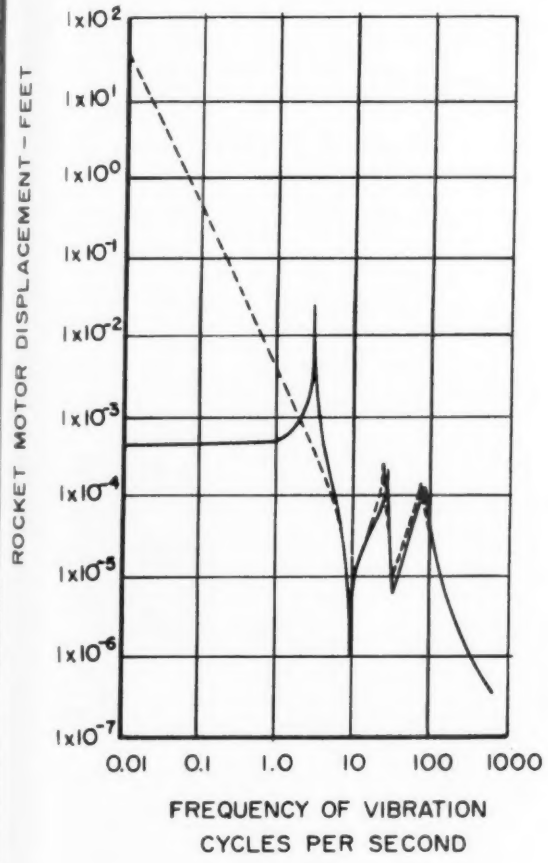


Fig. 4 Effect of placing a small missile on a mount designed for a larger missile

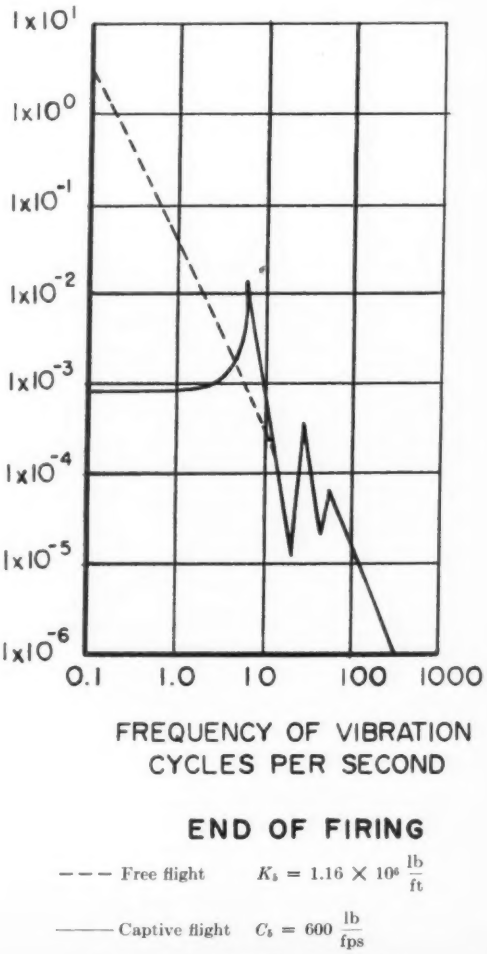


Fig. 5 Effect of emptying propellants

an inadequate method for preparing missiles to withstand the free flight vibration environment.

2 For frequencies above 6 cps, the soft mount gives excellent simulation of free flight.

3 Auxillary dampers and a control system need to accompany a soft mount if low frequency, between 0.01 and 6 cps, excitations occur. An uncontrolled low frequency excitation can tear the missile away from the test stand.

4 A soft mount test stand designed for a large missile with full tanks provides adequate free flight simulation for smaller missiles, as well as the large missile with empty tanks.

### References


1 Lieberman, P., "Simulation of Free Flight Missile Vibration in a Static Test Stand," Rocket Engine Test Laboratory, Edwards Air Force Base, June 1957.

2 Crede, C. E. and Lunney, E. J., "Establishment of Vibration and Shock Tests for Missile Electronics as Derived from the Measured Environment," WADC Technical Report 56-503, 1956; ASTIA Document AD 118133.

3 Lee, Y. C. and Miesse, C. C., "On the Structural Vibration and System Stability of a Captive Missile," Proceedings of the First Technical Symposium on Ballistic Missiles, June 1956 (Confidential).



ENGINEERS
SCIENTISTS
MATHEMATICAL ECONOMISTS

*for*

**WEAPON SYSTEMS**

ANALYSIS • SYNTHESIS
OPERATIONS RESEARCH

*at*

**GENERAL ELECTRIC'S**
TECHNICAL MILITARY PLANNING OPERATION
**(TEMPO)**

in Santa Barbara, California

Professional staff openings for graduates with advanced degree work in . . . .

MATHEMATICS • STATISTICS
MATHEMATICAL ECONOMICS
OPERATIONS RESEARCH
ENGINEERING OR PHYSICS

*Activities include:*

WEAPON SYSTEMS ENGINEERING

- Propulsion Systems
  Air-breathing, Nuclear, Rocket
- Military Electronics
  Undersea Communications
  Inertial & Radio Guidance
  Propagation Studies

OPERATIONS ANALYSES OF WEAPON SYSTEMS

- Logistics Analyses
- Mathematical Model Construction
- Cost Analyses

The Technical Military Planning Operation serves General Electric and its customers in studies of future military environments, synthesis of weapon systems, and analyses of the effectiveness of military systems.

TEMPO is located on the coast (100 miles west of Los Angeles) in beautiful Santa Barbara, between mountains and the sea.

*Please address your resume and salary requirements to:*
Mr. R. N. DYRUFF, Room M-6
Professional Personnel

GENERAL ELECTRIC

735 State Street
Santa Barbara, California

SCA *Producers of Guidance Slip Rings for*

**BOMARC ***
**POLARIS**
**THOR**

* 60-RING BOMARC SLIP RING

*Experience on Projects such as:*

- JUPITER "C"
- JUPITER
- REDSTONE
- ATLAS
- NIKE
- CORPORAL
- NAVAHOE
- AND OTHERS

*Write for illustrated brochure*
Dept. JP
SLIP RING COMPANY OF AMERICA
3612 WEST JEFFERSON BLVD.
LOS ANGELES 16, CALIF.

*Sales Engineers throughout the U.S. & Canada*

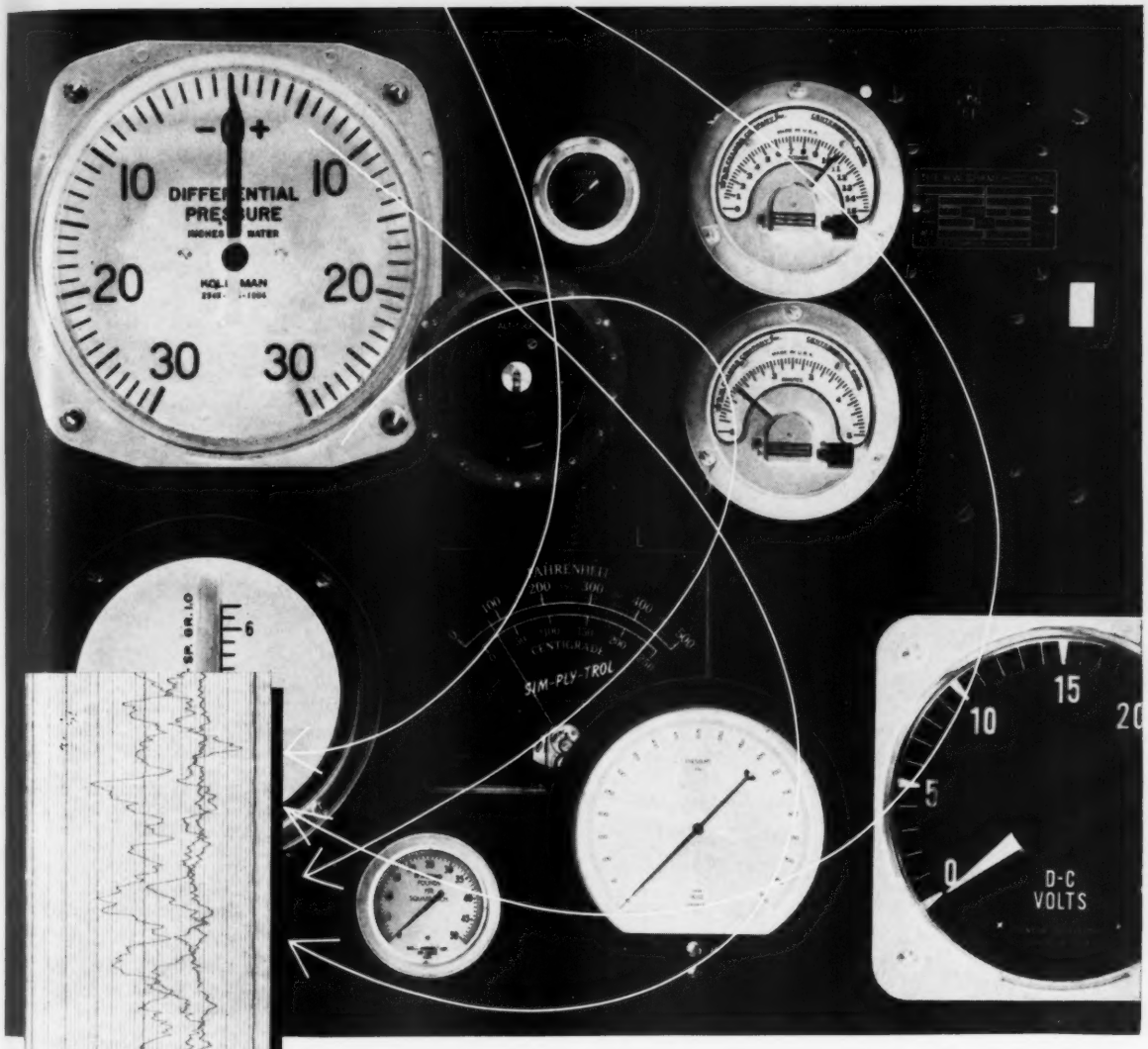


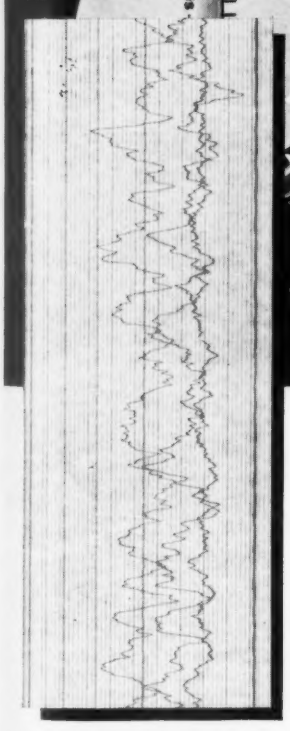

Kodak Linagraph Direct Print Paper is available in rolls of 5″ x 200′, 6″ x 100′, 7″ x 200′, and 12″ x 200′. Special sizes on request.

# Readout:

## *as fast as you can read a dial*

Now you can read oscillograph data as quickly as you read meters—with *no* wait for photochemical processing.

Kodak Linagraph Direct Print Paper, used in suitable moving-mirror galvanometer oscillographs, permits immediate record analysis.

Other advantages of Direct Print Paper: You can record frequencies from 0 to 3000 cps; you get sharp traces; you can write on it easily with pen or pencil; you can make it permanent by fixation.

**Get all the details on new Kodak Linagraph Direct Print Paper by writing to:**

**EASTMAN KODAK COMPANY**
**Graphic Reproduction Division**
**Rochester 4, N. Y.**

Kodak
TRADE MARK

## Aircraft Gas Turbine Engineers

# CONSULTANT POSITIONS in MECHANICAL DESIGN AERO-THERMODYNAMICS

***These are two parallel positions, with like lines of responsibility.***

You serve as a consultant on major (aerodynamic and thermodynamic) (mechanical design) problems encountered in conceiving and developing aircraft gas turbines.

In this capacity, you provide technical guidance on (aero-thermodynamic) (mechanical design) programs, contributing your broadest and most advanced engineering knowledge and understanding.

Specifically, you initiate and integrate the long-range planning required to exploit broad (aero-thermodynamic) (mechanical design) advances. You also promote acceptance of these plans by related engineering components, to assure coordinated engineering effort.

***Experience:***

You should have a minimum of 5 years' responsible (aero-thermodynamics) (mechanical design) experience in aircraft gas turbines, plus other work in the field, from preliminary design through production.

***Reply in complete confidence to:***

Mr. William Merrill

Professional Employment

SMALL AIRCRAFT ENGINE DEPARTMENT

1119 Western Avenue

West Lynn, Mass.

GENERAL ELECTRIC


# New Patents

**George F. McLaughlin,** *Contributor*

**Convertible aircraft with jet-driven lifting rotors (2,823,875).** A. C. Peterson, Edina, Minn.

Means are provided for rotational propulsion of the rotor unit or alternative translation propulsion of the aircraft.

**Fabricated gas turbine structures (2,824,359).** E. C. Rhodes and D. W. Rhys, Hounslow, England, assignors to The International Nickel Co., Inc.

Hollow blade of chromium alloy adapted to be subject to corrosive conditions prevailing at temperatures of about 600 to 850 C.

**External turbine jet engine (2,831,320).** W. E. Duncan, Miami, Fla.

Casing integral with an end wall and rotatably mounted on a stationary support. A fluid stream is directed against the periphery of the wall and through fluid guiding passages which interact with the stream to rotate the casing.

**Devices for releasably holding the rear ends of rockets (2,831,400).** H. Hosli, Geneva, Switzerland, assignor to Brevets Aero-Mechaniques, S. A.

Pressure from the rocket nozzle actuates a central piston connected to a pair of pivoted jaws holding the rear of a rocket, opening the jaws and releasing the rocket.

**Automatic parachute release (2,831,721).** R. Gross, Dayton, Ohio, assignor to USAF.

Load release for shroud lines, consisting of an explosive charge in the lower end of a cylinder. Slow-burning power charges ignite the main charge upon actuation of a trigger, blowing a closure member away from a hook holding a ring attached to the load.

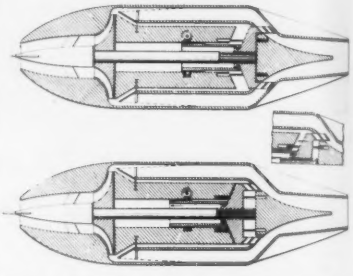

**Convertible turbojet and ramjet engine (2,832,192).** N. N. Budish, Seattle, Wash., assignor to Boeing Airplane Co.

Bladed gas turbine mounted for shifting in the axial direction between two positions. In first position, blades project within the gas flow passage; in second position, blades are withdrawn, leaving the gas flow passage unobstructed.

**Gas turbine fuel control system responsive to speed and compressor load (2,832,193).** H. J. Wood, Sherman Oaks, Calif., assignor to Garrett Corp.

Means for subjecting to differential pressure a movable wall connected to operate a fuel valve. A valve in the line

---

EDITOR'S NOTE: Patents listed above were selected from the Official Gazette of the U.S. Patent Office. Printed copies of patents may be obtained from the Commissioner of Patents, Washington 25, D. C., at a cost of 25 cents each; design patents, 10 cents.

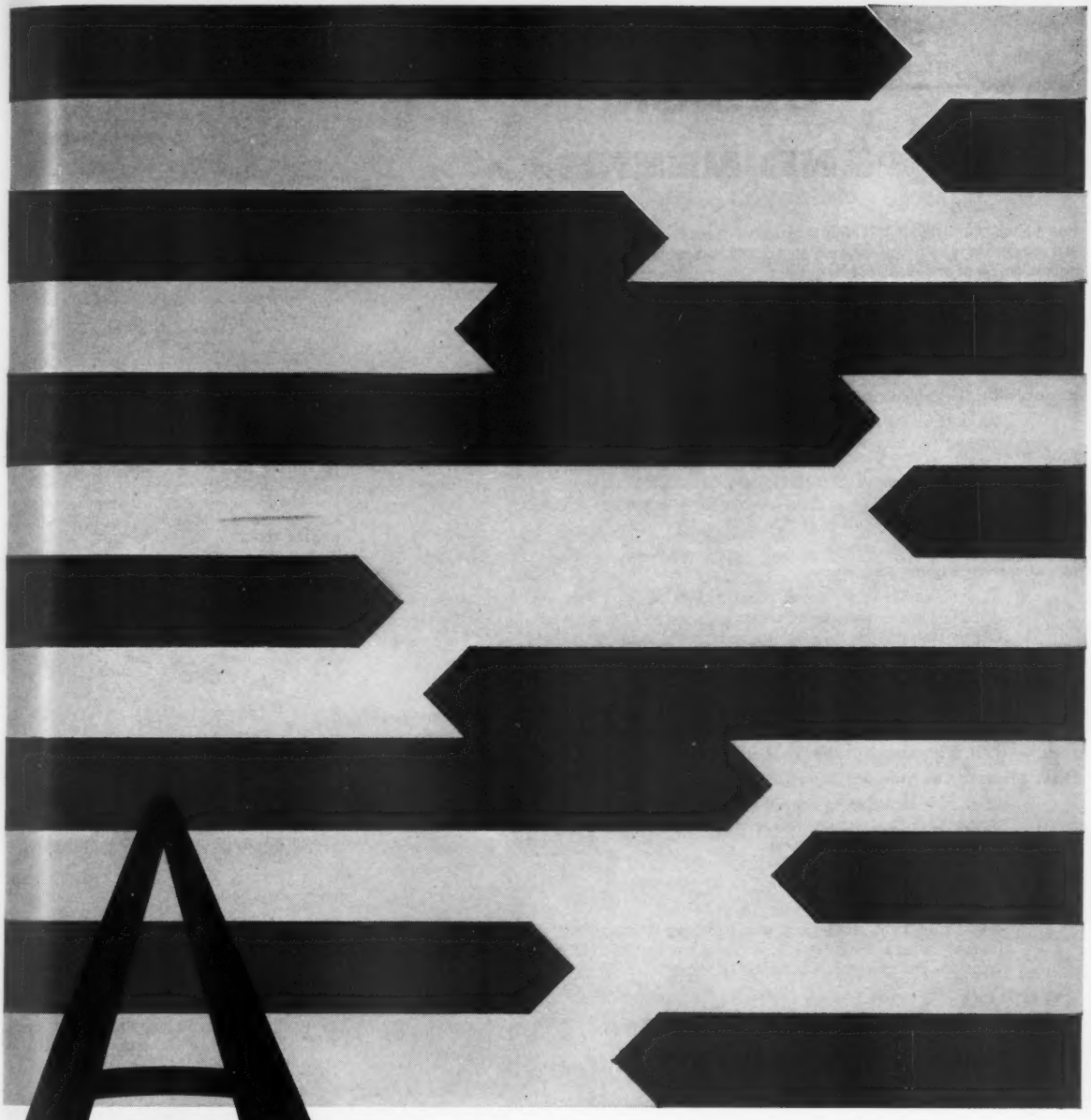

**ASTRODYNE** —aimed for the future in solid rocketry

Astrodyne was founded early this year to bring together in one productive group all the skills, experience, and facilities it takes to design and manufacture America's major solid propellant missile systems.

From Phillips Petroleum Company came men with impressive backgrounds in research, design, and manufacture of superior solid propellants. From North American Aviation came men who know missile systems management, and who have designed and built the largest rocket engines in use today.

Today Astrodyne has the experience to design, develop, and manufacture complete propulsion systems, extruded and cast propellants, solid propellant rocket motors, and boosters, and gas generator charges for auxiliary power units.

Inquiries are welcomed on any phase of the solid propellant field—from preliminary design to quantity production.

**ASTRODYNE, INC.**
McGREGOR, TEXAS

# ANALYSIS AND DESIGN ENGINEERS

New projects at GRUMMAN AIRCRAFT have created responsible positions for graduate engineers with initiative and imagination to carry out individual studies and participate in group efforts on propulsion systems and installations for advanced aircraft and missiles.

## PROPULSION DEPARTMENT

**Propulsion Aerodynamicist**

MS in AE with at least five years' experience in aerodynamics of fluid flow. Emphasis is on aerodynamics of propulsion systems—particularly external flow effects on induction system and exit system design of high-speed vehicles. Knowledge of supersonic and hypersonic flow theory mandatory. Experience in the propulsion aerodynamics of VTOL and STOL aircraft desirable. Will be responsible for setting up applied research projects and performing design and analysis work in support of advanced design effects.

**Missile Propulsion Engineer**

BS or MS in AE, ME, Physics or Chemistry with 3-5 years' experience in rocket and/or ramjet propulsion system analysis and system application. Additional experience involving supervision, military requirements, customer liaison, research, engine development, or testing is desirable.

**Engine Performance Analyst**

BS or MS in AE or ME with 3-5 years in turbojet and ramjet performance analysis. Experience required with IBM 704 programing application to engine performance.

**Heat Transfer Engineer**

BS or MS in AE, ME or Physics, with 3-5 years of research or analytical experience in applied heat transfer or thermodynamics. Work involves aircraft air conditioning, aerodynamic heating, engine installation cooling, and ice removal.

**Applied Mathematician**

Master's Degree in mathematics with experience in applied mathematics or mechanics. Work involves studies and investigations in the fields of heat transfer, aerodynamics, thermodynamics, propulsion and statistical computational techniques.

## POWER PLANT AND EQUIPMENT INSTALLATION DEPT.

**Fuel System Engineer**

BS in ME, CE or AE or equivalent with 2-5 years' experience in fuel system design for recent military jet aircraft. Technical knowledge and experience in the following fields required:

Basic jet aircraft fuel system design and analysis.

Design of fuel system components and accessories and attendant vendor and military service liaison problems.

Design and installation engineering of internal self-sealing, bladder and integral fuel tanks.

Design of pressure fueling and flight refueling systems and flight refueling packages.

**Power Plant Installation Engineers**

Graduate engineers with 5 or more years' experience in the design and installations of turbo-jet, turbo-prop, ramjet and rocket engines for aircraft and missile propulsion systems. Additional experience in supervision, manufacturing, or test development would be beneficial.

U. S. Citizenship required. We pay moving expenses.

For immediate interview, send your resume to:

MR. A. WILDER, Engineering Personnel Director

**GRUMMAN AIRCRAFT ENGINEERING CORPORATION**

**Bethpage • Long Island • New York**


connected to the downstream side of the throttle modulates the pressure level acting on the wall.

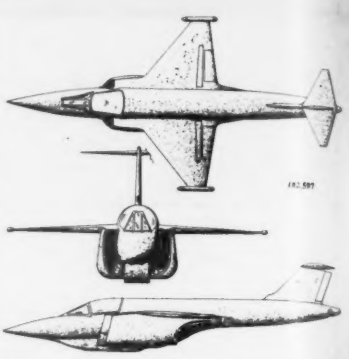

**Airplane design (182,597).** A. Kartveli, Huntington, N. Y., assignor to Republic Aviation Corp.

Twin-engine single-seater jet with exhausts close to the fuselage, below the wing roots.

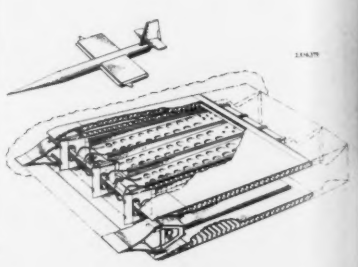

**Ramjet wing system for jet propelled aircraft (2,836,379).** B. T. Salmon, San Diego, Calif., assignor to General Dynamics Corp.

Ramjet propulsion integrated with the wings of an aircraft as to constitute a power plant which is compact in size and efficient in operation at supersonic speeds. The configuration propels and serves to sustain the aircraft in flight.

**Missile launcher (2,837,970).** H. A. Helstrom Jr., Dallas, Tex., assignor to Chance Vought Aircraft, Inc.

Device for successively launching rockets. Missiles are retractably mounted in guides, and positioned for launching by chains and sprockets actuated by an electrical motor.

**Hydraulic ejection equipment for missiles (2,837,971).** R. Wosak, Quaker Hill, Conn., assignor to General Dynamics Corp.

Balancing system for ejecting missiles from a submarine or other installation under the sea. A passageway connects a water cylinder with the sea whereby the hydraulic pressure from the sea is the same in the cylinder as it is at the muzzle end.

**Automatic emergency radio control system (2,838,255).** J. J. Hagopian, San Jose and S. R. Hennies, Los Altos, Calif., assignors to Northrop Aircraft Corp.

Control circuit for an aircraft to be initially launched and connected to operate a control member in accordance with radio signals from a manually operated remote transmitter. A time delay relay operates a reset switch after the switch is energized for a predetermined time interval. The relay is energized simultaneously with launching of the aircraft.

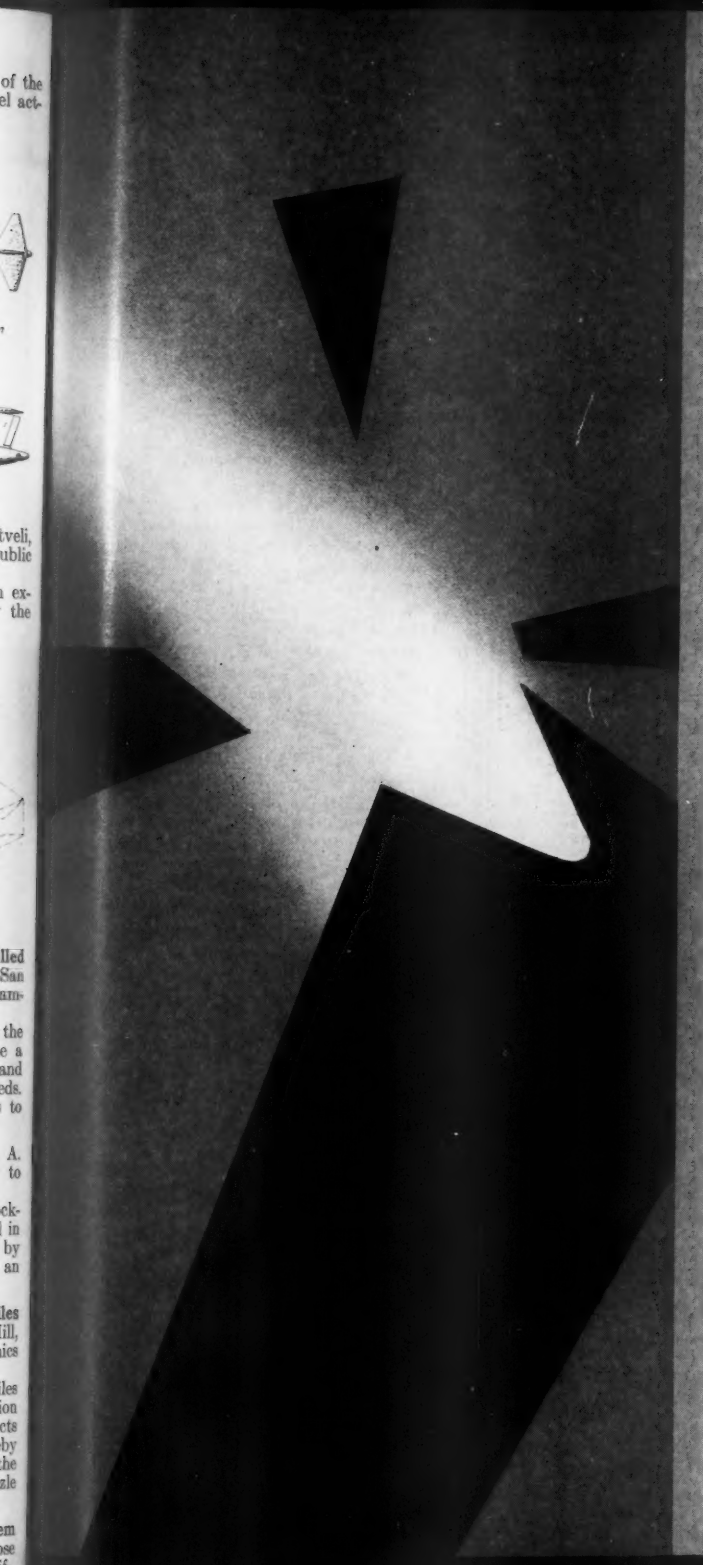

# THE PLASMA JET—

## a case of research and advanced development

Development of a re-entry simulation facility for the Air Force *Titan* ICBM nose cone required a method for heating air to extremely high temperatures. A special type of electrical discharge, sometimes called a "plasma jet," was considered. Both *fundamental* research—to obtain a quantitative understanding of the arc properties and mechanism—and *applied* research in actual aerodynamic and materials testing were needed. Advanced development—the actual design and construction of improved test facilities—was also an inherent part of the problem.

Theoretical and experimental physicists, aerodynamicists and physical chemists began a simultaneous attack on the fundamental processes. At the same time, and in close association with the others, instrumentation and mechanical engineers began to build and use a series of continually improved facilities for re-entry testing. Those inclined toward either fundamental or applied research in their particular specialty were able to maintain their integrity and their own research approach. At the same time they were able to benefit from the close working association with one another.

The results were especially fruitful. The plasma jet has proven an excellent tool for re-entry studies. Investigations of important applications in high-temperature chemistry, space propulsion and refractories are following as an added bonus.

Research and Advanced Development is more than a descriptive title at Avco. It is a concept that promotes creativity.

*For information on unusual career opportunities for exceptionally qualified scientists and engineers, write to: Dr. R. W. Johnston, Scientific and Technical Relations, Avco Research and Advanced Development Div., 201 Lowell Street, Wilmington, Mass.*

**Avco**

*Research & Advanced Development*

# SR. PERFORMANCE ANALYST

(AE or ME)

**TURBOJET MACHINERY**

*. . . a unique application of your skills on the*

AIRCRAFT NUCLEAR PROPULSION PROGRAM

Now in an advanced development stage at General Electric, the ANP program has an important new assignment for an engineer with 6 to 10 years of progressively more advanced experience in one or more of the following fields:

**Propulsion System Performance Analysis; Aero-Thermodynamics of Turbomachinery; Power Plant Installation (Aero-Thermodynamics)**

This engineer's primary responsibility will be to integrate, *cycle-wise*, the performance of turbomachinery with all-over power plant design for nuclear powered aircraft.

He will formulate and direct performance analysis projects to further these objectives; coordinate the work of contributing groups; assess the effectiveness of analysis, design and development work involved.

*Qualified Applicants, interested in the challenge of this pioneering assignment, are requested to write to:*

**Mr. P. W. Christos, Div. 34-MU**

AIRCRAFT NUCLEAR PROPULSION DEPT.

**GENERAL ELECTRIC**

**P.O. Box 132** **Cincinnati 15, Ohio**



# "MONOBALL"®

Self-Aligning Bearings

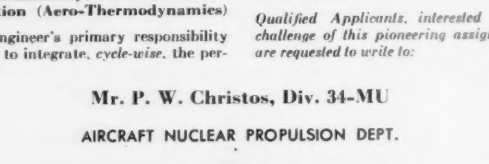


CHARACTERISTICS

| | ANALYSIS | RECOMMENDED USE |
|---|---|---|
| 1 | Stainless Steel Ball and Race | For types operating under high temperature (800-1200 degrees F.). |
| 2 | Chrome Alloy Steel Ball and Race | For types operating under high radial ultimate loads (3000-893,000 lbs.). |
| 3 | Bronze Race and Chrome Steel Ball | For types operating under normal loads with minimum friction requirements. |

**Thousands in use. Backed by years of service life. Wide variety of Plain Types in bore sizes 3/16" to 6" Dia. Rod end types in similar size range with externally or internally threaded shanks. Our Engineers welcome an opportunity of studying individual requirements and prescribing a type or types which will serve under your demanding conditions. Southwest can design special types to fit individual specifications. As a result of thorough study of different operating conditions, various steel alloys have been used to meet specific needs. Write for revised Engineering Manual describing complete line. Dept. JP-58.**

**SOUTHWEST PRODUCTS CO.**

1705 SO. MOUNTAIN AVE., MONROVIA, CALIFORNIA


# Book Reviews


**Ali Bulent Cambel,**
**Northwestern University,**
***Associate Editor***


**Microwave Measurements,** by Edward L. Giuyton, McGraw-Hill, New York, 1957, 476 pp. $12.


Reviewed by ARTHUR BRONWELL
Worcester Polytechnic Institute


"Microwave Measurements" serves the very valuable function of bringing together in one volume much of the significant material on this subject. The author's research experience in this field enables him to appraise the material accurately and also to bring this up to date with a wealth of information on recent developments, many of which have come out of researches of the laboratories which he directs at Stanford University. This book presumes a knowledge of basic material in electromagnetic theory. The derivations of the equations are not given, but most beginning texts in microwaves will supply this information.

The treatment of klystrons goes far beyond that of other texts in supplying both practical information regarding design and theoretical formulations for analyzing performance. It considers such aspects as klystrons used as oscillators, converters, amplifiers and frequency multi-


**COMPLETE TESTING FACILITIES**

★ **Qualification Tests**
★ **Evaluation Tests**
★ **Performance Tests**
★ **Environment Tests**

*Manufacturers of Metal Boss Seals to Military Specifications*

*Aetco*

**AIRCRAFT EQUIPMENT TESTING CO.**

**1812 Fleet St., Baltimore 31, Md.**

ORleans 5-8337 ORleans 5-2222

pliers, as well as methods of obtaining tunable klystrons. There is a section on re-entrant cavity oscillators and a short section on traveling wave tubes. The absence of information on the magnetron is unfortunate.

The sections on the generation and detection of laboratory signals will be extremely helpful to those engaged in laboratory practice. The chapter on measurement of microwave power reflects the excellent work done on balometer bridges and calorimeters during the war, which has not been much improved on in basic principle since. In the chapter on impedance concepts there is a rather shy treatment of Maxwell's equations, followed by an extensive analysis of standing waves on transmission lines, a subject which is further elaborated upon to good effect in the following chapter on impedance measurement.

Subsequent chapters deal with the measurement of wave length and frequency, as well as a rather thorough treatment of the measurement of $Q$ of cavities. An interesting innovation is the inclusion of a section on the use of molecular absorption as microwave frequency standards.

One gets the impression that the author is much more at home with circuit equations than with Maxwell's field equations. Perhaps it is in the nature of the text, dealing as it does with the entire gamut of microwave measurements, that circuit concepts should predominate. There is a dearth of information on waveguides and microwave filters using waveguide elements. However, the book is thorough in its treatment and contains a great deal of material of value to those who are working in the microwave field.

**Automatic Feedback Control System Synthesis,** by Prof. John G. Truxall, McGraw-Hill, New York, 1955, 675pp.

Reviewed by Scott H. Cameron
Armour Research Foundation

In spite of the fact that the years since World War II have seen the development of many new and powerful techniques for the synthesis of automatic feedback systems, much of the design of such systems is still carried out in our development laboratories by means of inefficient cut and try procedures. This book by Dr. Truxall should do much to correct this situation. While intended as a text for course work at the graduate level, the clarity of style and the well chosen examples render the book suitable for self study.

The book begins with a discussion of the LaPlace transform which is unusually good for a servomechanism text. The emphasis in this chapter is placed on the time domain-frequency domain relationships which are so essential to a firm grasp of the material to follow. The LaPlace transform discussion is followed by a chapter on signal flow diagrams as applied to feedback theory in which the signal flow diagram is used to derive and prove some of the more important Bode feedback theorems with astonishing simplicity. Other chapters treat the synthesis of RC networks, the synthesis of complete feed-

NOW IN VOLUME PRODUCTION AT C.A.E.

. . . the TC-106
(USAF TYPE MA-1A)
PORTABLE COMPRESSOR for GROUND SUPPORT APPLICATIONS

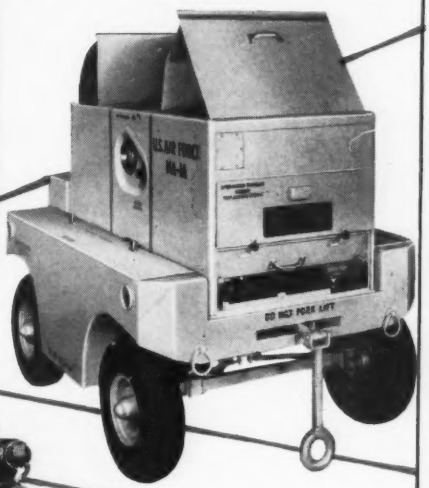

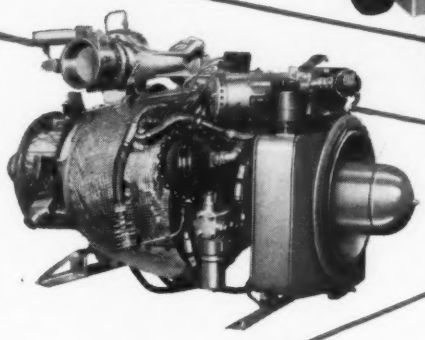

MODEL 141 TURBO-COMPRESSOR ENGINE

Typical of the finest results of Continental development is the TC-106 portable compressor unit for ground support applications. This advanced new model, with a high performance turbine compressor as its heart, weighs one-third less than its predecessor, yet has 17 per cent higher output, and in addition, other important qualities: greater mobility, less noise, and a completely automatic control system. . . . It is now in volume production at the Continental Aviation and Engineering Toledo plant.

C.A.E. gas turbine models—the J69-T-9, the J69-T-2, and the J69-T-19A are being built for Cessna's T-37A twin jet trainer, Temco's TT-1 Navy jet trainer, the Beech jet Mentor trainer, and the Ryan Q-2A Fire Bee target drone.

CONTINENTAL AVIATION & ENGINEERING CORPORATION
12700 KERCHEVAL AVENUE, DETROIT 15, MICHIGAN

SUBSIDIARY OF CONTINENTAL MOTORS CORPORATION

When you need an aluminum fuel pump this big for your rocket to the moon, Morris Bean & Company will cast it for you.

Actually, no such casting exists.

*It could.*

We have developed unique foundry techniques which we now use in production on castings weighing thousands of pounds. These castings have extensive areas 9 to 12 inches thick which must be porosity free.

We are also casting solid and hollow mandrels used to form solid propellant.

The outstanding contribution of our large aluminum castings is drastically reduced first and ultimate costs.

Telephone or write for information now.

Morris Bean & Company
Yellow Springs 6, Ohio

# large aluminum castings!

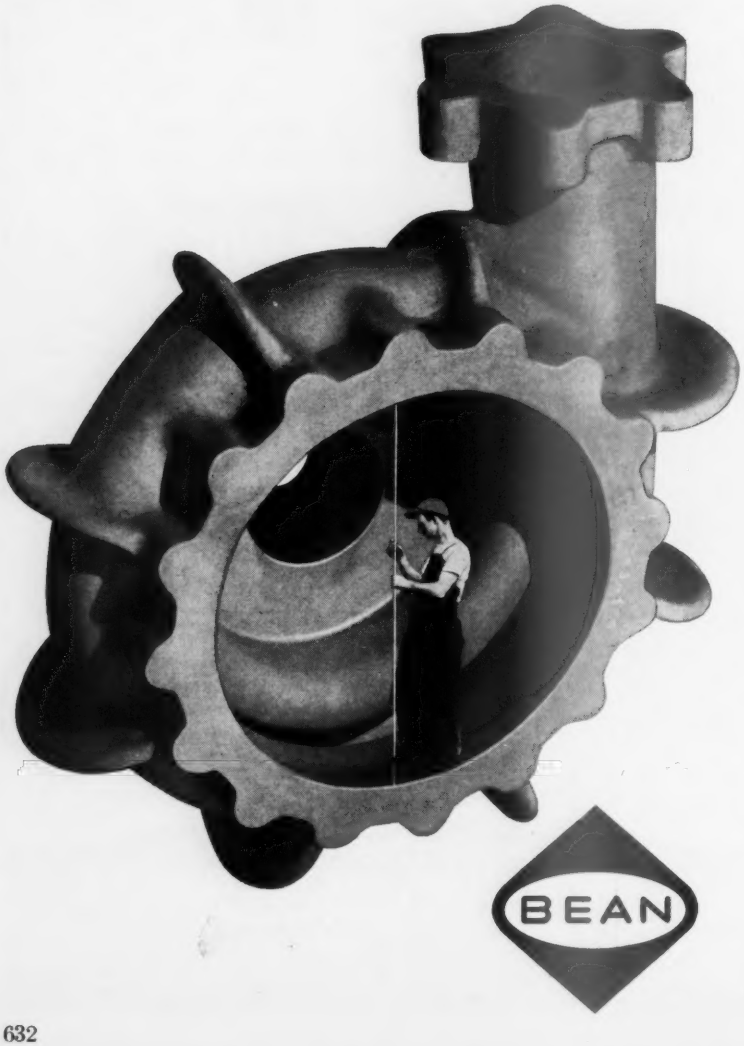


back control systems through zero-pole configurations, the root-locus method of Evans, the application of statistical design principles together with the appropriate background material, sampled data systems, and the analysis of nonlinear systems by means of the describing function and phase plane techniques. Much of the material in these later chapters appears here for the first time in book form, having appeared previously in the form of technical papers and unpublished Doctoral theses.

The book is entirely theoretical, and Dr. Truxall seems to be capable of extremely lucid theoretical discussions. He first presents the broad theoretical picture and then fills in the details by means of appropriate examples and well executed drawings. For those with a desire for still more detail the references are liberal and complete. This reviewer regards Dr. Truxall's book as essential for anyone concerned with the design or analysis of automatic feedback systems. The single criticism might be the omission of any problems which, it is noted, might have made this text, already long, somewhat unwieldy.

### Book Notices

**Elements of Engineering Thermodynamics,** by Rolf H. Sabersky, McGraw-Hill, 1957, 318 pp. $9.50. This book has been prepared for the undergraduate course in engineering thermodynamics. The author has succeeded in writing a concise and up-to-date book. The many illustrations related to jet propulsion should make it particularly suitable for students interested in this field.

**Engineering Thermodynamics,** by C. O. Mackey, W. N. Barnard and F. O. Ellenwood, John Wiley & Sons, 1957, 428 pp. $7.95. Although based on the well-known text, "Heat Power Engineering," by Barnard, Ellenwood and Hirshfeld, this book actually is an entirely new book. It is aimed at undergraduate engineering students.

### Books Received

**Strengthening Science Education for Youth and Industry,** by T. A. Edison Foundation Institute, New York University Press, New York, 1956, 162 pp. $5. This constitutes the Proceedings of the Seventh Thomas Alva Edison Foundation Institute, held Nov. 19–20, 1956.

**Fatigue in Aircraft Structures,** edited by A. M. Freudenthal, Academic Press, 1956, 456 pp. $12. This constitutes the Proceedings of the International Conference on Fatigue in Flight Structures which convened at Columbia University in 1956. It includes the contributions of the following authors: R. J. Atkinson, P. D. Brooks, J. Cornillon, S. Eggwertz, P. J. E. Forsyth, A. M. Freudenthal, E. Gassner, H. Giddings, R. F. Hanstock, R. A. Heller, M. Hempel, H. T. Jensen, W. W. Johnstone, P. Kuhn, B. Lundberg, A. O. Payne, C. E. Phillips, R. L. Schleicher, N. Thompson, F. Turner, W. Weibull, W. A. Wood.

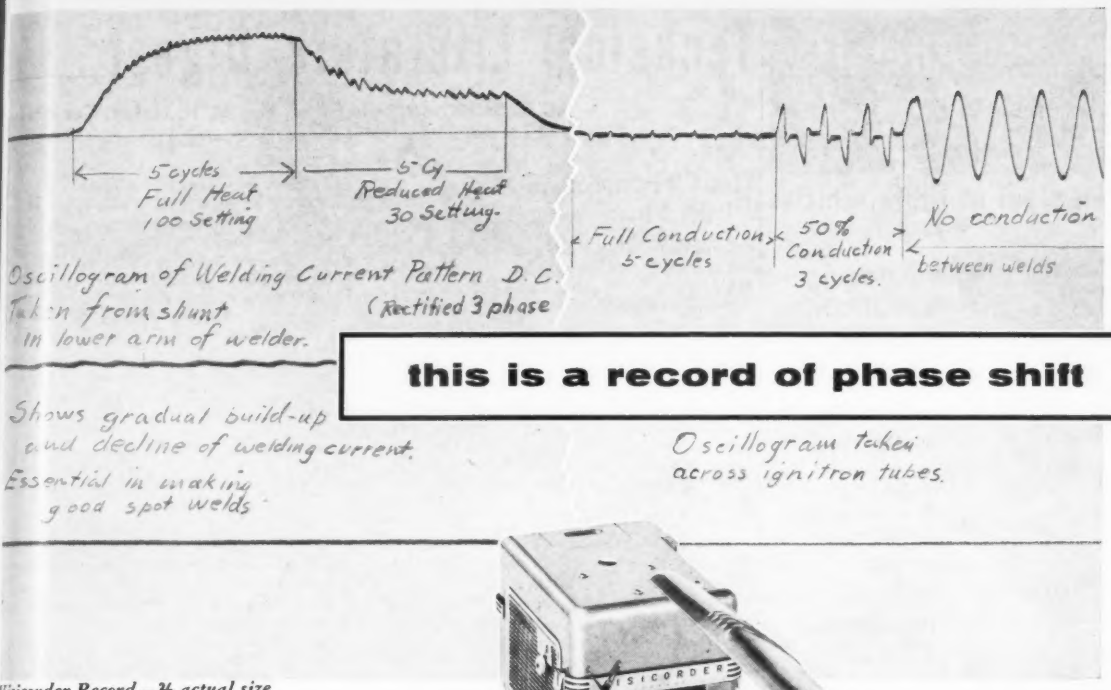


**this is a record of phase shift**

*Visicorder Record — ⅓ actual size*

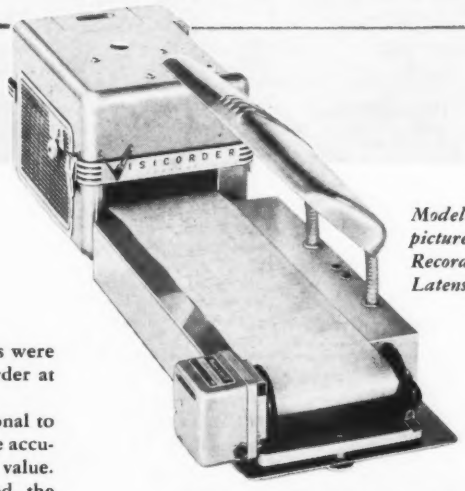


*Model 906A Visicorder pictured with Record Takeup and Latensifier Unit.*

These welder phase-shift heat-control patterns were directly recorded with a Honeywell 906 Visicorder at Bristol Aircraft (Western) Limited in Winnipeg.

Since the welding heat generated is proportional to the square of the current value, phase shift must be accurately controlled in order to determine the heat value. If the phase shift dial is not accurately calibrated, the result is too much or too little heat, and a poor weld.

In this application, the Visicorder is an essential guide to accurate calibration, since ink-type recorders do not cover the sensitivities and frequencies needed and an oscilloscope would present a continually changing pattern since most recording periods are less than 10 cycles. The directly-recorded Visicorder patterns allow a convenient study of the exact time when the current wave form was being cut off.

Here is the circuit used in this test.

*Input Circuit for Oscillogram of D. C. Welding Current*

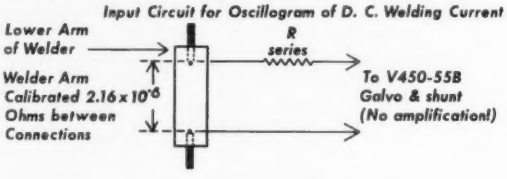


The Honeywell Visicorder is the first high-frequency, high-sensitivity direct recording oscillograph. In laboratories and in the field everywhere, instantly-readable Visicorder records are pointing the way to new advances in product design, rocketry, computing, control, nucleonics . . . in any field where high speed variables are under study.

The new Model 906A Visicorder, now available in 8- and 14-channel models, produces longitudinal grid lines simultaneously with the dynamic traces, time lines, and trace identification by means of new Accessory units.

To record high frequency variables—and monitor them as they are recorded—use the Visicorder Oscillograph. Call your nearest Minneapolis-Honeywell Industrial Sales Office for a demonstration.

# Honeywell

Industrial Products Group

**Reference Data: Write for Visicorder Bulletin**

*Minneapolis Honeywell Regulator Co., Industrial Products Group, Heiland Division, 5200 E. Evans Avenue, Denver 22, Colorado*

THE MARK OF QUALITY
BARBER COLMAN
Aircraft Controls
for all types of flight vehicles

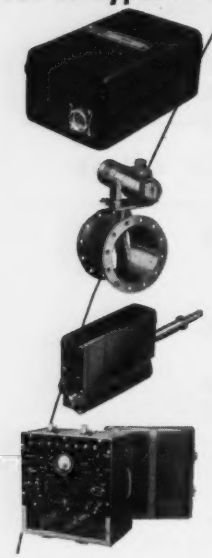

TEMPERATURE & POSITIONING CONTROLS
AIR VALVES
ACTUATORS
GROUND TEST EQUIPMENT

Write for complete data or consult the Barber-Colman engineering sales office nearest you: Los Angeles, Seattle, Fort Worth, New York, Baltimore, Montreal, Rockford.

BARBER-COLMAN COMPANY
Dept. I — 1470 Rock Street, Rockford, Illinois.

# Technical Literature Digest

**M. H. Smith,** *Associate Editor,* **and M. H. Fisher,** *Contributor*
**The James Forrestal Research Center, Princeton University**

## Heat Transfer and Fluid Flow

**Approximate Methods for Predicting Separation Properties of Laminar Boundary Layers,** by N. Curle and S. W. Skan, *Aeron. Quart.*, Aug. 1957, pp. 257–268.

**On the Calculation of Heat and Mass Transfer in Laminar and Turbulent Boundary Layers,** by D. R. Davies and D. E. Bourne, *Quart. J. Mech. Appl. Math.*, vol. 9, Dec. 1956, pp. 457–488.

**A Low-speed Experimental Investigation of the Effect of a Sandpaper Type of Roughness on Boundary-layer Transition,** by Albert E. von Doenhoff and Elmer A. Horton, *NACA TN* 3858, Oct. 1956, 45 pp.

**Investigation of Transient Pool Boiling Due to Sudden Large Power Surge,** by Robert Cole, *NACA TN* 3885, Dec. 1956, 44 pp.

**Two-phase, Steam-water Critical Flow,** by H. S. Isbin, J. E. Moy and A. J. R. DaCruz, *AIChE J.*, vol. 3, Sept. 1957, p. 361.

**Heat-Transfer to Boiling Methanol—Effect of Added Agents,** by A. J. Lowery Jr. and J. W. Westwater, *Ind. & Engng. Chem.*, vol. 49, Sept. 1957, pp. 1445–1448.

**On the Steady-state Temperature of a Flat Plate Placed in a Flow of Reacting Gas Mixture** (Russian—Ob ustanovivsheisia temperature ploskoi plastiny, obtekaemoi reagiruiushchei gasovoi smes'iu), by E. P. Vaulin, *Doklady Akad. Nauk SSSR*, vol. 113, Apr. 21, 1957, pp. 1235–1238.

**Heat Transfer to Flowing Gas-solids Mixtures in a Circular Tube,** by Leonard Farber and Morgan J. Morley, *Ind. & Engng. Chem.*, vol. 49, July 1957, pp. 1143–1150.

**One-dimensional Unsteady Flow of Magneto-gasdynamics,** by S. I. Pai, *Univ. Maryland, Inst. Fluid Dynamics Appl. Math., TN* BN-86 (AFOSR TN 56-537), (AD 110356), Nov. 1956, 14 pp.

**Heat Transfer in Fully-developed Flow between Parallel Plates with Variable Heat Sources,** by Albert L. Loeffler Jr., *Nucl. Sci. & Engng.*, vol. 2, Sept. 1957.

**Transient Air Temperatures in a Duct,** by S. E. Rea and C. M. Ablow, *Trans. ASME*, vol. 79, no. 7, Oct. 1957, p. 1536.

**Effect of Wall Roughness on Convective Heat Transfer in Commercial Pipes,** by J. W. Smith and Norman Epstein, *AIChE J.*, vol. 3, June 1957, pp. 242–248.

**New Finite-difference Technique for**

EDITOR'S NOTE: Contributions from E. R. G. Eckert, J. P. Hartnett, T. F. Irvine Jr. and P. J. Schneider of the Heat Transfer Laboratory, University of Minnesota, are gratefully acknowledged.

*The General Electric Jet Engine Dept. Announces the establishment of* **2** *new*

**Senior Engineering Design Analysis Positions**

Because of expanding activity we are broadening our organization to include two additional Senior Engineers, and we are inviting inquiries from qualified men who wish to join our organization at this level.

In keeping with General Electric's policy of parallel opportunities for specialists and managers, salaries established for these new positions are equivalent to those of high management level.

We are seeking design specialists with 12 to 20 years of practical hardware experience. To qualify, you must be thoroughly familiar with all mechanical, aerodynamic, hydraulic, control, and installation areas involved in aircraft gas turbine design, with heavy specialized practical experience in at least one of those areas. You will have been responsible for successfully putting engines through their 150 hour test and you will have had many years of experience in analyzing design problems relating to engines in operation, and will have provided valid engineering solutions.

Briefly, you must be able to accept any hardware problem that turns up in the field and stay with it until you get the answer.

The Engineers who fill these positions will be making important contributions to jet engine design and utilization. You will be responsible for both overall and detailed analysis of components and systems of the newest designs and developments to assure maximum utilization of special knowledge gained during factory, field, and service operations. As a member of the Senior Review Panel, you will incorporate results of your practical experience in our new designs. And, as a senior specialist in the field, you will represent the Jet Engine Department on major Government and Industry technical panels.

*If you qualify, call or write*
*M. L. Umble, Supervisor*
*Professional Placement, POplar 1-4100,*
*Extension 3828, Bldg. 501.*

GENERAL ELECTRIC
JET ENGINE DEPT. CINCINNATI 15, OHIO

PROGRESS REPORT FROM AVCO RESEARCH LABORATORY

# NEW LIGHT ON MHD*

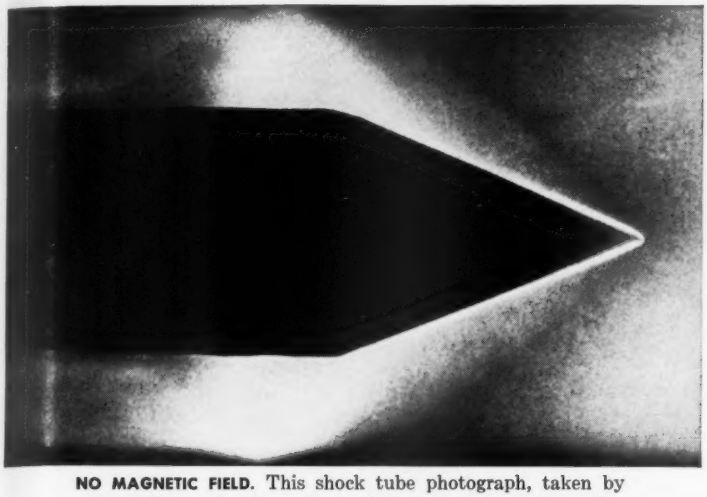

**NO MAGNETIC FIELD.** This shock tube photograph, taken by emitted light only, shows the typical shock wave configuration formed by high-velocity gas flowing around a pointed cone.

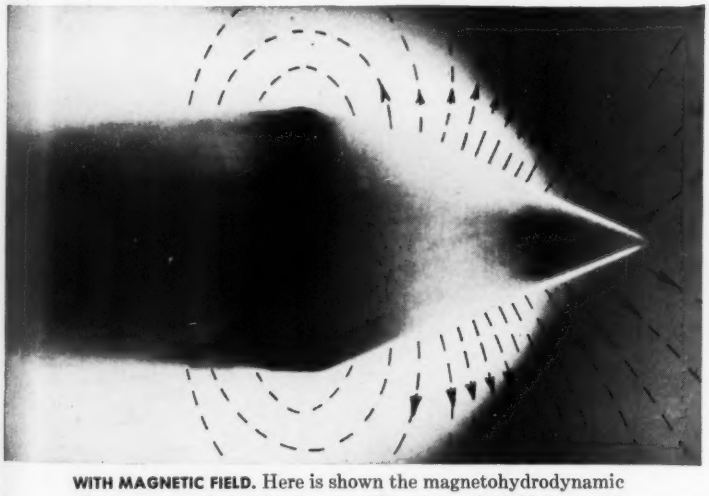

**WITH MAGNETIC FIELD.** Here is shown the magnetohydrodynamic displacement of the shock wave. The magnetic field is caused by electric current flowing through a coil of wire within the cone. This experiment qualitatively demonstrates the interaction of a high-temperature gas with a magnetic field. This effect would be expected to produce drag and reduce heat transfer to the body.

The Avco Research Laboratory was founded a little more than three years ago for the purpose of examining high-temperature gas problems associated with ICBM re-entry. The success of this research led to the birth of a new corporate enterprise, Avco's Research and Advanced Development Division.

The Research Laboratory, now established as a separate Avco division, has expanded to embrace all aspects of physical gas dynamics. We are currently gravid with several embryonic projects which we anticipate will likewise grow into new corporate enterprises. Our work in the physics, aerodynamics and chemistry of high-temperature gases is growing in the following areas:

**Magnetohydrodynamics—**
Flight and industrial power-generation applications

**Space flight—**
Manned satellites
Electromagnetic propulsion

These developments have created a number of openings for physicists, aerodynamicists and physical chemists. If your background qualifies you to work in any of these areas, we would be pleased to hear from you.

Arthur Kantrowitz

*Dr. Arthur Kantrowitz, Director*
*Avco Research Laboratory*

**P. S.** A listing of laboratory research reports indicative of the scope and depth of our activities is available. Address your request: *Attention: Librarian, Avco Research Laboratory, 2385 Revere Beach Parkway, Everett, Massachusetts.*

***Magnetohydrodynamics,** the study of the dynamics of electrically conducting fluids interacting with magnetic fields.

**Avco RESEARCH LABORATORY**

*A Division of Avco Manufacturing Corporation/Everett, Mass.*

*Other divisions and subsidiaries are:*

AK Division
Crosley Division
Ezee Flow Division
Lycoming Division
New Idea Division
Moffats Limited
Crosley Broadcasting Corporation
Research and Advanced Development Division

# Advanced Weapons

## *broad creative mission at Chance Vought*

**MILITARY ASTRONAUTICS: Vought studies toward space research vehicles and manned spacecraft include multistaging, space communications, nuclear and ionic propulsion, celestial navigation, and membership on Boeing's Dyna Soar space glider development team.**

**ASW RESPONSIBILITY: Under the Office of Naval Research, Vought antisubmarine specialists are conducting extensive research and development work in ASW detection and classification phases. Goal is to bring detection abreast of destruction capabilities.**

**Advanced Weapons Staff Engineer.** Ph.D. preferred, with at least 10 years background in guidance or navigation and control systems. To develop completely new concepts in guidance, navigation, or control systems.

**Electro-mechanical Systems Engineer or Specialist.** A.E., E.E., or M.E., (advanced degree preferred) with at least 7 years experience in autopilot, flight control, stability systems and inertial guidance systems and design work. To make high-level technical studies of various control and stabilization systems for advanced weapons.

**Guidance Design Engineer.** E.E. or Physics Degree, plus 2 or more years experience. To design various active and self-contained missile guidance systems, and to design and develop radar beacons.

**Lead Instrumentation Engineer.** B.S. or M.S. in E.E., plus 5 years electronics experience in telemeter applications of flight test instrumentation data. To guide a Research and Development group in the design and application of electronic gathering and reduction systems.

**Hydrodynamicist.** B.S. or M.S. in Engineering plus 5-7 years experience in hydrodynamics and cavitation of torpedoes and other fully submerged vehicles.

*Qualified engineers and scientists who would like to join Vought's development of advanced weapons are invited to inquire.*

A. L. JARRETT, Manager, Advanced
Weapons Engineering, Dept. JP-3.

CHANCE VOUGHT AIRCRAFT
INCORPORATED · DALLAS, TEXAS

**Solution of the Heat-conduction Equations, Especially Near Surfaces with Convective Heat Transfer,** by H. G. Elrod Jr., *Trans. ASME*, vol. 79, Oct. 1957, p. 1519.

**On the Use of Matrices for Solving Periodic Heat Flow Problems,** by G. W. T. White, *Appl. Sci. Res.*, vol. 6, Sec. A, Nos. 5–6, 1957, pp. 433–444.

**Influence of Turbulence on Transfer of Heat from Cylinders,** by J. Kestin and P. F. Meader, *NACA TN* 4018, Oct. 1957, 78 pp.

**Measurements of Heat Transfer from Fine Wires in Supersonic Flows,** by John Laufer and Robert McClellan, *J. Fluid Mech.*, vol. 3, Sept. 1956, pp. 276–289.

**Heat Transfer and Flow-Friction Characteristics of Woven-screen and Crossed-rod Matrixes,** by L. S. Tong and A. L. London, *Trans. ASME*, vol. 79, Oct. 1957, p. 1558.

**Heat Transfer to Lead-Bismuth in Turbulent Flow in an Annulus,** by R. A. Seban and D. F. Casey, *Trans. ASME*, vol. 79, Oct. 1957, p. 1514.

**Experiments on the Inhibition of Thermal Convection by a Magnetic Field,** by Y. Nakagawa, *Proc. Roy. Soc.*, Ser. A., no. 1220, vol. 2401, 1957, pp. 108–113.

**Cross Sections of Dissociative Recombination,** by Ernest Bauer and Ta-You Wu, *Can. J. Phys.*, vol. 34, Dec. 1956, pp. 1436-1447.

## Combustion, Fuels and Propellants

**Final Technical Report, Contract AF 18(600)-430,** *Texas Univ.* (*AFOSR-TN-56-63; ASTIA AD* 115028), Dec. 1956, 18 pp.

**Thermodynamic Calculations of the Performance of the Hydrogen Fluorine System,** by Rudolph Edse and William L. Doyle, *Wright Air Dev. Center, Tech. Rep.* 53-427, March 1956, 46 pp.

**Theoretical Combustion Performance of Ramjet Fuels: Hydrogen,** by Waldo T. Renich, *Johns Hopkins Univ. Appl. Phys. Lab.*, CF 2601, Dec. 1956, 3 pp. 5 fig.

**Research on Some Properties of Certain Propellants,** by Jacques Francon, *France, Ministere de l'Air, Publications Scientifiques et Techniques, Notes Techniques* 66, 1957, 46 pp. (in French).

**The Diesel Powered Ballistic Centrifuge** by W. Hendricks and W. M. Bogart, *Hercules Powder Co., Allegany Ball. Lab., Rep.* ABL/X-17, Aug. 1957, 13 pp.

**Flame Stabilizing Effects of Inclined Air Jets,** by D. P. Duclos, Allan Schaffer and A. B. Cambel, *Indust. & Engng. Chem.*, vol. 49, Dec. 1957, pp. 2063–2066.

**Investigations of the Detonation Properties of Condensed Explosives with Equations of State Based on Intermolecular Potentials, I: RDX with Fixed Product Composition,** by W. Fickett, W. W. Wood and Z. W. Salsburg, *J. Chem. Phys.*, vol. 27, Dec. 1957, pp. 1324–1329.

**The Thickness of Laminar Flames in Pre-mixed Reactants: Optical Considerations,** by F. J. Weinberg, *Proc. Royal Soc.*, vol. 243, Dec. 10, 1957, pp. 107-118.

**Progress Report on Study of Combustion for Supersonic Ram Jet (ODS Project) for Period Apr. 1–Sept. 30, 1945,** *CM* 174, (Report PDN-2980), by Esso Labs., Oct. 1945, 24 pp. 3 tab. (Declassified from Confidential by authority of Johns Hopkins Univ., Appl. Phys. Lab., letter dated 2/5/57, signed Paul E. Clark.)